


PUBLISHED PROJECT REPORT PPR901

Rainfall Thresholds for Landslides

Deterministic and Probabilistic Approaches

M G Winter, F Ognissanto and L A Martin

Report details

| | | | |
|------------------------------------|---|------------------------------------|---|
| Report prepared for: | Transport Scotland, Roads | | |
| Project/customer reference: | TS/TRBO/SER/2012/12/37 | | |
| Copyright: | © Queen's Printer for Scotland | | |
| Report date: | May 2019 | | |
| Report status/version: | Issue 1 | | |
| Quality approval: | | | |
| M G Winter (Project Manager) |  | M G Winter (Technical Reviewer) |  |

Disclaimer

This report has been produced by TRL Limited (TRL) under a contract with Transport Scotland. Any views expressed in this report are not necessarily those of Transport Scotland.

Whilst every effort has been made to ensure that the matter presented in this report is relevant, accurate and up-to-date, TRL Limited cannot accept any liability for any error or omission, or reliance on part or all of the content in another context.

When purchased in hard copy, this publication is printed on paper that is FSC (Forest Stewardship Council) and TCF (Totally Chlorine Free) registered.

Contents amendment record

This report has been amended and issued as follows:

| Version | Date | Description | Editor | Technical Reviewer |
|----------|------------|-----------------------------|----------------------------|----------------------------|
| Draft 1d | 29/10/2018 | Partial draft | L A Martin F Ognissanto | M G Winter |
| Draft 1f | 27/11/2018 | Complete draft | M G Winter | L A Martin F Ognissanto |
| Draft 1h | 12/12/2018 | Draft | L A Martin | M G Winter |
| Draft 1i | 17/12/2018 | Draft for customer comment | M G Winter | |
| Draft 1m | 02/04/2019 | Customer comments addressed | L A Martin M G Winter | M G Winter |
| Issue 1 | 15/05/2019 | DPA Approval | | P Langdale |

| | |
|--------------------------------|------------------|
| Document last saved on: | 16/05/2019 17:38 |
| Document last saved by: | Reviewer |

Table of Contents

| | |
|--|----|
| Executive Summary | 2 |
| 1 Introduction | 4 |
| 2 Debris Flow and the Scottish Trunk Road Network | 6 |
| 3 Rainfall Patterns and Landslides | 12 |
| 4 Scotland's Rainfall Climate | 18 |
| 4.1 Recent Trends and Future Change | 21 |
| 5 A Tentative Trigger Threshold | 22 |
| 5.1 Results and Interpretation | 25 |
| 5.2 Testing and Using the Threshold | 28 |
| 6 Development of a Probabilistic Threshold | 32 |
| 6.1 Data | 35 |
| 6.2 Analysis | 45 |
| 7 Conclusions and Recommendations | 66 |
| Acknowledgements | 70 |
| References | 72 |
| Appendix A The procedure for sorting and analysing 15-minute rainfall data | 76 |
| Appendix B Application of Bayes Theorem to a Hypothetical General Scenario | 78 |
| Appendix C Explanation of Probability of Rainfall Duration $P(D)$ | 82 |

Executive Summary

This report describes the development of a means of identifying and forecasting periods of time when the debris flow hazard is greater and the risk associated with those events is therefore increased.

The link between rainfall and debris flow is well-established in Scotland and a tentative threshold to describe the relation between rainfall and debris flow has been developed. The threshold is related to the Met Office heavy rainfall warning used to switch wig-wag warning signs on during periods of heavy rainfall and to thus indicate higher debris flow hazard and risk to road users.

This tentative, deterministic threshold is, however, limited by the lack of data proximal to the debris flow events that occur and has always been considered to underestimate the amount of rain required to trigger an event. To this end two rain gauges were installed in the area around the A83 Rest and be Thankful, in order to acquire data in this more remote, higher elevation location at which debris flow events occur relatively frequently.

This threshold is also limited by its deterministic nature, albeit at the time that it was developed there were no known probabilistic thresholds. Like all deterministic thresholds it simply divides the rainfall duration-intensity plane into two regions: one in which debris flow occurs and one in which debris flow does not occur. This binary approach is not well-matched to reality, which is significantly more complex, and in reality the two regions represent undefined, but greater and lesser, likelihoods of event occurrence. A probabilistic approach provides a more realistic, reliable and defensible rainfall trigger threshold for debris flow that is, additionally, based on similar principles to rainfall forecasts. This approach potentially yields a suite of rainfall thresholds, or rainfall states, that correspond to differing probabilities of debris flow occurrence given different rainfall duration-intensity pairings.

In this report the recent history of debris flow in Scotland as it relates to the trunk (strategic) road network is briefly and selectively described as is the rainfall climate of Scotland. A brief review of international rainfall trigger thresholds for landslides points out the potential for:

- 1) a probabilistic approach to be taken to the development of such thresholds; and
- 2) for rainfall event data that does not lead to a landslide, as well as rainfall event data that does lead to a landslide, to be incorporated into the analysis.

The development and use of the existing deterministic threshold and the development of the new probabilistic approach are both described. While the deterministic approach relies on cause and effect, with a set amount of rainfall in a defined period leading to a landslide, the probabilistic approach uses Bayes' theorem. This allows that a degree of randomness is present and that it is not possible to trace a unique path linking an event and a single outcome. In this way an evaluation of the likelihood is given that a result occurs as an outcome of certain inputs; that is, a probability is associated with its occurrence.

The probabilistic analyses use the prior probability of landslide occurrence and the posterior probability associated with rainfall and landslides to develop one-dimensional analyses for conditional landslide probability based on rainfall duration, rainfall intensity and total rainfall. This is then extended to encompass the more complete two-dimensional analysis to

derive the conditional probability of landslide occurrence dependent upon paired values of rainfall duration and intensity.

Probabilistic thresholds for the conditional probability of landslide occurrence dependent on rainfall duration and intensity $P(L|D,I)$ are derived in the range 0.05 (5%) to 0.3 (30%). This is considered to be a significant improvement on the deterministic approach to the forecast of periods during which landslide hazard and risk are elevated due to rainfall conditions.

It is proposed that a formal 'shadow' trial be undertaken of a probabilistic landslide forecast system at the A83 Rest and be Thankful, initially paralleling the trigger system already in use until its utility is proven. Such a forecast might be used, for example, to action specific landslide risk reduction actions such as the wig-wags that are currently in use at the site. The trial will require detailed, multi-stakeholder planning and preparation to ensure that it reflects the planned operational use and that clear success criteria are determined in advance. An outline programme for the development of such a trial is set-out in this report.

1 Introduction

Rainfall-induced debris flows, a form of landslide, are a common occurrence in Scotland. The events of August 2004, which adversely affected the Scottish trunk road network, led to the Scottish Road Network Landslides Study (Winter et al. 2005; 2006; 2009; 2013a).

The overall purpose of that study was to systematically assess and rank the hazards posed by debris flows and to put in place a management and mitigation strategy for the Scottish trunk road network. The ranking system allows lengths of the network subject to risk from debris flow events to be prioritised for action.

The approaches to management and mitigation were based upon exposure reduction and hazard reduction respectively (Winter et al., 2009). There are many forms of landslide management and mitigation (e.g. VanDine, 1996) and a strategic approach to landslide risk reduction has been developed (Winter, 2013; 2014a; 2019). That approach is intended to provide a common lexicon and to allow a clear focus on outcomes from such activities whilst avoiding an overemphasis on individual processes and techniques (Figure 1.1). This approach ought to be of particular value to those who fund such works, including infrastructure owners and local governments. Management involves the reduction of the exposure of road users to the hazard by one or more means of:

- 1) education;
- 2) geographical (non-temporal) warnings; or
- 3) response (including temporal, or early, warnings).

Mitigation primarily, but not exclusively, involves reduction of the actual hazard by means of:

- a) works to engineer or protect the elements at risk;
- b) remediation of the hazard to reduce the probability of failure; or
- c) removal, or evacuation, of the elements at risk.

One of the recommendations put forward by Winter et al. (2009) was that work to develop a tentative rainfall threshold for landslides in Scotland be continued with a view to establishing a more robust form of the threshold. Such thresholds can be used to enable periods when debris flow events are more likely and to thus deliver effective early warnings (see item 3 above).

The A83 trunk (strategic) road at the Rest and be Thankful is widely recognised as being amongst those sites subject to the highest risk of the sites identified by Winter et al. (2009): both to the physical road infrastructure, including its continuous and uninterrupted use (Winter et al., 2014), and to road users (Wong & Winter, 2018; Winter, 2018). The application of the strategic approach to landslide risk reduction at the A83 Rest and be Thankful, is extensive and incorporates both exposure and hazard reduction actions (Winter et al., 2013b; Winter & Corby, 2012; Winter & Shearer, 2017). Also included within those actions was the installation of two rainfall gauges in the area, in order to better enable the evaluation of the effects of rainfall on debris flow events. This action reflects the fact that the rainfall gauge network in Scotland is sparse in areas of interest for debris flow forecasting, not least as the primary function of meteorological observation stations is the collection of synoptic data; simple rainfall stations are more usually used for specific

purposes related to water resources and hydroelectric power, for example (Winter et al., 2010).

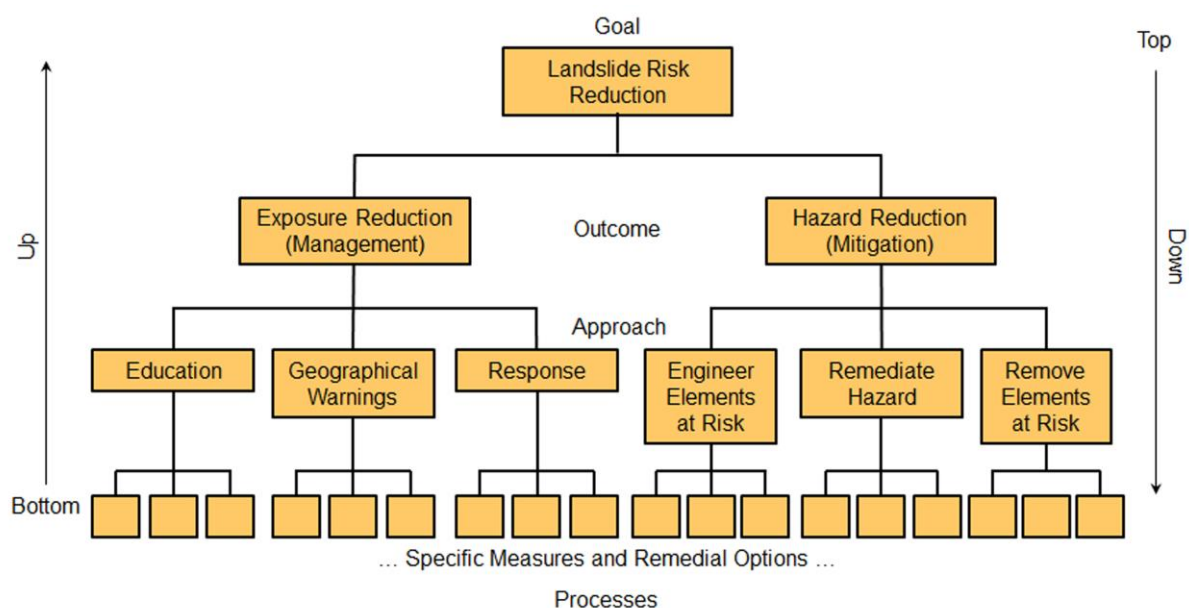


Figure 1.1: Classification for landslide management and mitigation to enable a strategic approach to risk reduction (from Winter, 2014a)

This report describes the development of a means of identifying and potentially forecasting periods of time when the likelihood of debris flow events is greater and the risk associated with those events is therefore higher.

Section 2 presents a brief background narrative on debris flow and the Scottish trunk road network.

Section 3 gives an overview of issues related to rainfall and landslides, including a commentary on how a deterministic threshold might be exploited within an early warning system.

Section 4 gives a brief overview of the rainfall climate of Scotland.

Section 5 describes the derivation of the tentative, deterministic, threshold reported by Winter et al. (2009) and further developed by Winter et al. (2010); this uses rainfall and debris flow data from a wide area of Scotland.

Section 6 describes the ongoing further work undertaken to develop a probabilistic framework for forecasting debris flow; this uses rainfall and debris flow data from the two rainfall gauges installed in the area of the A83 Rest and be Thankful.

2 Debris Flow and the Scottish Trunk Road Network

The Scottish Road Network Landslides Study (Winter et al., 2005; 2009) was instigated in response to the rainfall-induced landslide events of August 2004. The rainfall experienced in Scotland in August 2004 was substantially in excess of the norm. Some areas of Scotland received more than 300% of the 30-year average August rainfall (source: www.metoffice.gov.uk), while in eastern parts between 250% and 300% was typical. Although the percentage of the monthly average rainfall that fell during August reduced to the west, some parts still received 200% to 250%.

Long lasting and intense rainfall led to a large number of landslides, in the form of debris flows, in the hills of Scotland. Critically, some of these affected important parts of the trunk road network, linking not only cities but also smaller, remote communities. Notable events occurred at the A83 between Glen Kinglas and to the north of Cairndow (9 August), the A9 to the north of Dunkeld (11 August), and the A85 at Glen Ogle (18 August) (Figure 2.1).

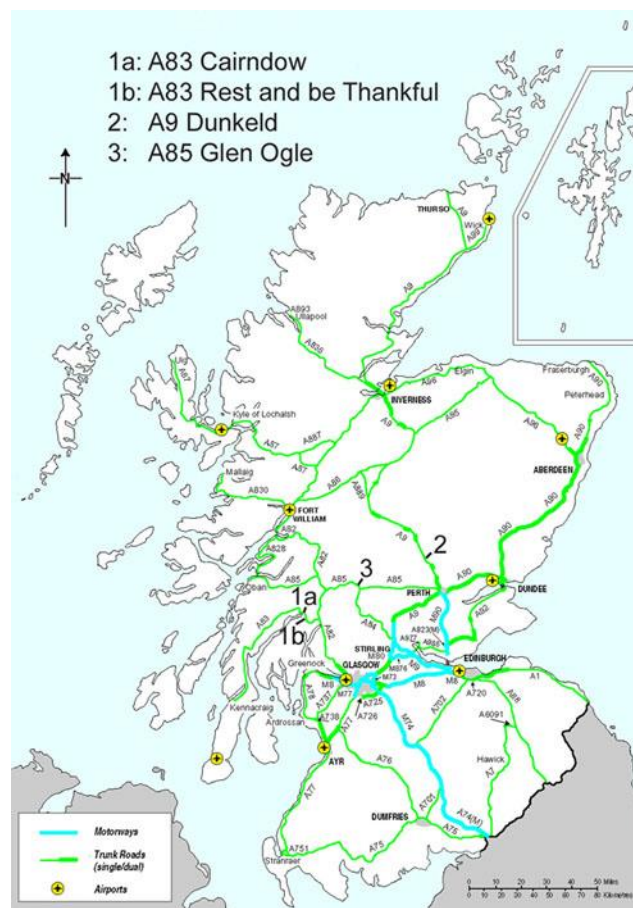


Figure 2.1: Map showing the trunk road network, including motorways, in Scotland. The locations of the three main debris flow event groups that affected the trunk road network in Scotland in August 2004 are shown

Subsequent analysis of radar data indicated that at Callander, 20km from the A85 events, 85mm of rain fell in four hours on 18 August. Some 48mm fell in just 20 minutes and the storm reached a peak intensity of 147mm/hour. The 30-year average August rainfall varies between 67mm on the east coast and 150mm in the west of Scotland (Anon., 1989).

While there were no major injuries, some 57 people were taken to safety by helicopter after being trapped between the two debris flows that reached the A85 in Glen Ogle. However, the real impacts were social and economic, in particular the severance of access to and from relatively remote communities. The A83, carrying up to 5,000 vehicles per day (all vehicles two-way, 24 hour annual average daily traffic, AADT) was closed for slightly in excess of a day, the A9 (carrying 13,500 vehicles per day) was closed for two days prior to reopening, initially with single lane working under convoy, and the A85 (carrying 5,600 vehicles per day) was closed for four days. The traffic flow figures are for the most highly trafficked month of the year (July or August). Minimum flows occur in either January or February and are roughly half those of the maxima reflecting the importance of tourism and related seasonal industries to Scotland's economy. Substantial disruption was thus experienced by local and tourist traffic, and goods vehicles.



Figure 2.2: View of the hillside above and below the approach to the Rest and be Thankful from the east (from NGR NN 23160 06559 on the opposite side of Glen Croe). Not only can the event dated 28 October 2007 be clearly seen but evidence of numerous past events can be seen on the surrounding hillside

The events of August 2004 are described by Winter et al. (2006). These events are by no means unique and further debris flows have affected the A9, A82 and A83, for example, since August 2004. The event pictured at the A83 in Figures 2.2 and 2.3 occurred at around 0330 hours on Sunday 28 October 2007. Figure 2.2 illustrates the event and the surrounding hillside; the photograph is taken from the opposite side of the valley and evidence of numerous past events can be clearly observed. Figure 2.3 illustrates the event in more detail and it is clear that the system of mass movement comprises two discrete but related events. The flow above the road commenced with a relatively small slide (or slides) into an existing drainage channel. This then triggered the movement of a large amount of marginally stable material in and around the stream channel depositing an estimated 400 tonnes of material

at road level. This material blocked the open drain which carries water along the upslope side of the road to a series of culverts beneath the road. While the material from above the road had limited impact upon the slopes below the road, water diverted from the drain was channelled across and over the edge of the road causing significant erosion and undercutting of the slope below the A83, and associated deposition further down the hill as can be seen in Figure 2.3.

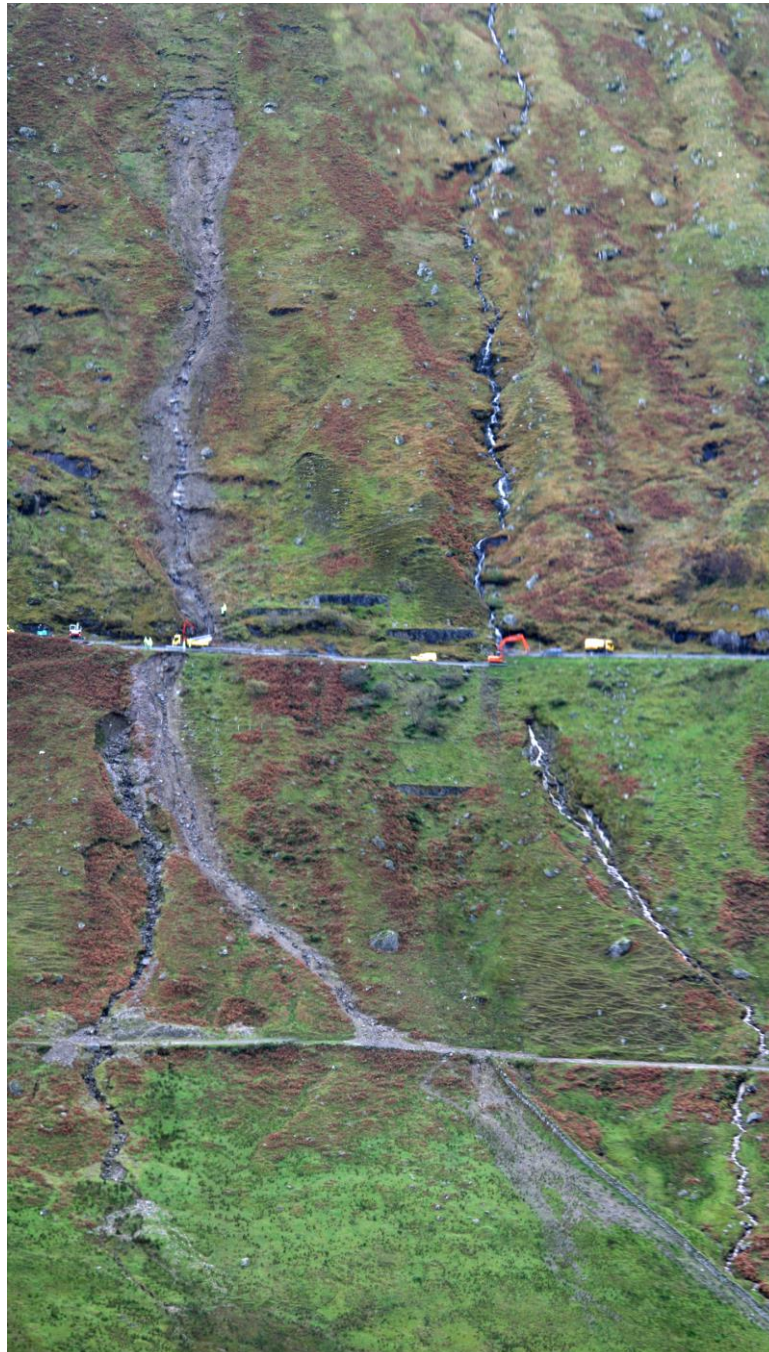


Figure 2.3: View of the debris flows above and below the A83 on the approach to the Rest and be Thankful (from NGR NN 23160 06559 on the opposite side of Glen Croe). The head scar is at approximately 370m AOD, the A83 at 240m AOD and the Old Military Road at 180m AOD

Due to the major contribution that tourism makes to Scotland's economy the impacts of such events can be particularly serious during the summer months, during which period debris flows usually occur in July and August. Nevertheless, the impacts of any debris flow event occurring during the winter months, during which debris flow usually occurs between October/November and January, should not be underestimated. Not surprisingly, the debris flow events described created a high level of interest in the media in addition to being seen as a key issue by politicians at both the local and national level. Indeed, the effects of such small events which may, at most, affect directly a few tens of metre of road cast a considerably broader vulnerability shadow (Winter & Bromhead, 2012); Winter (2014b) estimated the boundaries of the vulnerability shadow cast as illustrated in Figure 2.4.

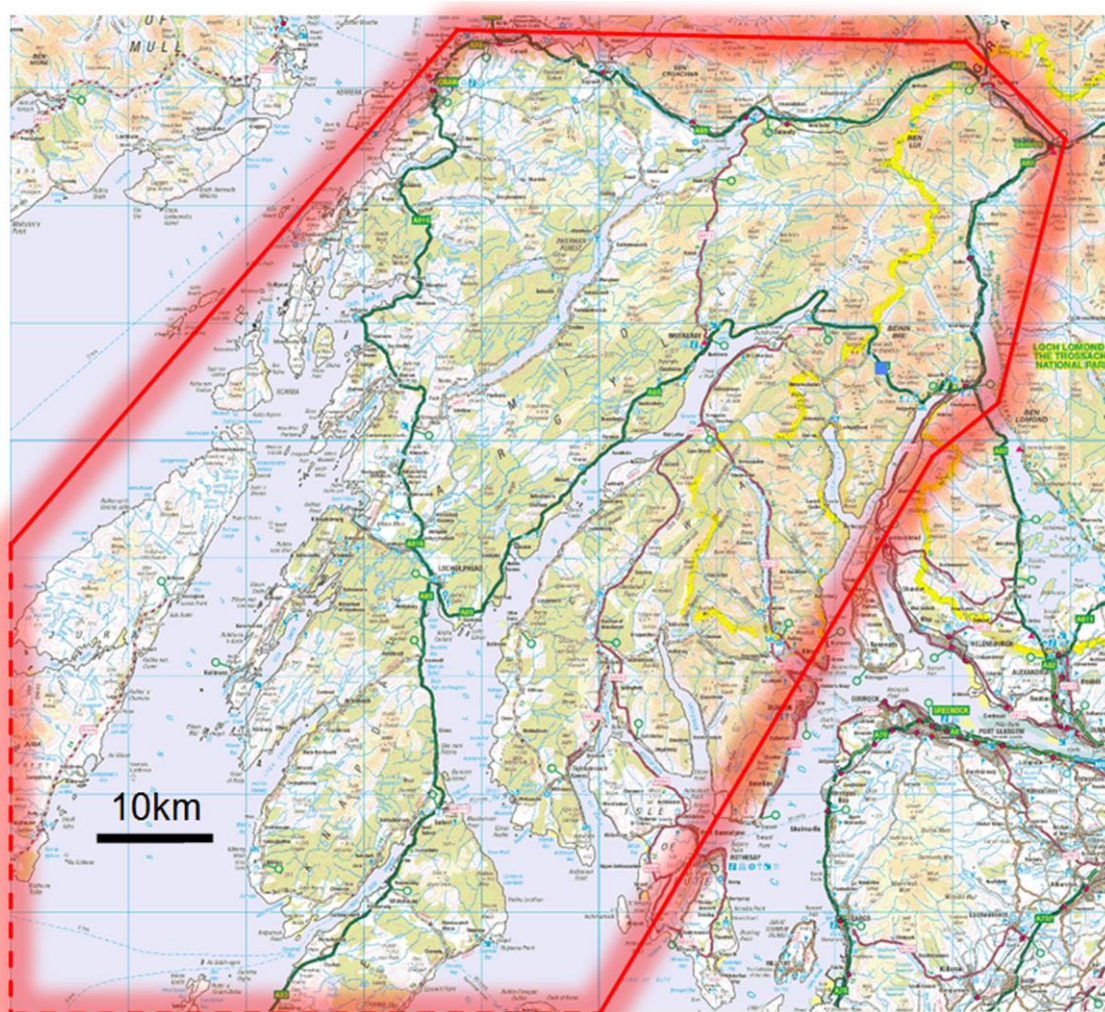


Figure 2.4: A relatively small debris flow event (blue square) closed the A83 at the Rest and be Thankful in October 2007; the vulnerability shadow that was cast (bounded in red) was extensive (Winter, 2014b)

The A83 Rest and be Thankful site has been extremely active in recent years with multiple debris flow events and associated closures and events in 2007, 2008 and 2009 had an adverse effect on the travelling public. Subsequent events in 2011 and 2012 have continued this trend through to much more recent events in October 2018 (the October 2018 events took place after the completion of the analysis presented in this report). This has meant that

the area has become the focus of not only concern but also of extensive landslide management and mitigation activity. This culminated in a study being commissioned to assess and make recommendations on potential landslide remediation actions (Anon., 2013; Winter & Corby, 2012).

3 Rainfall Patterns and Landslides

Landslides are often cited as being caused by rainfall and the link between high intensity-short duration, storm rainfall and debris flows has been documented in Japan (Fukuoka, 1980), New Zealand (Selby, 1976) and Brazil (Jones, 1973) amongst other places. However, the influence of longer term, antecedent rainfall prior to storm events was clear from the events experienced in Scotland in August 2004 (Winter et al., 2007a).

In a study based in the Santa Cruz Mountains of California, Wieczorek (1987) noted that no debris flows were triggered until 280mm of seasonal rain fell, thus clearly acknowledging the importance of antecedent rainfall, a factor that has also been recognised in studies in Southern California (Campbell, 1975), New Zealand (Eyles, 1979) and Alaska (Sidle & Swanson, 1982). Wieczorek (1987) also noted that for high permeability soils, such as those found in Hong Kong (e.g. Ko, 2005), the period of antecedent rainfall may be short or even that the amount of necessary antecedent rainfall may be supplied by the early part of the storm event itself.

Many studies have also included back analyses of rainfall records to define specific rainfall threshold levels that lead to conditions likely to cause landslides. These include, for example, Australia, Hong Kong, Italy, Jamaica, Nepal, Norway, Singapore, Slovenia, Switzerland, UK and the USA. Many authors of such studies state that their methodologies either could be, or will be, used for actively forecasting conditions likely to lead to landslides, but relatively few report such practical implementation and use of their work (Winter et al., 2010).

The back analyses use a wide range of methodologies; however, these are dominated by intensity-duration analyses (e.g. Ahmad, 2003; Aleotti, 2004; Caine, 1980; Flentje & Chowdury, 2006; Hurlimann, et al., 2003) which is a viable and well-established technique. Further details are given by Winter et al. (2009) and a wider-ranging review of rainfall thresholds is presented by Anon (2007).

The rainfall intensity-duration pattern of each storm during, or immediately after, which landslides have occurred can be analysed and a series of points representing a range of rainfall durations (x) and associated intensities (y) can be plotted. An example using hypothetical data is presented in Figure 3.1. Each event produces a data series containing a point representing each of the rainfall durations used in the analysis. Further events may be similarly analysed and if the same durations are used, a series of vertical data columns will be achieved, each one representing events associated with different rainfall intensities of a given duration. The solid data points in Figure 3.1 represent such data and the lower boundary of these data points represents the threshold above which rainfall-induced landslides may be expected to occur.

It is also important to note that most analyses consider storm and antecedent rainfall, the latter usually for periods between five and 40 days, or more. Those geographical regions in which antecedent rainfall is not considered, or is considered over shorter periods, tend to be those that experience particularly intense storm rainfall and/or where geomorphological and geological conditions favour the rapid onset of instability.

An additional element to this approach can be to undertake the same analysis but to additionally include data from storm events that do not trigger landslides (Winter et al., 2007b). However, assumptions must be made about the most appropriate point from which

to back-calculate (e.g. maximum storm intensity), as there is no causal event to define this point in time. This allows the threshold to be defined from below as well as from above, lending an additional degree of surety to the process. Figure 3.1 illustrates the development of a purely hypothetical threshold in this manner – the ‘open’ data points representing such ‘non-events’. The additional advantage of this approach in Scotland is that the relatively small number of rainfall events that are associated with landslide events are supplemented by those significant rainfall event that are not associated with landslide events, thus significantly increasing the amount of data available for analysis (see Section 6).

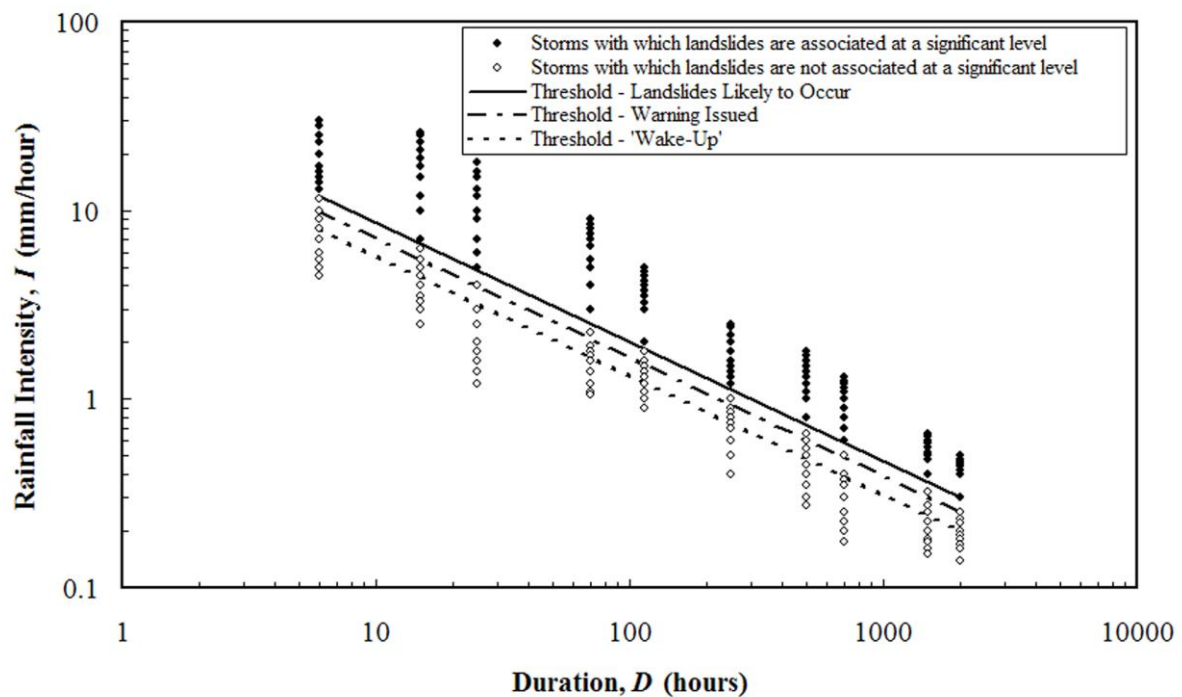


Figure 3.1: Development of a purely hypothetical rainfall intensity-duration threshold for landslides

The hypothetical rainfall data of Figure 3.1 have been used to illustrate a total of three (hypothetical) threshold levels:

- A threshold level above which landslides might be expected to occur (as described above).
- A threshold level at which a warning is issued and action taken – set at a lower level to give adequate time for effective notification and action.
- A still lower threshold level at which instruments are checked and key personnel alerted to the possibility of the development of conditions likely to lead to landslides – a precursor to the issue of a landslide warning.

It is important to recognise that threshold levels developed in this way are in no way absolute. They may, for example, simply represent the transition between the landslide density and/or short-term frequency in a given area reaching a limit that is significant in the context of infrastructure operation. This transition is likely to be more complex in larger areas of varied and complex geology such as Scotland. Indeed such thresholds may potentially change at discrete locations not only as a result of climatic variations but also as

a result of changes in vegetation/land cover, anthropogenic activity and recent geomorphological activity including debris flows. It is clear from observation of Scotland's hillsides, including that illustrated in Figures 2.2, that debris flow activity may render a given section of hillside less prone to further movement in the short-term but also that other areas where any previous activity is further in the past may present hazards that are just as significant. It is also important to note that if relevant to a wide enough area then thresholds can be a good long-term indicator, or forecast, of the increased likelihood of debris flow in a given region at a given point in time as opposed to a prediction of an event at a given site at a given time.

Intensity-duration relations for a number of different areas are plotted in Figure 3.2. All of the thresholds plot reasonably close together and broadly parallel, although in order to achieve a readable graph, log-log scaling has been used. The data are however sufficiently spaced to indicate that a unique threshold for all areas of the world is unlikely to exist in any practical sense, as would be expected from variations in climate and geology. The threshold plot for Scotland suggests a lower intensity for a given rainfall duration than others and has been, at least provisionally and in part, attributed by Winter et al. (2010) to the nature of the rainfall gauge network which primarily targets synoptic data and is therefore most often located close to sea level and thus a long way, horizontally and vertically, from the landslide events that are of interest here (see also Section 5).

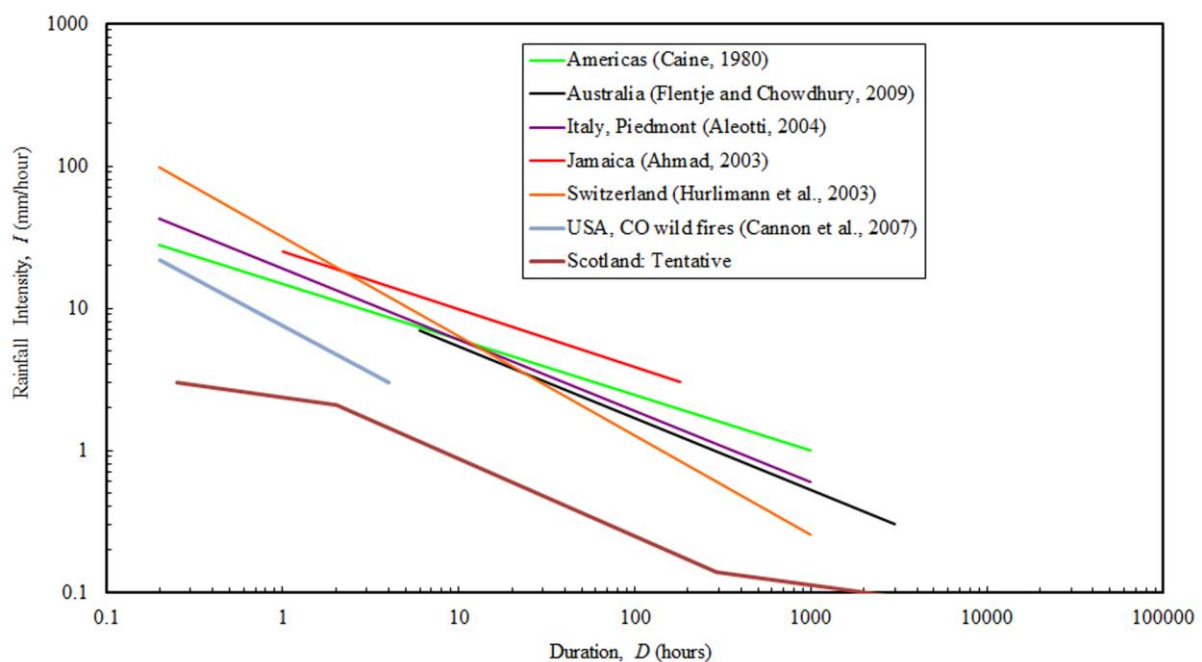


Figure 3.2: International rainfall intensity-duration trigger thresholds for rainfall-induced landslides showing the tentative threshold reported by Winter et al. (2009; 2010)

Clearly any tool of this nature must be fit for the purpose defined by the end user. While engineering geologists may be concerned by the concept of false alarms (false positive), experience would indicate that network operators are generally much more concerned by the possibility of events that are not forecast (false negative) occurring and relatively willing to accept false positives. This is especially so when the planned actions when an event is forecast involve issuing relatively low key warnings, which are appropriate to the local risk

level, rather than, for example, closing infrastructure. While both false alarms (false positives) and un-forecast events (false negatives) have the potential to undermine public, media and political confidence in a system it is the latter which is generally considered to have the more serious potential consequences from the point-of-view of inter alia potential liability.

The foregoing deals entirely with the development of deterministic thresholds. An interesting and potentially very useful development is the use of Bayesian probability to determine thresholds that are associated with the conditional probability of a landslide given a particular rainfall input.

Brunetti et al. (2010) employ a Bayesian inference method based on the relationship:

$$I = \alpha D^{-\beta} \quad (3.1)$$

where I is the rainfall mean intensity (mm/h),

D is the duration of the rainfall event (in hours) that results in a landslide, and

α and β are unknown shape and scale parameters to be estimated.

Estimating these parameters relies on a Bernoulli probability distribution, and Bayesian analysis (using the program WinBUGs) provides posterior probability (see second paragraph after Eq. (3.2) below for a contextual definition of posterior probability) distributions for their estimates. The parameters lead directly to a landslide threshold. It is important to note that for these probabilistic estimates it is explicitly assumed that landslide events are always associated with rainfall.

The Brunetti et al. (2010) Bayesian approach does not use rainfall events that do not result in landslides, as proposed by Winter et al. (2007b) and as a result is not considered further.

Berti et al. (2012) use a probabilistic approach to evaluating rainfall that led to a landslide event and rainfall that did not lead to a landslide event. The probabilistic approach allows uncertainty and variability to be incorporated and results in a distribution of probabilities which allow extreme events (such as landslides) to be estimated more robustly.

This method revolves around Bayes' theorem:

$$P(L|R) = \frac{P(R|L) \cdot P(L)}{P(R)} \quad (3.2)$$

which states that the probability of landslide (L) occurring given that rain (R) has occurred, $P(L|R)$, is proportional to the probability of rain given that a landslide has occurred $P(R|L)$ multiplied by the probability of a landslide occurring $P(L)$, divided by the probability of rain, $P(R)$. These probabilities can be computed using relative frequencies, for example $P(L) = N_L / N_R$ where N_L is the number of landslides and N_R is the number of rain events over a certain period.

It is important to note, not least to enable a full understanding of the probabilistic analyses presented in Section 6, that both $P(L|R)$ and $P(R|L)$ are conditional probabilities as each refers to the probability of one event occurring given that the other has occurred. In terms of Eq. (3.2) $P(R|L)$ is a special case of conditional probability and is thus also referred to as posterior probability as it is derived directly from evidence or observations of, in this case, rainfall and landslides: i.e. the number of rainfall events that were associated with a

landslide divided by the total number of landslide events. In contrast, $P(L|R)$ is derived from Eq. (3.2) which includes the posterior probability $P(R|L)$ and prior the probabilities $P(R)$ and $P(L)$.

Bayes theorem can be extended to two or more dimensions to consider the probability of a landslide based on the joint likelihood of rain duration and intensity.

The method contains a series of steps:

- Identify rainfall episodes including their duration, amount of precipitation and intensity.
- Identify rainfall episodes that triggered landslides (considering antecedent rainfall).
- Apply Bayes theorem to rainfall events, rainfall duration, antecedent rainfall;
- Apply two-dimensional Bayes analysis to evaluate the joint effect of rainfall duration and intensity on landslide likelihood.

These analyses lead directly to a distribution of thresholds each associated with a conditional probability in terms of $P(L|R)$. The approach proposed by Berti et al (2012) has the advantage of not only producing a conditional probability for a landslide event given a particular level of rainfall, but also of incorporating Winter et al.'s (2007b) proposal to use additional data from rainfall events that do not lead to landslides and to thus increase the available data significantly. While Berti et al. (2012) had data from 1,168 rainfall triggered landslides, they were able to analyse a total of 250,177 rainfall events; at best a few 10s of landslide events are available for analysis in Scotland.

4 Scotland's Rainfall Climate

The climate of Scotland in terms of its rainfall may be very broadly divided into the relatively dry east and the relatively wet west, where almost twice as much rain falls on average each year (Figure 4.1, which shows data for the United Kingdom in its entirety). The trend towards greater rainfall in the more westerly parts is broadly maintained throughout, with the possible exception of the south-east of Northern Ireland. However, what is also important to note is that the areas subject to high rainfall are much smaller, both in absolute terms and by proportion, in the southern part of Great Britain (England and Wales) than in Scotland in the north.

The debris flow events that disrupt the Scottish trunk road network are, in the main, located in the wet west of Scotland, albeit that there are notable exceptions (see Section 5). Winter et al. (2009) present figures comparing those events that occurred nominally in the east to the remainder that occurred in the west and conclude that the combined data sets for each of the east and west occupy broadly the same space on the intensity-duration diagram. Notwithstanding this, it is worthwhile to examine the quite marked contrast in the rainfall between the east and west which is also highlighted, at a site-specific level, in Figure 4.2.

Data presented by the Met Office (Anon, 1989) indicates that in the lowland regions in the east of Scotland, overall annual rainfall levels are relatively low, being broadly comparable with drier parts of England. The monthly average rainfall data for Edinburgh (Figure 4.2), which is broadly representative of the east and one of the driest locations in Scotland, indicates that in the main the monthly variations in rainfall are relatively slight. Notwithstanding this, in the past (Winter et al., 2010) rainfall was generally greatest in the summer months of July and August (1951 to 1980 averages); however the highest rainfall months for 1981 to 2010 averages (Figure 4.2) are January and October. Edinburgh may not be well known for debris flow events but (McAdam, 1993) reported that in 1744 a cloud burst resulted in the erosion of, and associated flow from, the gully below the summit of Arthur's Seat known today as the Guttled Haddie; this feature remains clearly visible. More recently some evidence of debris flow has been examined by the first author in the nearby Pentland Hills, although it should be noted that orographic effects may come into play here.

In the wetter west, maximum rainfall levels are reached during the period September to January (e.g. Tiree in Figure 4.2). Perhaps most marked is the variation in the monthly averages with the driest month of May receiving, on average, less than half of the rainfall experienced in the wettest month of October. Although rainfall levels in the west are relatively low in August, they do increase from a low point in May. It is worth noting that while Tiree shows rainfall levels significantly in excess of those for Edinburgh and Aberfeldy (1,255mm on average per annum compared to 704mm and 1,086 respectively) other locations in the west Scotland experience significantly more rainfall: e.g. Inverinan with around 2,369mm of rainfall on average per annum (Figure 4.2). Such average values mask large annual variations. Barnett et al. (2006a; 2006b) indicate that the annual average rainfall for the west of Scotland varies between around 1,200mm and 2,100mm for the period 1914 to 2004, equivalent figures for the east of Scotland indicate an equivalent range of between around 770mm and 1,450mm; such figures can of course mask significant variations within these areas.

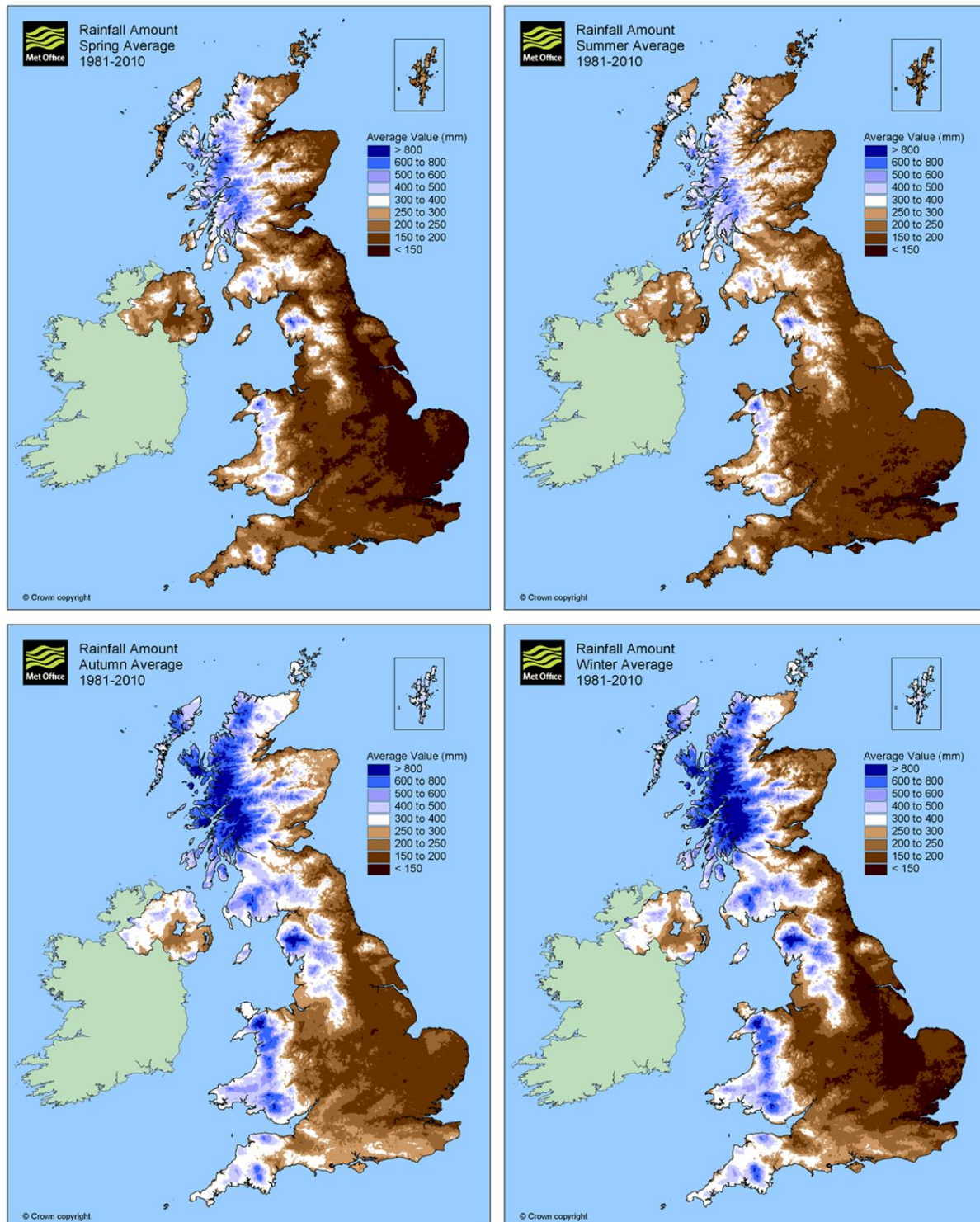


Figure 4.1: Example of Met Office 30-year monthly average rainfall data (1981 to 2010) for the UK for Spring (top left), Summer (top right), Autumn (bottom left) and Winter (bottom right) (images courtesy of the Met Office)

Additionally, the majority of meteorological monitoring stations, including rainfall gauges, are inevitably located in generally more accessible low-lying areas. While developments in remote sensing have seen an increase in the number of observation sites in the more remote areas it remains the case that the station network is sparser in mountainous areas

(McGregor & MacDougall, 2009). It is also the case that the network of observations is designed to meet general synoptic uses and climate monitoring requirements. Rainfall amounts in the higher elevation, mountain areas are usually greater due to orographic effects, albeit that accumulations are likely to be generally higher on the westward-facing, windward, side of Scottish mountain ranges than on the eastward-facing, leeward, side where rain shadow effects may come into play. In broad terms these orographic effects are borne out at the macro scale for Scotland, and the UK as a whole, in Figure 4.1. However, scenarios in both the west and the east indicate that the soil may commence undergoing a transition from a dry to a wetter state at or around August and that in the period October/November to January the soil is likely to be in a wet, if not saturated, state and that rainfall continues to be at relatively high levels. This indicates an increased potential for debris flow and other forms of landslide activity during these periods.

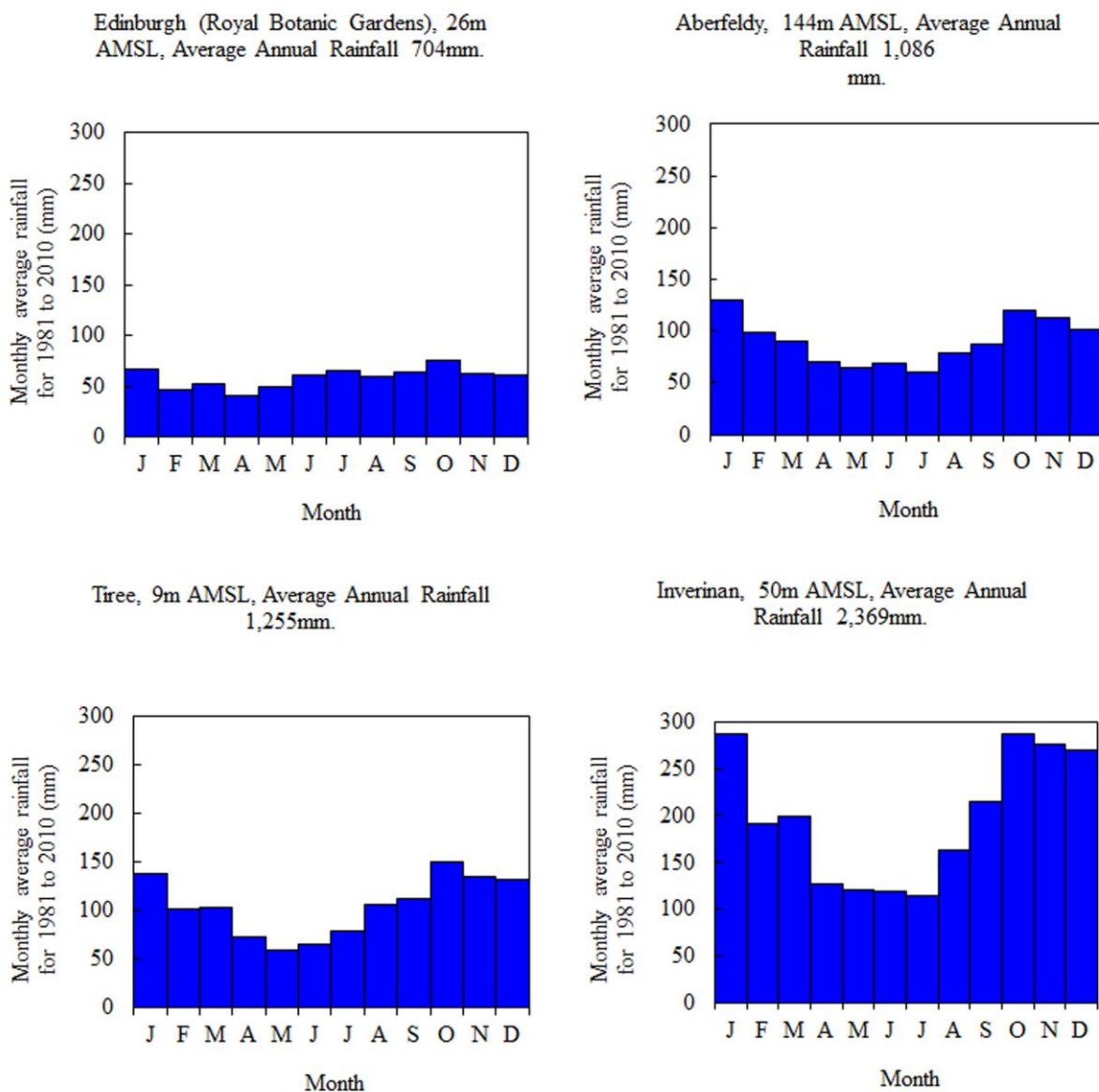


Figure 4.2: Average rainfall patterns for selected locations in Scotland, based upon 30-year 1981 to 2010 averages (data courtesy of the Met Office)

Clearly, the soil water conditions necessary for debris flows may be generated by long periods of rainfall or by shorter intense storms. It is however widely accepted that Scottish debris flow events are usually preceded by both extended periods of (antecedent) rainfall and intense storms (e.g. Winter et al., 2009; 2010).

4.1 Recent Trends and Future Change

It is instructive to consider not only the predictions for future climate change but also what trends may be observed in the climate of the recent past. Work by the Met Office (Barnett et al., 2006a; 2006b) describes trends in climate across Scotland during the last century. The figures presented (for 1914 to 2004) indicate a small increase in the running average annual rainfall for the north and, particularly, the west of Scotland while figures for the east of Scotland are broadly stable.

Interestingly the 30-year averages for Edinburgh and Tiree, where data from the same locations are available, show that the 1981 to 2010 averages are around 12% to 13% higher than those reported (Anon., 1989; Winter et al., 2010) for 1951 to 1980. These increases may well be due to improved gauge measurement accuracy and must be taken in the context of just two stations. Indeed, while the Met Office has observed an increasing trend in rainfall across Scotland the reasons behind the observed trend is an area of ongoing research. The *State of UK Climate Report* has been published annually since 2014 (Kendon et al. 2015; 2016; 2017; 2018) and therefore will, in time, provide the latest information about UK climate and trends.

Examining the available climate change data (Winter & Shearer, 2013) suggests that this is likely to be part of an ongoing trend with increased rainfall during the winter months seemingly likely to increase the prevalence of landsliding in Scotland, particularly in the context of the likelihood of more intense rainfall events. The reduced soil moisture during the summer, as a result of both predicted temperature increases and rainfall decreases, could potentially persist through the early part of autumn depending upon precisely when the transition from a dry to a wet state occurs; this may mean that the short-term stability of some slopes, particularly those formed from granular materials, may be enhanced by the suction pressures that may develop in such conditions. However, although climate models are not best suited to predicting storm events, the available evidence for climate change does point to an increase in such short duration, high intensity rainfall events, even in summer. Soils under high levels of suction are vulnerable to rapid inundation (Toll, 2001), and a consequent reduction in the stabilising suction pressures, under precisely the conditions that tend to be created by short duration, localised summer storms.

5 A Tentative Trigger Threshold

The rainfall gauge network in Scotland is sparse in areas of interest for debris flow forecasting, not least as the primary function of meteorological observation stations is the collection of synoptic data; simple rainfall stations are more usually used for specific purposes related to water resources and hydroelectric power, for example. In addition, while the rainfall radar system covers some of the areas of interest at a resolution of 2km, many are resolved at just 5km, sufficient for the primary function of the weather radar network in monitoring precipitation patterns and their movement as input to general weather forecasting. Additionally, issues surrounding the performance of radar rainfall in mountainous, and indeed other areas, appear to be some way from being fully resolved. Roberts et al. (2009) state, in relation to an analysis performed in an area with 5km radar resolution, that "... rainfall amounts estimated by the [UK] radar network were generally less than those measured by gauges [at the same locations] and distributed somewhat differently".

Nonetheless work was undertaken and reported (Winter et al., 2009; 2010) to develop a rainfall threshold for debris flow potential from analyses of rainfall data, from the pre-existing rainfall gauge network and rainfall radar, in the lead up to debris flow events. This work is summarised and updated with new data in this section. The events were selected on the basis that they:

- 1) Caused disruption at a known location on the road network.
- 2) That the date and time at which they occurred were known with a reasonable degree of certainty, although in some cases the timing of the peak rainfall was taken as the event time in the absence of any direct observation.
- 3) That there was good coverage of the site by rainfall data from both gauges and radar.

It proved possible to identify 16 events that met these conditions (Table 5.1; Figure 5.1). Some of the events were known in detail while others were recommended for analysis by colleagues within both Government and the private sector. Not all of the events can be described in detail although Winter et al. (2006) were able to describe the events of August 2004 in detail and Milne et al. (2009) supplement those descriptions of the events at A85 Glen Ogle. Discussions at the time of selection indicated that most of the events follow the pattern of relatively small slides into existing stream channels which then through consequent erosional activity became debris flows. The primary exception is the series of events at the A9 in August 2004, the triggers for which were erosional rather than sliding (Winter et al. 2006).

Table 5.1: Summary of information for analysed events

| Event location | Date | National Grid Reference and Road Number | Daily Rain Gauge Locations (Distance in km and direction from landslide location) | | | Hourly Rain gauge location | Maximum hourly rainfall, mm (gauge) | Time and date of maximum rainfall (gauge) | Maximum hourly rainfall, mm (radar) | Time and date of maximum rainfall (radar) |
|-------------------------------------|----------------|---|---|-------------------------------|-------------------------------|----------------------------|-------------------------------------|--|-------------------------------------|---|
| | | | 1 | 2 | 3 | | | | | |
| 1. Loch Carron, Stromferry Bypass | October 2001 | NG 910 373: A890 | Loch Carron (2.7 NNW) | New Kelso (6.4 NNE) | Plockton (11.5 WSW) | Lusa, Skye (24.0 SW) | 3.6 | 10:00, 30/10 | 5.8 | 15:00, 29/10 |
| 2. Glen Croe, Rest and be Thankful | January 2003 | NN 235 071: A83 | Lochgilphead (6.5 SSW) | Clachan Pwr St (7.2 NW) | Inveruglas (8.8 ENE) | Sloy (9.0 ENE) | 5.4 | 04:00, 25/1 | 6.7 | 04:00, 25/1 |
| 3. Glen Croe, Rest and be Thankful | November 2003 | NN 234 072: A83 | Lochgilphead (6.5 SSW) | Clachan Pwr St (7.2 NW) | Inveruglas (8.8 ENE) | Sloy (9.0 ENE) | 7.4 | 09:00, 29/11 | 10.5 | 11:00, 29/11 |
| 4. Glen Croe, Rest and be Thankful | January 2004 | NN 235 070: A83 | Lochgilphead (6.5 SSW) | Clachan Pwr St (7.2 NW) | Inveruglas (8.8 ENE) | Sloy (9.0 ENE) | 3.0 | 18:00, 18/1 | 5.4 | 18:00, 18/1 |
| 5. Laide, Wester Ross | February 2004 | NG 901 924: Unclassified | Sand 2 (1.2 SE) | Aultbea (5.6 WSW) | Poolewe (11.3 SSW) | Aultbea (5.6 WSW) | 4.6 | 06:00, 5/2 | 2.7 | 06:00, 5/2 |
| 6. Glen Kinglas | August 2004 | NN 208 096: A83 | Clachan Pwr St (3.7, NNW) | Glenfyne Lodge (6.0, N) | Lochgilphead (8.0, S)*(1) | Sloy (11.3, E) | 9.4 | 22:00, 8/8 | 13.7 | 22:00, 8/8 |
| 7. Cairndow, Glenfyne | August 2004 | NN 186 115: A83 | Clachan Pwr St (1.8, NNE) | Glenfyne Lodge (5.3, NE) | Allt na Lairige (8.6, NE)*(2) | Sloy (13.6, E) | 9.4 | 22:00, 8/8 | 14.1 | 22:00, 8/8 |
| 8. N of Dunkeld, Perth | August 2004 | NO 005 443: A9 | Inver No.2 (2.5, SSE) | Meikle Tombane (7.0, SW) | Balinluig (9.4, NNW) | Faskally (17.8 NNW) | 17.6 | 12:00, 9/8 | 13.1 | 12:00, 9/8 |
| 9. Glen Ogle, Lochearnhead | August 2004 | NN 573 266 and NN 576 262: A85 | Killin, Monemore (5.6, N) | Strathyre S. Wks. (10.0, S) | Ardalnaig (18.1, NE) | Tyndrum #3 (21.4, W) | 6.2 | 11:00, 18/8 | 12.7 | 17:00, 18/8 |
| 10. Pitcalnie, Easter Ross | August 2004 | NH 804 722: U150A | Tain Range (10.9, N) | Gleanies House (11.5, NE) | Hill of Fortrose (16.6, SSW) | Tain Range (10.9, N) *(3) | 12.8 | 04:00, 19/8 | 5.7 | 02:00, 19/8 |
| 11. Eathie, Black Isle | August 2004 | NH 775 643: U231 | Hill of Fortrose (8.3, SSW) | Nairn, Dunbar (13.9, ESE) | Tain Range (19.3, NNE) | Tain Range (19, NNE) | 4.0 | 16:00, 18/8 and 05:00, 19/8 | 4.1 | 01:00, 19/8 |
| 12. Avoch-Fortrose, Black Isle | October 2004 | NH 717 559: A832 | Hill of Fortrose (1.9, NE) | Allangrange Hse (9.5, WSW) | Inverness (10.8 SSW) | Tain Range (29.0, NNE) | 5.6 | 08:00, 21/10 | 3.8 | 07:00, 21/10 |
| 13. Cnoc Fhionn, Shiel Br., Glenelg | December 2004 | NG 876 198: C46 | Nostie (7.8, NNW) | Achnagart (9.7, ESE) | Plockton (15.4, NNW) *(4) | Skye Lusa (17.7, WNW) | 5.6 | 07:00, 6/12 | 5.8 | 11:00, 6/12 |
| 14. Letterfinlay, Loch Lochy | January 2005 | NN 250 912: A82 | Clunes Forest (5.3, WSW) | South Laggan #3 (7.2, NE) | Braeroy Lodge (8.7, E) | Tulloch Br (16.3, SE) | 5.0 | 19:00, 6/1 | 8.0 | 03:00, 7/1 |
| 15. Inverinate-Morvich | September 2005 | NG 944 212: U152W | Achnagart (6.3, SSE) | Plockton (18.6, NW) | None | Skye Lusa (24.0, W) | 15.6 | 17:00, 13/9 | 7.5 | 16:00, 13/9 |
| 16. Kylerhea Glen, Skye | September 2005 | NG 775 208: C72 | Skye Lusa (8.0, WNW) | Broadford, Rockbank (12.5, W) | Plockton (12.0, N) | Skye Lusa (8.0, WNW) | 15.6 | 17:00, 13/9 | 5.0 (4.6) | 09:00, 13/9 (16:00, 13/9) |

Timing for hourly rain gauge and radar maxima is for hour-ending.

Additional rain gauge information: (1) Allt Na Lairige (8.7, NNE); (2) Lochgilphead (10.0, S); (3) Kinloss (30.0 ESE); (4) Skye Lusa (17.7, WNW).

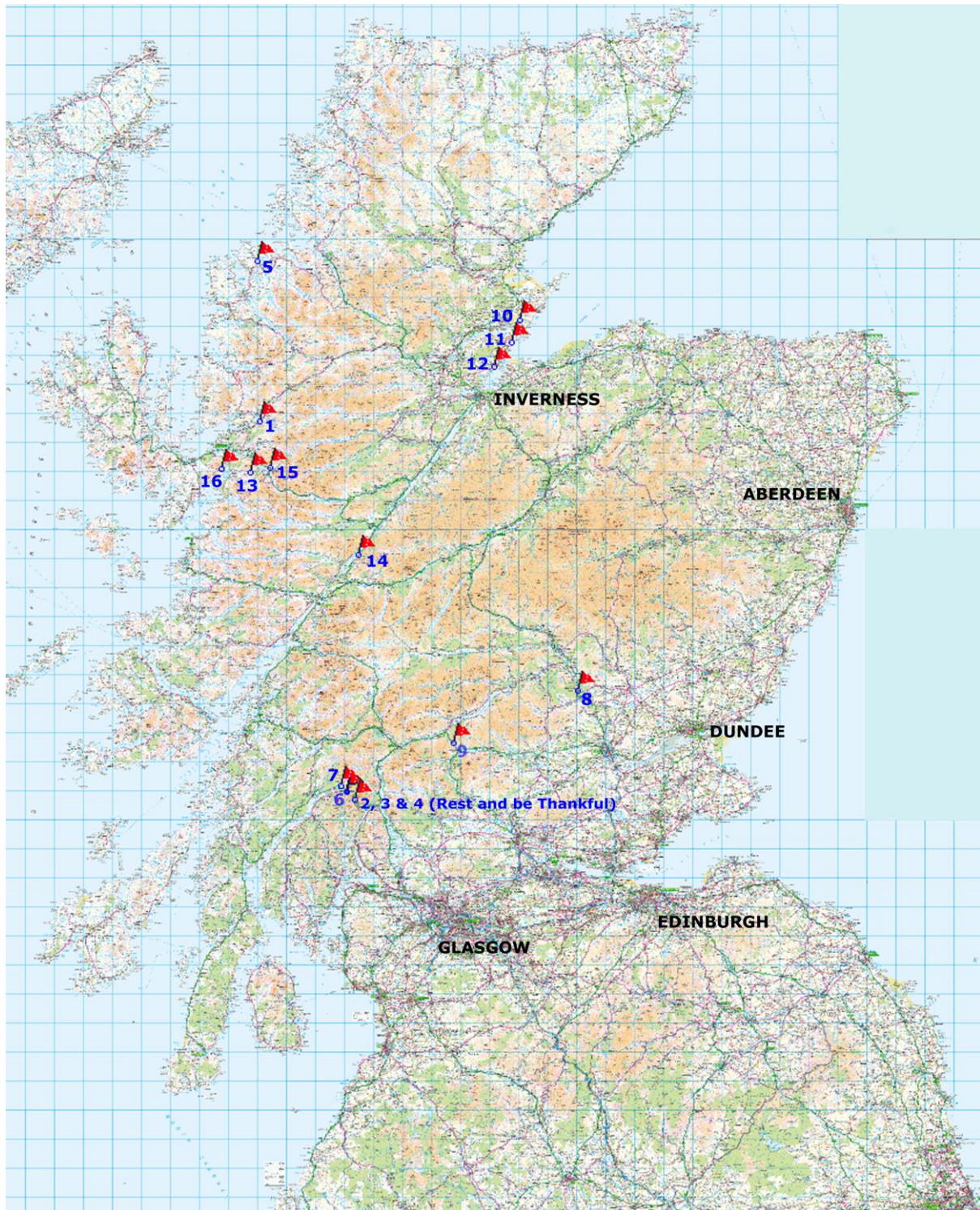


Figure 5.1: Map of mainland Scotland (omitting the south-west) showing the location of the events listed in Table 1. Locations 6 and 7 represent the events at the A83 Glen Kinglas and north of Cairndow (9 August), Location 8 represents the events at the A9 to the north of Dunkeld (11 August) and Location 9 the events at the A85 at Glen Ogle (18 August). Locations 2, 3, and 4 represent events at the Rest and be Thankful, events from which area have also been used to help validate the threshold

The analyses considered both short duration and extended antecedent periods and tested analytical methods that could have an application to forecasting similar events in the future. The work thus included the following activities:

- Extraction of comprehensive data sets of rainfall from rain gauge and radar sources for each of the 16 events.
- Analysis of the data in order to make graphical representations for each of the 16 events:
 - Cumulative antecedent rainfall data over 150 days from standard UK Met Office daily rainfall gauges. (Note that 150 days was used in the analysis to ensure that all relevant rainfall was included therein.)
 - Accumulated storm rainfall and intensity for a period of 18 to 24 hours leading up to the time of the event using both radar and hourly rain gauge data.
 - The relations between intensity and duration for the combined storm and antecedent periods, to compare the intensity-duration relations for individual events and also on a seasonal and geographical basis.
- Preparation of a spreadsheet for analysis of future events ('Future Back Analysis'), based on the methods for data manipulation and analysis above, in order to simplify and increase the speed of the analysis response to events.

5.1 Results and Interpretation

This section summarises the analyses of the 16 events, more detailed results and associated discussion are given by Winter et al. (2009).

The following rainfall information was extracted:

- 1) Daily rainfall from the three stations closest to the location of the landslide, for a period of 150 days prior to the event. The distance and bearing of the gauge from the landslide location was obtained.
- 2) Hourly rainfall from the tipping bucket rain gauge (TBR) closest to the landslide location for the four to five day period covering the time of the event. Distance and bearing information was also given.
- 3) Radar measurements of rainfall intensity at intervals of five minutes (for 2 km pixels) or 15 Minutes (5 km pixels) for the pixel square that includes the landslide location, covering a period of two to three days up to and including the storm event.
- 4) Radar measurements of rainfall intensity for a three by three array of pixels, which includes the debris flow location pixel at its centre.

Analyses for the specific storm event, covered an 18-hour period, and an antecedent period of 150 days prior to the event.

Ideally, the storm rainfall information should be analysed back from the point in time when the landslide occurred, the assumption being that this time marks a point when either an intensity or accumulation threshold was reached which caused the landslide process to occur. This timing information was not known precisely for all events, so an initial time had

to be chosen from the period of most intense rainfall, using the hourly rainfall data from the relevant TBR, or if the TBR was some distance from the landslide location (sometimes in excess of 20 km), the hourly radar rainfall record at the radar pixel covering the landslide location was used.

Details of storm rainfall depth and intensity were determined using the radar data from the pixel containing the landslide location. Although there are a number of ways in which errors can arise in radar rainfall estimation and these are discussed earlier in this section, it is considered that in the absence of proximal TBR(s) that using radar represents a consistent approach, and will not, like non-proximal TBR data, introduce problems of variable gauge locations, intervening topography, and movement in the rain producing system. The analysis of the antecedent daily rainfall, using cumulative rainfall totals over fixed periods prior to the date of the landslide event, was made from the rain gauge nearest the landslide location. Where this gauge had missing data, the data set for the next nearest rain gauge was used.

In terms of understanding how rainfall may cause debris flow, groups of plots for intensity-duration were examined for summer and winter events (Figure 5.2), and for events that occurred in the eastern and western parts of Scotland (Winter et al. 2009). The most important observation is that all of the different groups of data sets (e.g. summer and winter, and eastern and western) broadly occupy the same area on the intensity-duration diagrams and that there is thus no compelling case for different thresholds on either a seasonal or geographical basis. It is thus appropriate to combine the intensity-duration data for the 16 events onto a single diagram (Figure 5.3).

As expected there is considerable scatter in the data. However, once 'outlying' data points are removed from consideration (Winter et al. 2009) then a reasonably clear tentative trigger threshold can be drawn (Figure 5.3). While the removal of such points may or may not be justifiable on a statistical basis it is important to understand that the development of the threshold is not a data-fitting exercise. In contrast, the driver for the work is the development of a practical tool which does not trigger at a very low rainfall level that might only occasionally lead to debris flow. Indeed, there is a strong suspicion that the rainfall preceding the 'outlier' data from Events 5 and 12, which correspond to falling rainfall intensities, may have been sufficient to lead to the event. In the case of the 'outlier' data from Event 13 there were some doubts regarding the timing of the event from the outset and the available rainfall data was from relatively distant stations which may have been less than representative of the rainfall at the event location.

As noted earlier the maximum rainfall event duration of 150 days was used to ensure that all relevant rainfall as captured within the analysis. Now that the threshold has been drawn (and tested, see Section 5.4) it seems likely that the inflection point towards the right-hand end of the line in Figure 5.3 (288 hours or 12 days) defines the maximum duration of the rainfall that leads to debris flow. It also seems likely that the inflection point (at 2 hours) towards the left-hand end of the threshold in Figure 5.3 defines the time before an event which broadly corresponds to the point in time at which an event becomes inevitable (i.e. the condition of the soil has already reached a point at which movement is inevitable and that in this short period in the immediate run-up to the event rainfall may be less important than infiltration). If both of these assertions prove to be correct then this would mean that the threshold would be presented in an entirely linear fashion which, notwithstanding the

slightly ‘s’-shaped curve presented by Flentje & Chowdury (2006), is generally more reflective of findings from other parts of the World (Winter et al. 2009). For context it should be clear that breaching the intensity threshold at, say, a duration of 200 hours is not necessarily indicative of a landslide occurring. At such lengthy durations the threshold is likely to need to be breached at much lower durations. However, what it is indicative of is that the ground is more pre-disposed to landslide triggering and less intense storms are likely to be required to trigger an event.

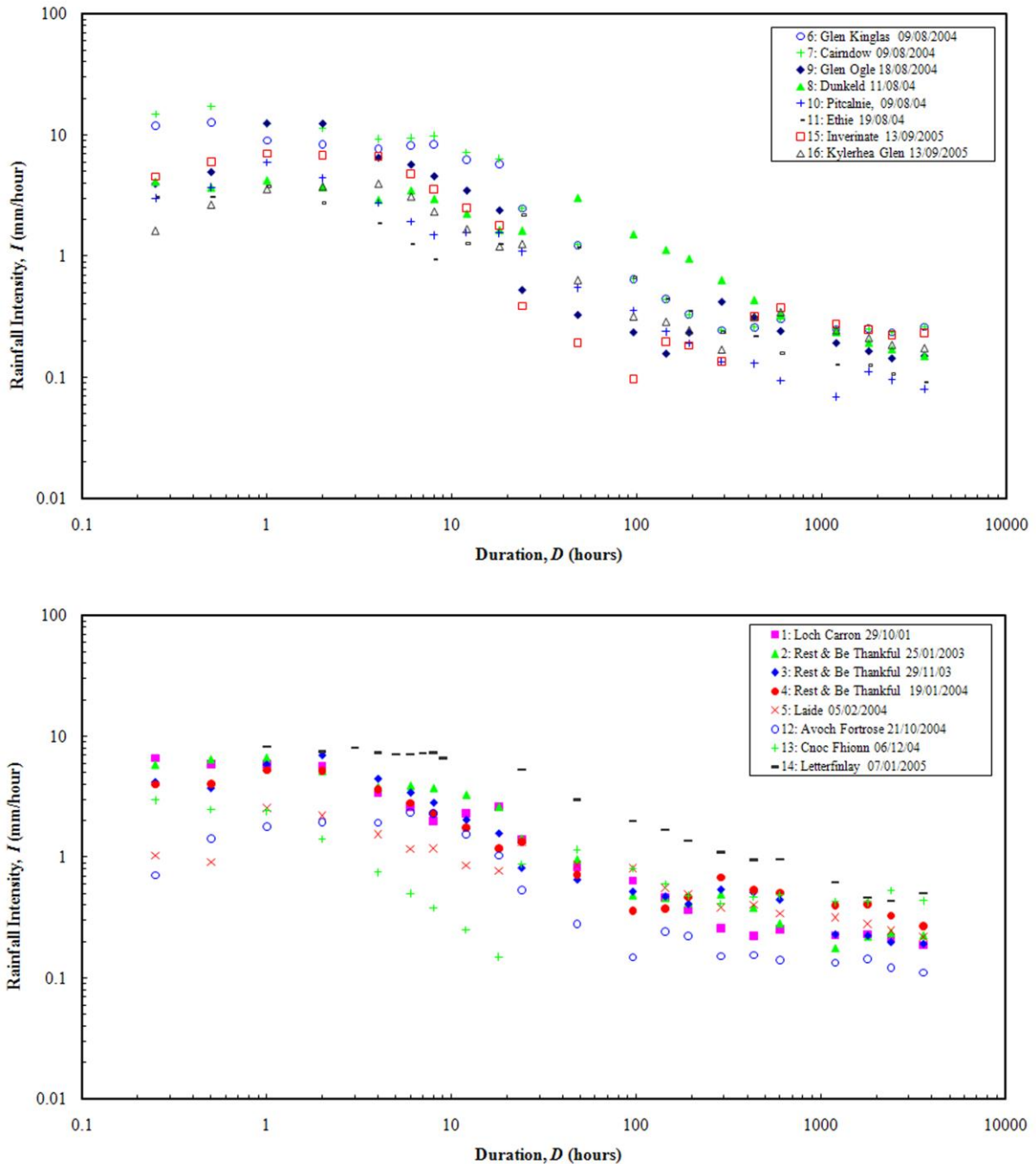


Figure 5.2: Intensity versus duration data for the 16 debris flow events presented for (top) Summer events and (bottom) Winter events

It seems clear that the threshold is generally low. Indeed, and to illustrate this point, it is not too dissimilar to those reported by Cannon et al. (2008) for debris flow in ash resulting from wildfires for which low thresholds have been established. There are a number of possible reasons for this:

- 1) That the mechanisms represented in Cannon et al.'s (2008) data are different. Certainly their thresholds are much more focused upon short-term storm events with a period of up to around 12 hours, while the rainfall analysis reported here stretches out to 3,600 hours (150 days) the true antecedent period is more likely to be around 12 days (288 hours) (see above).
- 2) That the materials that initiate debris flows in Scotland, often very wet and weak amorphous peat, are highly susceptible to rainfall-induced movement. (This is not such an issue at the Rest and be Thankful site that forms the focus of Section 6.)
- 3) The rainfall data used is not entirely representative of that experienced at the location of the debris flow event. Certainly the distance between the rainfall gauges used in the analysis and the actual debris flow events ranges between 1.2km and 29km.

These observations emphasise the importance of the threshold testing and validation work.

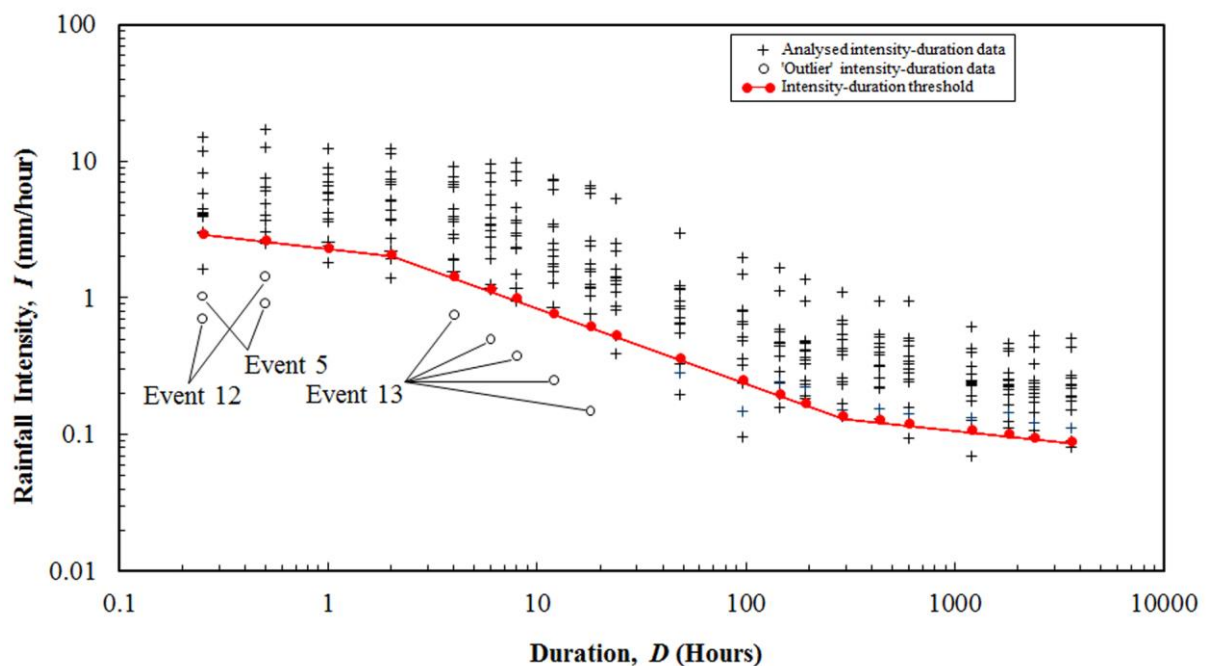


Figure 5.3: Combined plot of intensity versus duration data for the 16 debris flow events showing the tentative trigger threshold

5.2 Testing and Using the Threshold

Clearly the tentative threshold required validation and/or development using data derived from later events. These analyses were intended to test the efficacy of the threshold using data from events that post-date the development of the threshold. Winter et al. (2009; 2010) presented initial data and in Figure 5.4 this, along with additional previously unpublished data, is presented.

Testing of the threshold was undertaken using the results of the analyses of rainfall that led to debris flow events at the A83 Rest and be Thankful between October 2007 and February 2012. The form of analysis was the same as that used to develop the tentative rainfall intensity-duration threshold. The important difference being that these analyses were carried out after the threshold had been determined, thus providing a degree of validation to the threshold. The new and old data are illustrated in Figure 5.4.

For most of the events the data plot above the threshold for most of the antecedent period, but then between one and two hours preceding the event the data plot below the threshold. This may mean that sufficient rainfall had already fallen by this point for the debris flow to be inevitable (see also Section 5.1).

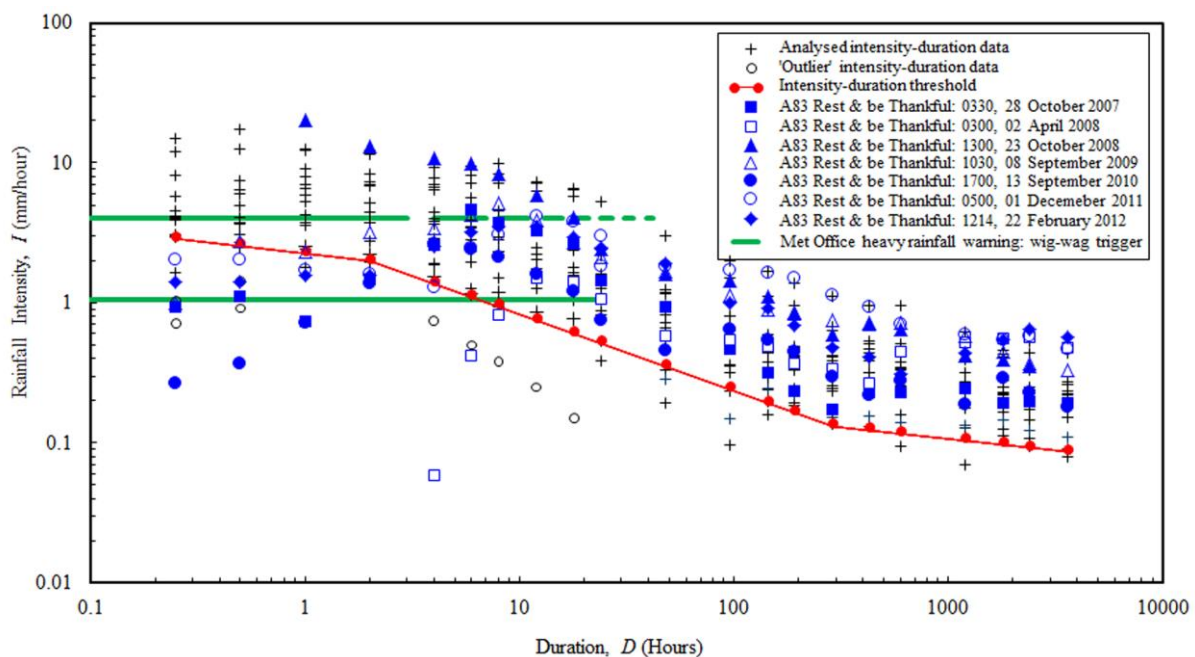


Figure 5.4: Tentative trigger threshold for Scottish debris flows in terms of rainfall intensity-duration showing events at the Rest and be Thankful that have been used for validation purposes. The wig-wag heavy rainfall warning triggers are also shown

The 2 April 2008 event, at an estimated time of 0300 hours, and 23 October 2008 event, at around 1300 hours (Figure 5.4), exhibit slightly different patterns. The 2 April 2008 event appears to have been driven by rainfall that occurred prior to around 10 to 12 hours before its occurrence and is thus more strongly related to antecedent rainfall. The data for the 23 October 2008 event, in contrast, sits well above the tentative threshold until around one hour before the event thus indicating a relatively large storm.

The inflexion points in the data at 288 hours (12 days) and at 2 hours lend weight to the earlier, tentative, assertion that these are correspondent with the effective antecedent period (i.e. earlier rainfall may have limited influence upon subsequent debris flow events) and the point beyond which debris flow becomes inevitable.

Notwithstanding the foregoing, simpler, single- or dual-period forecast thresholds (primarily the forecast 24-hour rainfall level) have been used to determine periods of higher risk from debris flow and to thus determine times when wig-wag warning signs should be switched on

to alert drivers of this elevated risk at the Rest and be Thankful. Figure 5.4 illustrates these heavy rainfall warnings as either:

- rainfall accumulation of 25mm in a 24 hour period, or
- rainfall expected to fall at a rate of 4mm/hour or more, giving a total of 12mm or more within 3 hours.

While these triggers are derived from the Met Office heavy rainfall warning system, careful comparison was undertaken prior to implementation and the close relation between the '25mm in a 24 hour' period and the trigger threshold can be clearly seen in Figure 5.4. An evaluation of the use of the wig-wag signs (Winter et al., 2013b; Winter & Shearer, 2017) suggests that around 90% of events occurred when the signs were activated. There were, however, at least two instances of 'false negatives' being indicated when landslides occurred when the wig-wags were inactive. Further a significant number of 'false positives' was reported (Winter et al., 2013b; Winter & Shearer, 2017), broadly correlating with the wig-wags being switched on seven times for each landslide event. Comparison of the threshold in Figure 5.4 with similar thresholds from other parts of the world indicates that it may underestimate the amount of rainfall required to trigger debris flows (Figure 3.2). Indeed, the work by Cannon et al. (2008) on debris flow triggering in areas that have been subject to wild fires appears to support this. In such areas debris flows are generally considered to trigger with relatively little rainfall due to the hydrophobic nature of the ash left after the fires. The tentative rainfall threshold for Scotland suggests triggering at lower rainfall levels than those that would be expected to trigger debris flow in areas subject to wild fires (Figure 3.2). Notwithstanding this the rather short duration of the threshold for wildfires in Figure 3.2 also indicates that these events are caused by short duration/high intensity rainfall with relatively little influence from longer duration/lower intensity (antecedent) rainfall.

The intention was that once a validated threshold was available, with any suitable adjustments made, it would be possible to set both 'Wake-Up' and 'Warning' thresholds (Figure 3.1). In viewing such data from events that occurred in the past (e.g. Figure 5.5) there is a tendency to view it from a position close to time, $t=0$ (although as the scale is logarithmic this is simply a very low number), which is broadly equivalent to the actual time of the event. However, when such data is used in the form of a threshold for forecasting purposes then it must be viewed as if from a point in time that precedes the event.

It was suggested (Winter et al. 2010) that the 'Wake-Up' be viewed from a point that is a maximum of three days ($t=72$ hours) in advance of any potential event, with the 'Warning' being viewed from a point half of one-day ($t=12$ hours) in advance, again as a maximum, and actual event threshold being observed from the point of view of a very short time in advance of any actual event. These viewpoints are illustrated in Figure 5.5 (which is based upon Figure 3.1) with the threshold observation point being set at time, $t=6$ hours. These timings have been assigned very much on an initial basis and require further work prior to the finalisation of a fully-developed threshold suitable for implementation.

It was anticipated that forecasts and warnings might be issued up to a few hours in advance of an event, the temporal extent of the tentative threshold being simply a means of reaching the point at which a forecast may be made.

The intention remains that, once sufficient confidence in the use of the threshold has been established, that the system be introduced to practical trial forecasting of debris flow events as part of the debris flow risk management procedure in the A83 Rest and be Thankful area using the full threshold rather than selected points as is done for the wig-wag warning signs. If that proves successful, its introduction to the broader north-west region of Scotland for other areas prone to rainfall-induced debris flows can be considered.

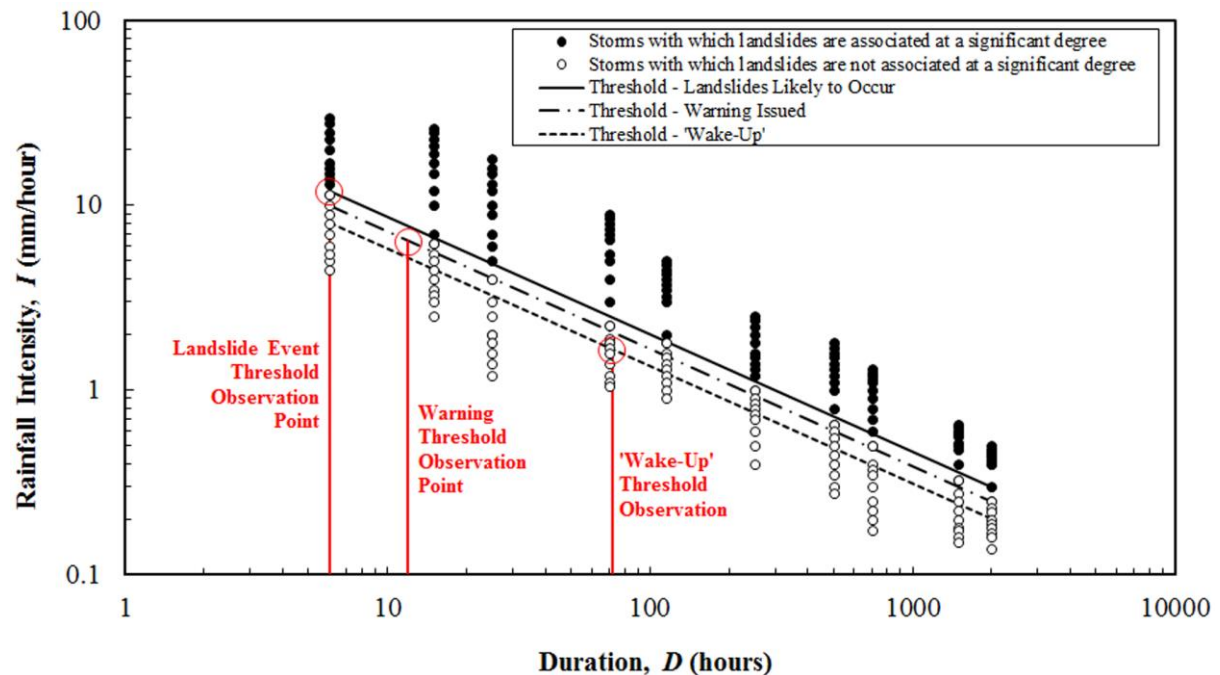


Figure 5.5: Hypothetical rainfall intensity-duration threshold for landslides, illustrating observation points for the different thresholds, described in Figure 3.1 may be used

The A83 Rest and be Thankful locality is known for the frequency with which debris flow events occur, which is much more than any on other part of the trunk road network in Scotland. It is thus well-suited to the use of temporal warnings such as the wig-wags signs. However, the much lower frequency of events at other sites suggests that the potential application of such direct and site-specific warnings is limited and that any proposals should be the subject of detailed location-specific assessment (Winter et al., 2013b; Winter & Shearer, 2017). The application of broader regional forecast-type warnings may be applied more widely although a trial period for such warnings is likely to be advisable.

6 Development of a Probabilistic Threshold

It can be difficult to justify expenditure on discrete analyses of rainfall that does not lead to debris flow, 'non-events'. However, analysis of data from a period of a year or more places a rather different complexion on this scenario as it is a relatively straightforward exercise to include rainfall events that both lead to and do not lead to debris flows.

Two rainfall gauges were installed, as part of a trial, on land close to the A83 at the Rest and be Thankful (Figure 6.1): close to the Rest and be Thankful car park (National Grid reference NN 22835 06967) and on the hillside to the northeast of Loch Restil (NN 23249 08496). This site is one of the most active debris flow areas in Scotland (see Figures 2.2 and 2.3) and is part of the major road network most frequently affected. This area can be defined in a number of ways but in essence it is the hillside to the east of the A83 trunk road along a near-7km length between Ardgartan and the Rest and be Thankful car park (Figure 6.1). However, by far the greatest hazards affect the southwest facing slopes of Beinn Luibhean which border the A83 for a distance of approximately 1.7km (Wong & Winter, 2018).

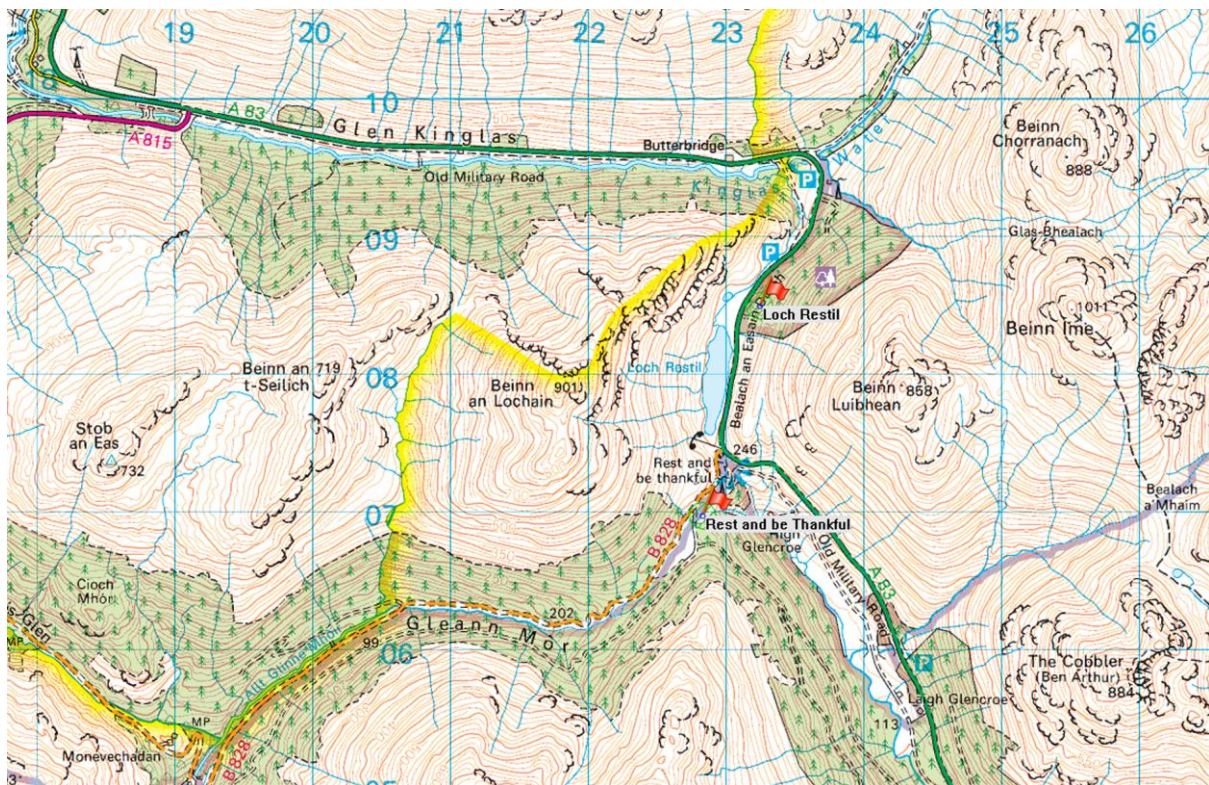


Figure 6.1: 1:50,000 Ordnance Survey map showing the position of the two rainfall gauges installed in the vicinity of the A83 Rest and be Thankful. Reproduced by permission of the Ordnance Survey, on behalf of HMSO, © Crown copyright and database rights, 2019. All rights reserved. Ordnance Survey Licence number 100046668

The potential to develop a rainfall threshold on a probabilistic basis and using rainfall data that both leads and does not lead to debris flows is described in Section 3. The installation of rain gauges in the area of the A83 Rest and be Thankful means that many of the previously expressed concerns regarding the applicability of the available rainfall data (see Section 5) are of very much less concern.

Data on debris flow events in the area between Ardgartan and Cairndow has been collected for the period between 29 April 2012, when the gauges were activated, and 27 March 2018, the date for which the most recent rainfall data was available when the analysis commenced (Table 6.1).

Table 6.1: Debris flow events between April 2012 and March 2018 in the A83 Rest and be Thankful area (extended and from Winter & Shearer, 2017)

| Time | Date | Event Description |
|---------|---------------------------|---|
| 20:00 | 22 June 2012 | A failure raft from a previous translational failure at the Rest and be Thankful was observed to be breaking up high on the slope. The event did not reach the carriageway. |
| Unknown | On or before 29 June 2012 | This relatively small debris flow did not reach the road although some small boulders did (this event may have occurred on 29 June or earlier) on the easterly approach to the Rest and be Thankful. |
| 16:00 | 01 August 2012 | A significant event on the easterly approach to the Rest and be Thankful. |
| 07:15 | 19 November 2012 | A significant event on the easterly approach to the Rest and be Thankful. |
| 07:00 | 03 October 2013 | A significant event in Glen Kinglas and Rest and be Thankful. Old Military Road used as detour. |
| Unknown | 09 January 2014 | A small volume of material (<2.5m ³) was successfully collected in the Phase 9a barrier with further material diverted toward the neighbouring catch pit (as per the design intention). Material did not reach A83. |
| 16:45 | 15 January 2014 | Rest and be Thankful. Shallow translational failure below debris flow barrier, approximately 90t reached carriageway. |
| 11:30 | 23 February 2014 | Glen Kinglas/Honeymoon Bridge, debris flow reached forestry car park but not the A83. |
| 01:35 | 06 March 2014 | Rest and be Thankful, deposits reaching both lanes of the A83. |
| 12:15 | 06 October 2014 | Glen Kinglas, a debris flow that washed a small amount of fines onto the road. |
| 06:30 | 28 October 2014 | Rest and be Thankful (and Glen Kinglas), the first significant 'live' test of the debris fences at the Rest and be Thankful. |
| 11:20 | 15 January 2015 | Small events at Rest and be Thankful and Glen Kinglas, no debris reported to have reached road. |
| 10:00 | 07 March 2015 | Slip below A83. |
| 08:18 | 11 November 2015 | Rest and be Thankful, contained by fence and did not reach A83. (There were two further events reported in November 2015 but neither date nor time are known so cannot be analysed.) |

Table 6.1: (... Continued). Debris flow events between May 2012 and March 2018 in the A83 Rest and be Thankful area (after Winter & Shearer, 2017)

| Time | Date | Event Description |
|-----------------|------------------------|--|
| 10:08 | 05 December 2015 | Rest and be Thankful, three events arrested by fences. |
| 07:40 | 30 December 2015 | Rest and be Thankful, arrested by fence. |
| 18:30 to 07:45* | 01 to 02 October 2017 | Small movement on hillside, did not reach A83. |
| 18:45 to 10:15* | 10 to 11 October 2017 | Small movement on hillside, did not reach A83 and water/debris overflow of the road. |
| 18:00 to 07:45* | 21 to 22 October 2017 | Small movement on hillside, did not reach A83. |
| 14:15 to 07:00* | 01 to 02 November 2017 | Small movement on hillside, did not reach A83. |
| 16:30 to 07:15* | 06 to 07 November 2017 | Reactivation of the 21-22 October 2017 event. |

* The identification of events from late-2014 onwards was aided by the use of time-lapse photography, LiDAR (Sparkes et al. 2017; 2018) and high resolution panoramic photography (Winter et al. 2017) and the associated follow-on arrangements; the precise time of events cannot be determined during the hours of darkness and/or during periods of poor visibility.

This data used in the subsequent analyses is derived from:

- Rainfall data from SEPA rain gauge station located to the south of the B828 near the beginning of the forestry road that traverses the west side of Glen Croe (Station Name: Rest and be Thankful; Station Number: 485490; National Grid Reference: NN 22835 06967, elevation 280m) (data from 29 April 2012).
- Rainfall data from SEPA rain gauge station located to the east of the A83 on the westerly approach to the Rest and be Thankful opposite the northern end of Loch Restil (Station Name: Loch Restil; Station Number: 485489; National Grid Reference: NN 23249 08496, elevation 260m) (data from 29 April 2012).
- The times and dates of debris flow events in the area. This data set is from a variety of sources including from TRL records and BEAR Scotland records which update those used by Winter et al. (2013b) and Winter & Shearer (2017).
- Time-lapse photography for events that occurred in 2017. The precise timing of these events cannot be identified during the hours of darkness and/ or during periods of poor visibility. For these, and the other events with an unknown time, the timing of the event has been estimated by taking the maximum 15-minutes rainfall during the day or period identified.

The debris flow events that occurred during this period are summarised in Table 6.1; Winter & Shearer (2017) provide more detailed narratives relating to the individual debris flow events listed between 2012 and 2015.

6.1 Data

6.1.1 *Rainfall and Landslide Events*

The first step in the development of a probabilistic threshold was to undertake a detailed analysis of the available data that both leads and does not lead to landslides. This was undertaken by the UK Met Office under contract to TRL.

The raw data consisted of 15 minute rainfall totals (mm) and no quality checks had been applied to the data other than scrutiny of the relatively crude quality control marker associated with each value, i.e. either 'U' (not validated), 'G' (good) or 'S' (suspect). Each 15 minute rainfall (mm) total is converted into average rainfall intensity (mm/hour) by multiplying by four so it is assumed that the rainfall in each 15 minute time-slot took 15 minutes to fall which may not always be the case. It is this parameter that is used to determine the antecedent conditions.

Although daily rainfall totals do not strictly form part of the antecedent analysis, it is useful to plot the daily totals (00:00 to 24:00) for the whole period to illustrate the conditions prior to and on the days of landslides at Rest and be Thankful and Loch Restil. These are shown in Figure 6.2 and Figure 6.3 with the rainfall total on the day of the landslide events are shown in red.

Correspondence with Data Quality Assurance team at SEPA (who maintain the rain gauges) and Met Office has highlighted several periods within the 2015 data record which have data issues associated with them.

It is understood that snowfall during January 2015 may have affected the precipitation amounts recorded at the Rest and be Thankful. The data has been retained within the analysis as it provides the best available estimate of the conditions contributing to the landslide on 15 January 2015 may have been augmented in the area. A few values on 13 and 14 January 2017 were also marked as suspect, these were also believed to be due to snowfall, and were excluded from the analysis.

The rainfall is recorded by two gauges at each site, referred to as the 'prime gauge' and the 'check gauge'. If issues are identified with the 'prime gauge', the data for the period affected may be substituted with the corresponding data from the 'check gauge'. During the July 2015, a blockage of the 'prime gauge' at Rest and be Thankful meant that the rainfall data was instead taken from the 'check gauge'.

The 'check gauge' data has also been used to cover a five day period from 14:00 26 November 2015 when the Rest and be Thankful 'prime gauge' was under-reporting the rainfall in the area, identified through 'buddy checks' with local gauges. This time period coincides with antecedent conditions of major landslide event on 5 December 2015.

A further issue developed with the 'prime gauge' at Rest and be Thankful in mid-December with the gauge not recording rainfall values. This 13 day period, from 10 to 22 December 2015, was identified by SEPA and has been excluded from the analysis. This has implications for the calculations of antecedent conditions of the landslide which occurred on 30 December 2015. The handling of the data from 23 December 2015 is discussed in further detail in Section 6.1.2.

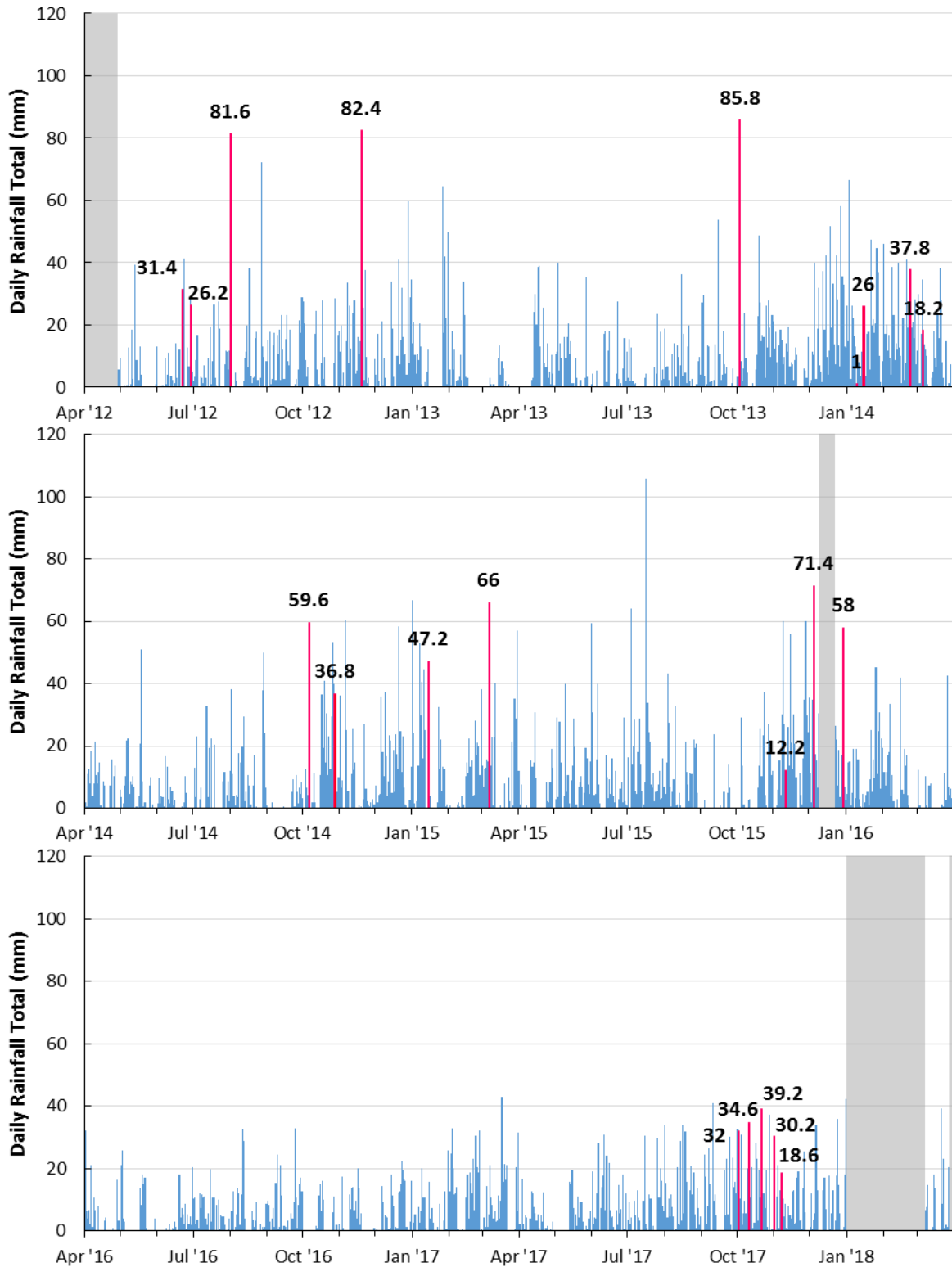


Figure 6.2: Daily rainfall totals (mm from 00:00 to 24:00) at Rest and be Thankful from late-April 2013 to late March 2018. The daily totals on days for which a landslide occurred are shown in red and the associated daily totals marked. The x-axis of each graph is for two years, from 1 April to 31 March the following year

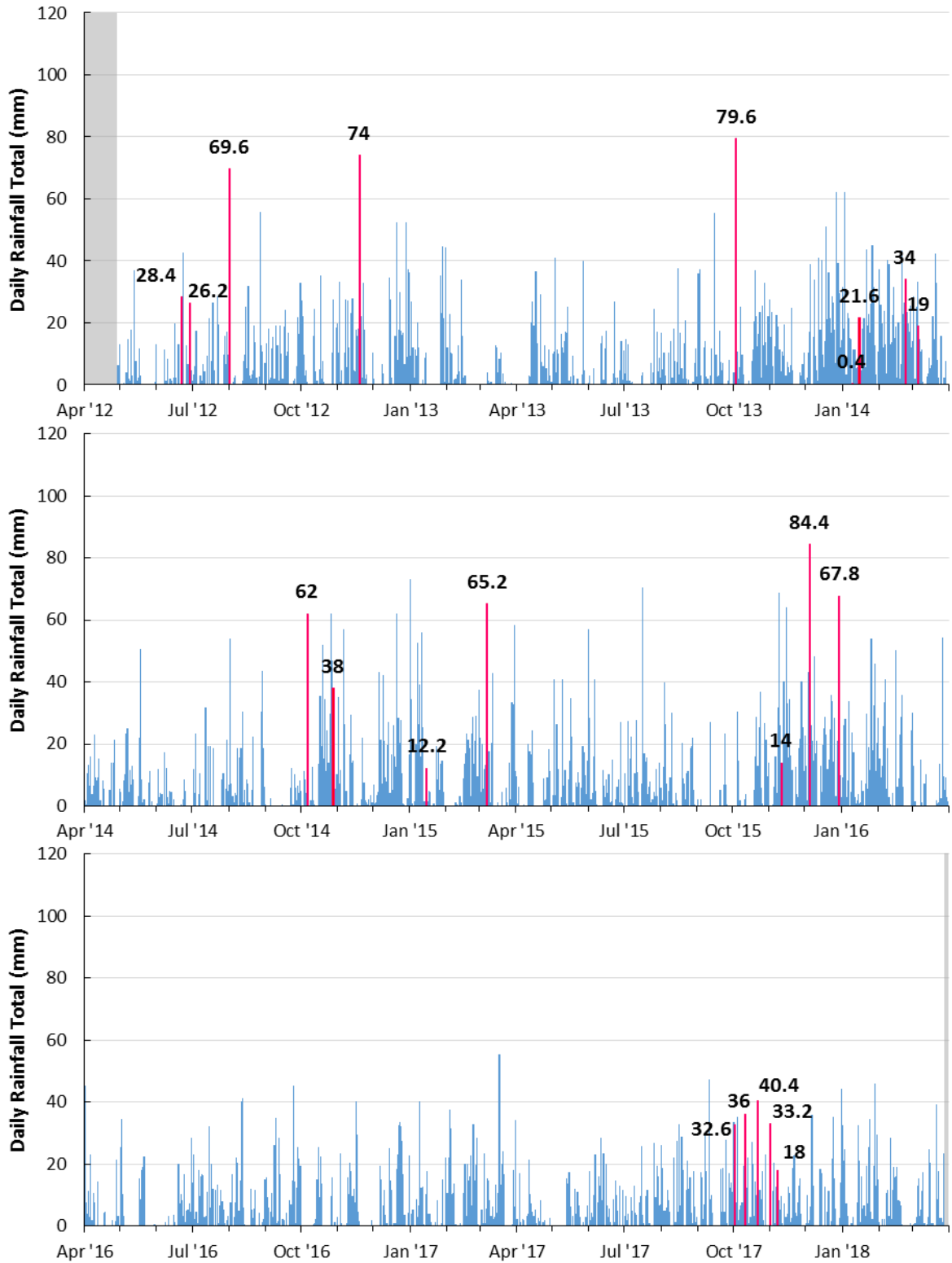


Figure 6.3: Daily rainfall totals (mm from 00:00 to 24:00) at Loch Restil late-April 2013 to late March 2018. The daily totals on days for which a landslide occurred are shown in red and the associated daily totals marked. The x-axis of each graph is for two years, from 1 April to 31 March the following year

Data from the Rest and be Thankful rain gauge is missing for the period 1 January to 7 March 2018; it has not been possible to identify the reason for this.

There is one landslide event that occurred before 02:00 on its recorded day, at 01:35 on 6 March 2014. For this event, the daily rainfall total of the previous day has been highlighted within Figure 6.2 and Figure 6.3. For other landslide events, the daily rainfall total for the day on which the landslide occurred is used.

The following comments about daily rainfall patterns are from the perspective of the use of the Rest and be Thankful gauge (Figure 6.2) as the primary source of rainfall data for the slopes above the A83. The Loch Restil gauge typically experienced similar patterns but less extreme rainfall and being further from the slopes is treated as a secondary rainfall data source. Landslide events usually coincide with either a period of persistently high rainfall (e.g. 1 August 2013), a high daily rainfall total on the day of the events (e.g. 6 October 2014) or both (e.g. 5 December 2015).

For seven of the landslide events, extremely high daily rainfall totals in excess of 50mm occurred on the day of the landslide (three in excess of 80mm). Whilst the midnight to midnight rainfall totals include rainfall which is likely to have occurred after landslide event, landslides almost exclusively happen on days with more than 25mm of rainfall. There are three exceptions to this, two landslide events on 9 January 2014 and 11 November 2015 which both occurred after previous days of high rainfall and one landslide event on 7 October 2017 which occurred as a reactivation of recent a landslide.

It is worth noting that there are seven occasions at the Rest and be Thankful where the daily rainfall totals are greater than 60 mm and no landslide occurs. The highest rainfall total from the time period featured, 105.8mm on 17 July 2015, is not linked to any known landslide event. There are many days in 2015 that contain daily rainfall totals that are similar or exceed those that have previously been associated with any recorded landslides. It is therefore difficult to identify what might have triggered some of the events and why apparently similar or higher rainfall conditions on the other days did not trigger any landslides.

During 2016 and 2017 daily rainfall totals greater than 60mm did not occur. Table 6.2, which shows the mean daily rainfall, highlights that in 2016 the Rest and be Thankful was 31% lower than Loch Restil, whereas in all other years the two sites had rainfall totals within 5% of each other. This raises the question of whether there are any quality issues with the data for this period at the Rest and be Thankful. Table 6.2 also confirms that the years 2016 and 2017 were drier overall than the preceding years of 2014 and 2015. This may explain why there were no landslides reported in 2016. There was a wet period with a succession of moderately high rainfall totals in October 2017 with landslides reported on several of the wettest days during this period.

The period of missing data during December 2015 at the Rest and be Thankful (Figure 6.2) coincides with several days of rainfall at Loch Restil (Figure 6.3), where five days with more than 20mm of rainfall was recorded. It can be assumed from the close proximity of the two sites that the Rest and be Thankful would also have experienced high rainfall during the period of missing data.

A more detailed approach is pursued in the remainder of the report analysing average rainfall intensities up to 12 days prior to all landslide events and non-events.

Table 6.2: Annual mean daily rainfall for each location

| Year | Mean daily rainfall (mm) | | % difference |
|------|--------------------------|----------------------|--------------|
| | Loch Restil | Rest and be Thankful | |
| 2013 | 8.4 | 8.3 | -1 |
| 2014 | 10.4 | 9.9 | -5 |
| 2015 | 11.3 | 11.3 | 0 |
| 2016 | 8.1 | 5.6 | -31 |
| 2017 | 8.6 | 8.8 | 2 |

6.1.2 Data analysis

The 15-minute rainfall data was analysed by the Met Office UK in the following manner with Excel spreadsheets:

1. For days on which a landslide occurred, the 15 minute rainfall intensity that relates to the time of the landslide was identified. For every other day (or a day when a landslide occurred but the timing is unknown) the highest 15 minute rainfall intensity in the day was identified (from the 96 values in the 24 hour period). If there was more than one 15-minute data-point with this value, the one that was later/latest in the day was chosen. The timing of this value becomes the time-slot for that day from which all antecedent rainfall was calculated.
2. The average intensity for the 30 minute, 1 hour, 2 hours, 4 hours, 6 hours, 8 hours, 12 hours, 18 hours, 24 hours, 48 hours, 96 hours, 144 hours, 192 hours and 288 hours prior to the time of the value identified in (1) above was calculated. This resulted in one value for each antecedent time period for each date i.e. there will be 15 intensities allocated to each date (one for each of the time slots plus the initial 15 minuet maximum value itself).
3. Days with no rainfall recorded were excluded from any further analysis.

This results in two datasets of 'wet days', those that resulted in a landslide and those that did not which were sorted and analysed. On days when the landslides occurred it is possible for periods of several hours prior to the landslide to have higher rainfall intensities than those at the time of the landslide (occasionally the rainfall intensity was zero at the time of the landslide). Unlike a non-landslide event, the intensity was chosen to coincide with the timing of the landslide which may not necessarily be the highest rainfall intensity on that day. This produces an inconsistency in sorting between the two datasets but it cannot be avoided. However, it was considered to be useful to retain the hour with the highest rainfall intensity on the day of a landslide (as long as it was prior to the time of the landslide) even though it did not coincide with the landslide, as such events may also be worthy of future investigation. It is acknowledged that such events will be catered for in the antecedent intensities prior to the time of the landslide. Following discussions within the project team,

it was decided that this information was not relevant and played no further part in the analysis. However, the values are retained in the spreadsheet and are termed 'maximum intensity on landslide day'.

In practice this procedure is quite complex within the Excel spreadsheet. The precise steps taken are described in Appendix A.

Due to the period of missing data from 10 to 22 December 2015, the period from 23 to 29 December 2015 was excluded from the dataset as there was insufficient data to calculate the antecedent rainfall conditions. The landslide event that occurred on 30 December 2015 at 07:40 was retained within the analysis, despite the fact that the average rainfall intensities for 192 and 288 hours prior to the landslide event overlapped with the period for which data was missing. Although the intensities for 192 and 288 hours prior to the events were averaged over missing data it was decided to keep these values in the analysis. Similarly the non-events 'wet day' on 31 December 2015 was retained, with the average intensity for 288 hours prior to the time being averaged over missing data.

The analysis method described above has resulted in 1,563 occasions of interest at Rest and be Thankful (21 days with landslides and 1,542 non-landslide days) and 1,606 occasions at Loch Restil (21 days with landslides and 1,585 non-landslide days). As up to 12 days' antecedent rainfall is considered, a natural consequence will be an overlapping in data from day to day but the sorting of the data results in sensible allocation of the data as time progresses. It was decided to treat the datasets from the two sites separately and not to find 'average' conditions to ensure that any extreme values were retained.

6.1.3 Results

The data has been analysed to reveal over 1,500 non-landslide days together with 21 landslide days. Plots of the average intensity (mm/h) versus the rainfall duration (hours) of the 21 landslide events are shown in Figure 6.4 and Figure 6.5 for Rest and be Thankful and Loch Restil respectively, together with the dates on which these events occurred. Differences in the distribution of the antecedent rainfall can be observed from the relative ranking of the landslide events at each of the considered time periods.

It should be noted that some rainfall intensities in Figure 6.4 and Figure 6.5, such as those of the landslide event on 11 November 2015, do not show when their value is zero. The landslide on the 7 November 2017 has the highest 15 minutes rainfall intensity at both locations, but when examining the average intensities from 6 hours onwards it has one of the lowest average rainfall intensities; this is also one of the three landslide events with the lowest daily rainfall as described in Section 6.1.1. By contrast, the landslide event on 9 January 2014 has the lowest rainfall intensities between 15 minutes and 24 hours (excluding those with zero) but at durations of 192 and 288 hours has rainfall above the average, this landslide event is associated with the lowest level of daily rainfall relative of all landslide events.

Figure 6.6 and Figure 6.7 show plots of all the events (landslide and non-landslide events). The red circles of the 21 landslide events are seen mainly, although not exclusively, at the top of each column plot as would be expected. However, there are still significant numbers of non-landslide black circles visible at the same high rainfall intensities. Both Figure 6.6 and

Figure 6.7 show that landslides do not typically occur in higher average intensities over a shorter duration, but do occur at high average intensities over a longer duration.

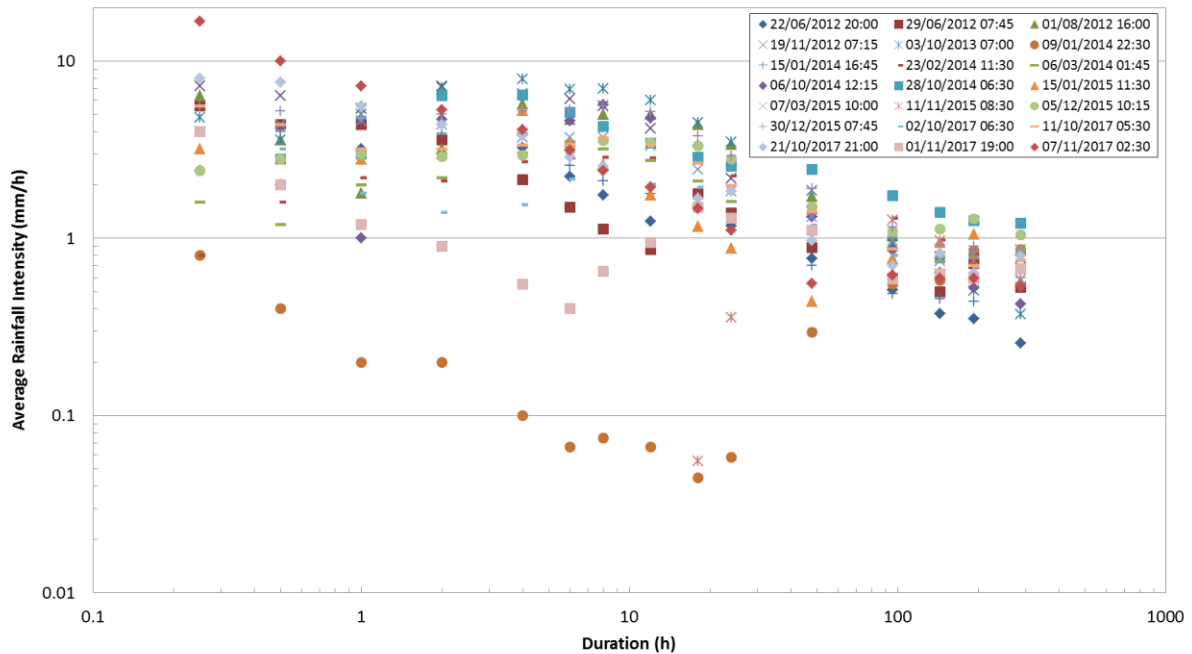


Figure 6.4: Plot of antecedent average rainfall intensities over different time periods prior to each of the 21 landslide events at Rest and be Thankful

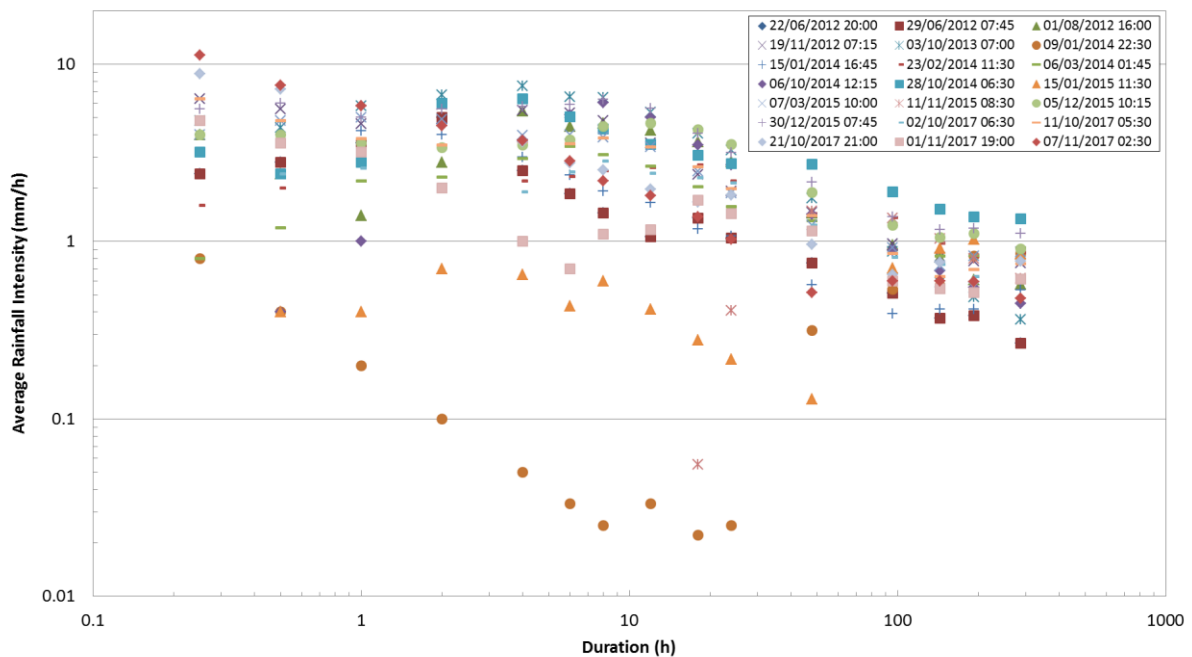


Figure 6.5: Plot of antecedent average rainfall intensities over different time periods prior to each of the 21 landslide events at Loch Restil

Some filtering of the data was undertaken to enable the patterns to emerge more fully. The final selection filtered the data for those events with a 24-hour antecedent rainfall total $\geq 12\text{mm}$ (an average rainfall intensity of $>0.5\text{mm/h}$) retaining the other coincident

antecedent rainfall intensities associated with those events. The two landslide events that fell below this filter on the Rest and be Thankful records were kept in the analysis. This resulted in 620 events at Rest and be Thankful and 680 events at Loch Restil. The graphs using this final filter are shown in Figure 6.8 and Figure 6.9. Many of the less significant non-landslide events experiencing similar to or higher antecedent rainfall intensities than landslide events still remain.

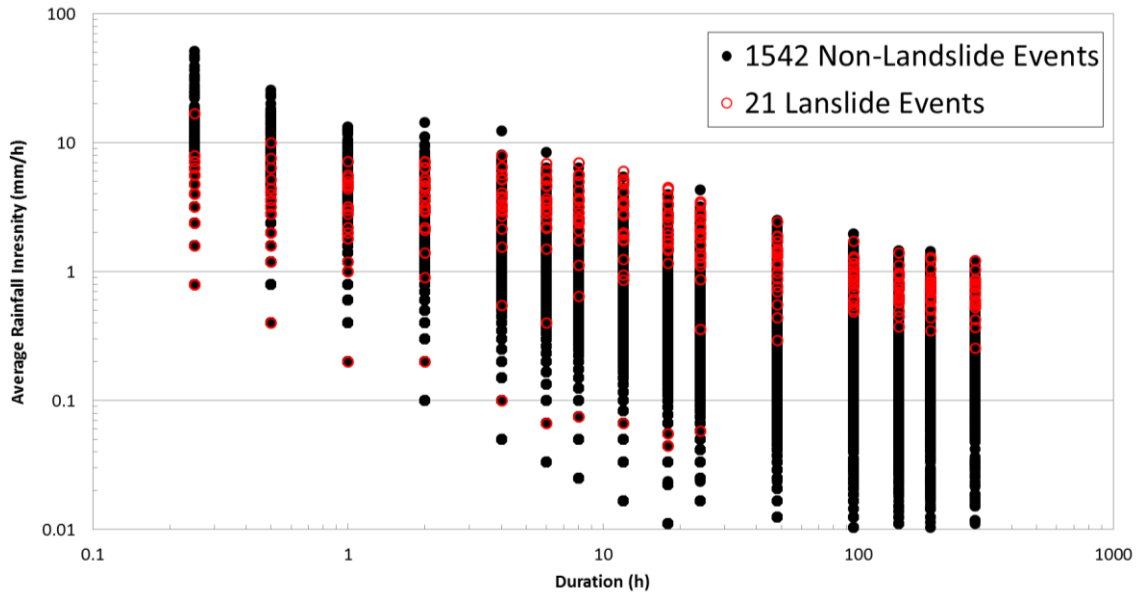


Figure 6.6: Plot of all antecedent rainfall intensities over different time periods prior to the 1542 non-landslide events and each of the 21 landslide events at the Rest and be Thankful

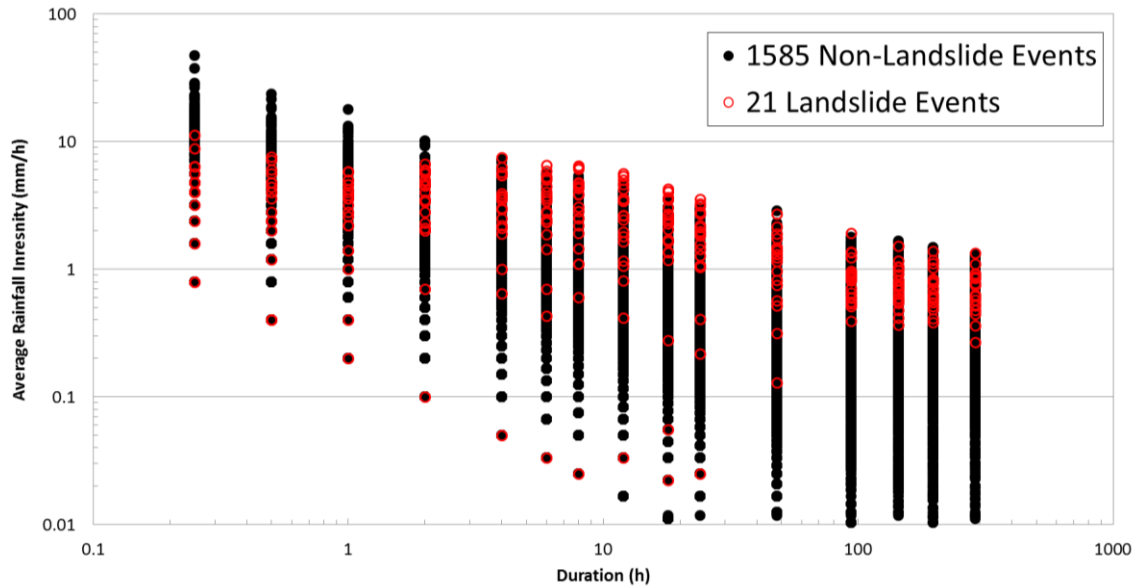


Figure 6.7: Plot of all antecedent rainfall intensities over different time periods prior to the 1585 non-landslide events and each of the 21 landslide events at Loch Restil

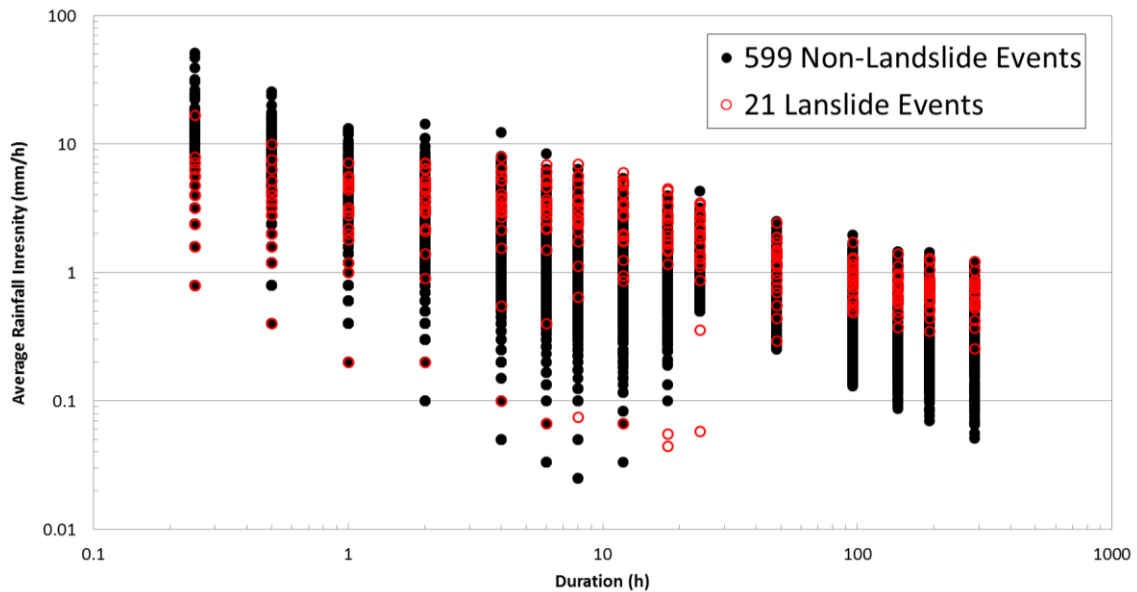


Figure 6.8: Plot of all antecedent rainfall intensities with a 24 hour rainfall total $\geq 12\text{mm}$ (average 24 hour intensity $\geq 0.5\text{mm/h}$) (a 24 hour accumulation prior to the time slot of highest 15 minute intensity on that day) over different time periods at Rest and be Thankful

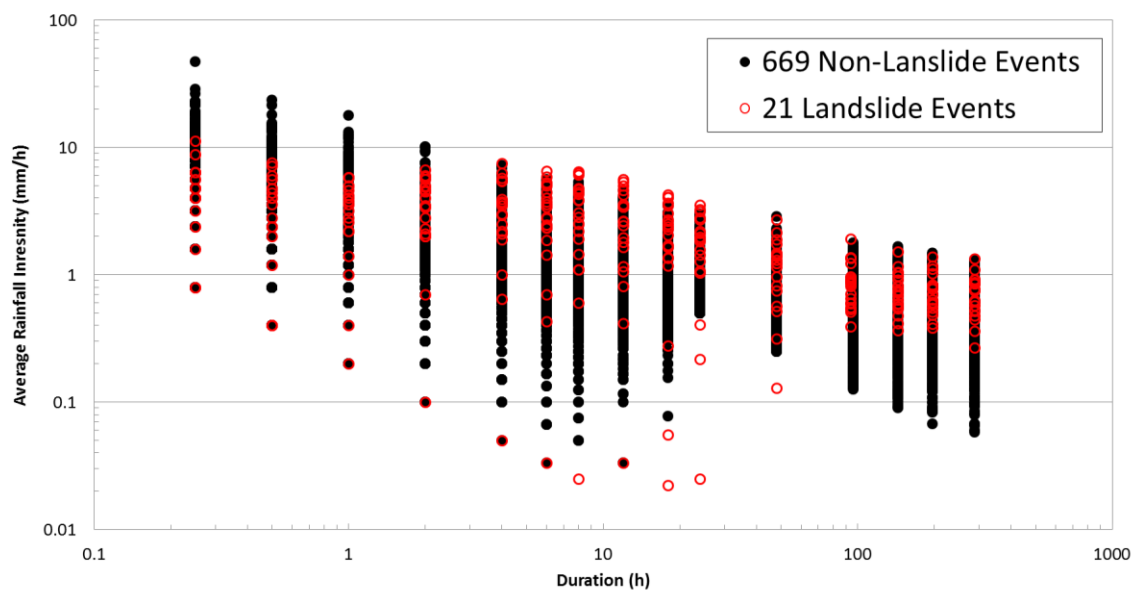


Figure 6.9: Plot of all antecedent rainfall intensities with a 24 hour rainfall total $\geq 12\text{mm}$ (average 24 hour intensity $\geq 0.5\text{mm/h}$) (a 24 hour accumulation prior to the time slot of highest 15 minute intensity on that day) over different time periods at Loch Restil

6.1.4 Summary

The purpose of this part of the work was to produce rainfall intensity-duration graphs incorporating data for rainfall events that do not lead to landslides. The data then feeds into the next stage that is the development of the probabilistic rainfall intensity-duration threshold for landslide triggering.

The current analysis has been performed from just under six-years of 15-minute rainfall data for Rest and be Thankful and Loch Restil.

Various methods of isolating rainfall events, using the 15 minute to 12 day duration data, were trialled; around 1,500 non-landslide events were identified together with 21 known landslide events.

In order to reduce some of the number of non-landslide events for plotting purposes and to give an appropriate scale to the rainfall events considered, a 24-hour daily rainfall total (prior to the timing of each event or prior to the highest intensity hour for a non-landslide event) in excess of 12mm (average hourly rainfall intensity of 0.5mm/h) was selected as a useful and appropriate filter. The final rainfall intensity-duration graphs are presented in Figure 6.8 and Figure 6.9.

Subsequent analyses focus on data from the Rest and be Thankful gauge as described Section 6.1.1.

6.2 Analysis

Predictions of the outcomes of physical events can be made using either a deterministic or a probabilistic approach.

The deterministic method is based on the principle of 'cause and effect', that is, given a certain set of parameters defining a system, there is only one possible outcome. In other words, no random elements are involved: each time that specific conditions occur, the same result is inevitable. It is therefore possible to derive rules from observations and employ them in order to formulate a forecast whenever the specific conditions recur. An example is the boiling point of liquid; the relationship between this characteristic temperature of a liquid and the environmental pressure is well known, if pure water is heated at sea level (i.e. one atmosphere of pressure) then it will boil when it reaches 100°C.

However, there are scenarios where a certain degree of randomness is present and it is not possible to trace a unique path linking an event and a single outcome. In this case, a conclusion cannot be drawn about the consequences of a particular scenario. Instead a validation of the likelihood that a result occurs as an outcome of certain inputs; that is, a probability is associated with occurrence. A probabilistic (or statistical) model makes inferences about all of the possible outcomes and attributes and a measure of how likely each one is to happen: i.e. it provides a probability distribution of outcomes.

The criterion on which to base the choice of the method to apply when analysing a phenomena, is the absence of uncertainties in the system. The origin of uncertainties can be related to various factors, including:

- That the measurement process itself can introduce uncertainties (e.g. due to random instrument or system errors).
- Missing observations (e.g. failure in the instruments, maintenance works, etc.).
- Temporal inconsistencies, arising for instance from uncertainties surrounding the time of initiation of an event as opposed to the recorded time at which the event was observed.

Probabilistic analyses find application also in cases in which the variables that come into play are so many that it not possible to account for them all in a deterministic model. The study here presented is an example of such complexity. As discussed in Section 3, it is not possible to identify a threshold of values beyond which a definitive assertion can be made that a landslide is going to occur by measuring the most significant rainfall variables (such as intensity, duration, etc.). Physical variations are responsible for introducing complexity within the system. For example, variations in soil depth, structure, type, properties, stress history, hydraulic conductivity amongst other properties and behaviours can all influence the way in which failure occurs as a result of water ingress.

Given the nature of the study of connection between rainfalls and landslides, it follows that a probabilistic approach is required (Sections 3 and 4).

6.2.1 Methodology

As mentioned in Section 3, the method followed here for describing the relations between rainfall events and landslide relies on the Bayes' theorem, an approach which makes use of the concepts of prior and posterior probabilities.

Prior probabilities are based on the principle of indifference, that is, it is assumed that there is no reason for expecting that one possible outcome is more likely than another. In practice, the same probability is assigned to all the possible outcomes prior to any empirical evidence.

Within this study, the two prior probabilities are defined as:

- $P(R)$ is the probability that a rainfall with specific characteristics R occurs (' R ' is described as rainfall for simplicity and could, in practice, be the rainfall duration, the mean rainfall intensity or another rainfall variable);
- $P(L)$ is the probability that a landslide L occurs during a rainfall event (independently of the characteristics of the rainfall).

Using the relative frequency method for calculating the probabilities (i.e. the probability that a specific outcome happens is equal to the ratio between its occurrence and the total number of outcomes), the following equations can be derived:

$$P(R) = \frac{N_R}{N} \quad \text{and} \quad P(L) = \frac{N_L}{N} \quad (6.1)$$

Where N is the total number of rainfall events, N_R is the number of rainfall events with specific characteristics, denoted by R for simplicity, and N_L is the number of landslide episodes.

When there is evidence of a link between an event and some variables, this information can be included in the posterior probability. This quantity gives the likelihood of the event occurrence in the presence of the specific variables. It is also referred to as conditional probability, since it represents a probability provided that certain conditions are verified (i.e. posterior probability is a special case of conditional probability).

In the context of this study, the following conditional probabilities are defined:

- $P(L|R)$ is the conditional probability that a landslide L occurs given that a rainfall, with characteristics R , has occurred.
- $P(R|L)$ is the posterior probability (a special case of conditional probability, see Section 3) that rainfall event with characteristics R is associated with an observed landslide L .

The former can be obtained from the Bayes' theorem (see Section 6.2.2), while the latter can be derived from the relative frequencies as follows:

$$P(R|L) = \frac{N_{(R|L)}}{N_L} \quad (6.2)$$

Where $N_{(R|L)}$ is the number of rainfall events, with characteristics R , that are associated with landslides and N_L is as defined in Eq. (6.1).

6.2.2 Bayes' Theorem

Bayes' theorem gives the likelihood of an event if certain conditions take place: i.e. it provides a conditional probability of an event (in this study, a landslide), based on potential causes (rainfall).

The Bayesian relation between potential cause and effect is expressed in terms of the posterior probability of the cause and the prior probabilities of the cause and the effect. This is expressed mathematically by Eq. (6.3), which states that the conditional probability that a landslide L is due to a rainfall event with characteristics R , $P(L|R)$, is equal to the ratio between the posterior probability of R given L , $P(R|L)$, and the prior probability of a rainfall event R , $P(R)$, multiplied by the prior probability of a landslide occurrence L , $P(L)$:

$$P(L|R) = \frac{P(R|L)}{P(R)} \cdot P(L) \quad (6.3)$$

This means that, if there is a link between an event R and an outcome L , the probability of observing L is not simply given by its prior probability $P(L)$.

Because of the cause-effect connection between the observables R and L , there is a multiplicative factor to take into account, namely the ratio $P(R|L)/P(R)$. It can be stated that:

1. The larger the value of $P(R|L)/P(R)$ then the higher the likelihood of rainfall R causing a landslide L .
2. The larger the value of $P(R|L)/P(R)$ then the larger the difference between the conditional probability $P(L|R)$ and the prior probability $P(L)$, that is, the stronger the link between rainfall events and landslides.
3. If $P(R|L) \approx 0$ then $P(L|R) \approx 0$, then there is no evidence that rainfall events with characteristics R trigger landslides.

It is worthwhile noting that calculating the probability using the relative frequency method (Eq. (6.1) and Eq. (6.2)), allows the formulation of the theorem to be simplified as follow:

$$P(L|R) = \frac{P(R|L)}{P(R)} \cdot P(L) = \frac{\frac{N_{(R|L)}}{N_E}}{\frac{N_R}{N}} \cdot \frac{N_E}{N} = \frac{N_{(R|L)}}{N_R} \quad (6.4)$$

The application of Bayes' Theorem to a hypothetical general scenario is presented in Appendix B. This is intended to illustrate the rather complex process in a more readily-understood form.

6.2.3 Data and analysis

As described in Section 6.1, from the data recorded at the Rest and be Thankful rainfall gauge 1,563 rainfall events were identified, 21 of which were associated with landslides. The rainfall events were filtered in order to consider only those characterised by total rainfall of at least 12mm in 24 hours (equivalent to an average intensity of 0.5mm/h or higher) or to have been associated with a landslide; this left 599 non-landslide events and 21 landslide events (a total of 620 events). The final set of rainfall intensities is organised in tabular form with fifteen columns, corresponding to the set number of time intervals that preceded

either the maximum 15 minute rainfall intensity of the day or the landslide event used to define the time of event occurrence. Table 6.3 which refers to non-landslide episodes has 599 rows, while Table 6.4 which refers to rainfall events associated with landslides has 21 rows.

The average antecedent rainfall intensities of the resulting 620 rainfall events are shown in Figure 6.10, for time intervals from 0.25 hours to 288 hours (12 days). The data for the 21 events that are associated with landslides mostly lie above the deterministic threshold (Section 5) particularly at longer durations.

For the calculation of the probabilities used in the Bayes' equation, the frequency method is used. Specifically, for the one-dimension case (Section 6.2.4), it has been carried out using the following procedures:

- A. **$P(L)$** : The prior probability of a landslide is the ratio between the number of landslides observed and the number of rainfall events recorded, that is, N_L/N . In this study this corresponds to 21 divided by 620; $P(L) = 0.0339$ (or 3.4%).
- B. **$P(D)$** : This is the prior probability of a rainfall event of duration D . The available data include 15 time intervals for each of the 620 rainfall events, and the corresponding average rainfall intensity (columns and cells in Table 6.3, respectively). Since the variable is the duration, a certain interval for the intensity can be fixed, ΔI .

$P(D)$ is given by the ratio between the number of rainfall events with duration D and the total number of rainfall events (both for a given ΔI interval), that is $N_D/N_{\Delta I, tot}$ (see also Appendix C for further explanation).

To calculate N_D , each time interval (i.e. column) is counted for the number of cells containing intensity values in the chosen interval. Therefore the number of rainfall events (with intensity in the range ΔI) characterised by certain duration D is obtained.

Table 6.5 present the number of events in each time interval that have an average intensity of $1 \leq I < 30\text{mm/h}$. The total number of readings with an average intensity within this range is 4,780 and therefore $P(D)$ can be calculated for each time interval using the equation $P(D) = N_D/N_{\Delta I, tot}$.

- C. **$P(D|L)$** : The probability that a rainfall event of duration D is associated with an observed landslide can be calculated using Eq. (6.2). The quantity is written as the ratio between the number of rainfall events of duration D which are associated with a landslide and the total number of rainfall events which are associated with landslides, that is $N_{(D|L)}/N_{D, tot}$.

The procedure followed is the same as that followed in Procedure B above for the quantity N_D , now applied to the 21 rainfall events that are associated with landslides. For each time interval, the number of cells with intensity in the fixed interval ΔI were counted, in order to obtain $N_{(D|L)}$.

The number of data corresponding to rainfall events connected with landslides is 315, i.e. 15 time intervals multiplied by 21 landslide events. If data is filtered to the chosen ΔI , in this study $1 \leq I < 30\text{mm/h}$ (values highlighted blue in Table 6.3), $N_{(D|L)}$ is obtained for each time interval by summing up the number of events which are within this range (values highlighted red at the bottom of Table 6.3). The total

number of average rainfall intensities that are associated with a landslide ($N_{D,tot}$) is 207. Therefore $P(D|L)$ can be calculated for each time interval using $N_{(D|L)}/N_{D,tot}$.

Table 6.3: Extract of the rainfall intensity table used for the Bayesian analysis (values are given in mm/h)

| Antecedent time interval (h) | 0.25 | 0.5 | 1 | 2 | 4 | 6 | 8 | 12 | ... | 288 |
|------------------------------|------|------|------|------|------|------|------|------|-----|------|
| Rainfall event 1 | 4.80 | 4.80 | 3.40 | 2.40 | 2.50 | 2.30 | 1.90 | 1.62 | ... | 0.34 |
| Rainfall event 2 | 3.20 | 2.80 | 1.60 | 0.80 | 0.40 | 0.27 | 0.20 | 0.13 | ... | 0.28 |
| ... | ... | ... | ... | ... | ... | ... | ... | ... | ... | ... |
| Rainfall event 599 | 5.60 | 4.80 | 4.80 | 4.20 | 4.50 | 4.40 | 3.88 | 3.02 | ... | 0.88 |

Table 6.4: Extract of the rainfall intensity table used for the Bayesian analysis for the rainfall events which are associated with landslides (values are given in mm/h). Calculations are given at the bottom of the table to aid in the explanation of Procedure C (below)

| Antecedent time interval (h) | 0.25 | 0.5 | 1 | 2 | 4 | 6 | 8 | 12 | ... | 288 |
|--------------------------------|------------------|------------------|------------------|------------------|------------------|------------------|------------------|------------------|-----|-----------------|
| Rainfall event 1 | 16.80 | 10.00 | 7.20 | 5.30 | 4.10 | 3.13 | 2.40 | 1.93 | ... | 0.53 |
| Rainfall event 2 | 4.00 | 2.00 | 1.20 | 0.90 | 0.55 | 0.40 | 0.65 | 0.95 | ... | 0.67 |
| Rainfall event 3 | 8.00 | 7.60 | 5.60 | 4.40 | 3.80 | 2.87 | 2.55 | 1.95 | ... | 0.80 |
| Rainfall event 4 | 5.60 | 4.40 | 3.20 | 3.20 | 3.35 | 3.40 | 3.68 | 3.40 | ... | 0.75 |
| Rainfall event 5 | 5.60 | 3.20 | 1.80 | 1.40 | 1.55 | 2.17 | 2.45 | 2.02 | ... | 0.69 |
| Rainfall event 6 | 5.60 | 5.20 | 4.80 | 5.00 | 5.20 | 5.30 | 5.60 | 5.17 | ... | 0.60 |
| Rainfall event 7 | 2.40 | 2.80 | 3.00 | 2.90 | 2.95 | 3.13 | 3.55 | 3.48 | ... | 1.04 |
| Rainfall event 8 | 0.00 | 0.00 | 0.00 | 0.00 | 0.00 | 0.00 | 0.00 | 0.00 | ... | 0.58 |
| Rainfall event 9 | 4.00 | 4.40 | 4.60 | 4.40 | 3.70 | 3.70 | 3.73 | 3.32 | ... | 0.87 |
| Rainfall event 10 | 3.20 | 2.80 | 2.80 | 3.00 | 5.25 | 3.50 | 2.63 | 1.75 | ... | 0.86 |
| Rainfall event 11 | 4.00 | 2.80 | 3.00 | 6.40 | 6.45 | 5.13 | 4.28 | 3.43 | ... | 1.22 |
| Rainfall event 12 | 0.00 | 0.00 | 1.00 | 4.70 | 3.85 | 4.60 | 5.68 | 4.77 | ... | 0.43 |
| Rainfall event 13 | 1.60 | 1.20 | 2.00 | 2.20 | 3.05 | 3.50 | 3.20 | 2.75 | ... | 0.87 |
| Rainfall event 14 | 0.80 | 1.60 | 2.20 | 2.10 | 2.70 | 2.83 | 2.88 | 2.83 | ... | 0.82 |
| Rainfall event 15 | 4.00 | 4.00 | 4.60 | 3.90 | 3.25 | 2.57 | 2.10 | 1.78 | ... | 0.55 |
| Rainfall event 16 | 0.80 | 0.40 | 0.20 | 0.20 | 0.10 | 0.07 | 0.08 | 0.07 | ... | 0.86 |
| Rainfall event 17 | 4.80 | 3.60 | 5.00 | 7.10 | 7.95 | 6.93 | 7.00 | 6.00 | ... | 0.37 |
| Rainfall event 18 | 7.20 | 6.40 | 5.40 | 7.20 | 6.55 | 6.10 | 5.60 | 4.17 | ... | 0.77 |
| Rainfall event 19 | 6.40 | 3.60 | 1.80 | 3.20 | 5.70 | 4.70 | 5.03 | 5.02 | ... | 0.57 |
| Rainfall event 20 | 5.60 | 4.40 | 4.40 | 3.60 | 2.15 | 1.50 | 1.13 | 0.87 | ... | 0.53 |
| Rainfall event 21 | 2.40 | 2.00 | 3.20 | 6.50 | 3.25 | 2.23 | 1.75 | 1.25 | ... | 0.26 |
| $N_{(D L)}$ | 17 | 18 | 19 | 18 | 18 | 18 | 18 | 18 | ... | 2 |
| $P(D L) = N_{(D L)}/N_{D,tot}$ | $\frac{17}{207}$ | $\frac{18}{207}$ | $\frac{19}{207}$ | $\frac{18}{207}$ | $\frac{18}{207}$ | $\frac{18}{154}$ | $\frac{18}{207}$ | $\frac{18}{207}$ | ... | $\frac{2}{207}$ |

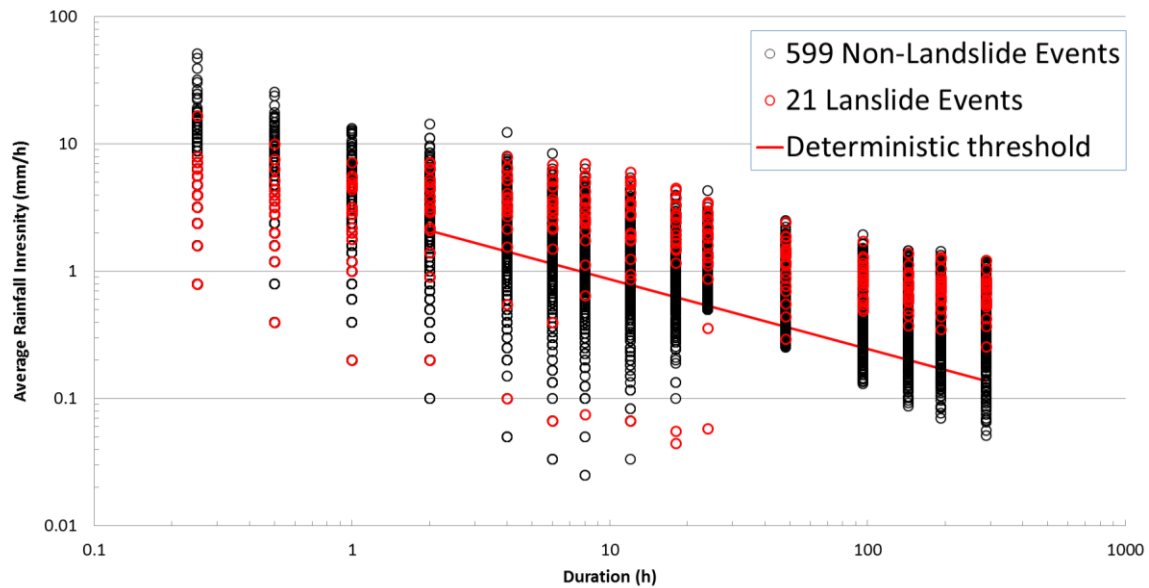


Figure 6.10: Rainfall events at Rest and be Thankful ranked by hour total $\geq 12\text{mm}$. Red dots refer to events which are associated with landslides. The red line is the deterministic threshold developed by Winter et al. (2010)

Table 6.5: Calculations of $P(D)$ for each time period prior to a rainfall event for average rainfall intensities of $1 \leq I < 30\text{mm/h}$

| Rainfall event duration, D (h) | Number of events, N_D | $P(D)=N_D/N_{\Delta I,tot}$ |
|--------------------------------------|-------------------------|-----------------------------|
| 0.25 | 598 | 0.13 |
| 0.5 | 598 | 0.13 |
| 1 | 574 | 0.12 |
| 2 | 517 | 0.11 |
| 4 | 459 | 0.10 |
| 6 | 412 | 0.09 |
| 8 | 394 | 0.08 |
| 12 | 344 | 0.07 |
| 18 | 273 | 0.06 |
| 24 | 232 | 0.05 |
| 48 | 160 | 0.03 |
| 96 | 95 | 0.02 |
| 144 | 64 | 0.01 |
| 192 | 39 | 0.008 |
| 288 | 21 | 0.004 |
| $N_{\Delta I,tot}$ | 4,780 | |

D. $P(I)$: The prior probability of having a rainfall event of intensity I , is given by the ratio between the number of observed rainfall events with intensity I , N_I , and the total number of events, N_{tot} , regardless of the duration (in this case, 15 time intervals multiplied by 620 rainfall events is 9,300). Although the intensity is a continuous

variable, for practical reasons, the data are grouped in ranges: therefore, the calculation of N_i has been carried out counting the number of cells with intensity values in the different ranges. For the purposes of this study, an interval of 1.5mm/h was chosen, results are presented in Table 6.6.

- E. $P(I|L)$: The probability that a rainfall event of intensity I is associated with an observed landslide L can be calculated using Eq. (6.2). This quantity is written as the ratio between the number of rainfall events having intensity I which are associated with a landslide and the total number of events which are associated with a landslide, that is $N_{(I|L)}/N_{i,L}$.

As in Procedure (D) above, $N_{(I|L)}$ has been calculated by counting the number of cells/ events corresponding to a certain intensity range, but this time considering only to data associated with landslides (i.e. $N_{i,L}$ is equal to 15 time intervals multiplied by 21 rainfall events associated with landslides, $N_{i,L}=315$). Results, using an interval 1.5mm/h, are presented in Table 6.7.

Table 6.6: Calculations of $P(I)$ over all rainfall events using an average rainfall intensity interval of 1.5mm/h

| Intensity (mm/h) | Number of events, N_i | $P(I)=N_i/N_{tot}$ |
|-----------------------------|-------------------------|--------------------|
| 0-1.5 | 5,833 | 0.63 |
| 1.5-3 | 1,650 | 0.18 |
| 3-4.5 | 827 | 0.09 |
| 4.5-6 | 441 | 0.05 |
| 6-7.5 | 252 | 0.03 |
| 7.5-9 | 117 | 0.01 |
| >9 | 180 | 0.02 |
| N_{tot} | 9,300 | |

Table 6.7: Calculations of $P(I|L)$ using an average rainfall intensity interval of 1.5mm/h

| Intensity (mm/h) | Number of events, $N_{(I L)}$ | $P(I L)=N_{(I L)}/N_{i,L}$ |
|-----------------------------|-------------------------------|----------------------------|
| 0-1.5 | 143 | 0.45 |
| 1.5-3 | 69 | 0.22 |
| 3-4.5 | 54 | 0.17 |
| 4.5-6 | 30 | 0.10 |
| 6-7.5 | 14 | 0.04 |
| 7.5-9 | 3 | 0.01 |
| >9 | 2 | 0.01 |
| $N_{i,L}$ | 315 | |

6.2.4 One-dimensional analysis

Following the method described in Section 6.2.3, the prior and posterior probabilities of rainfall events characterised by a given variable have been calculated and used in the Bayes' equation for obtaining the conditional landslide probability. The variables considered were duration, D , and intensity, I , of the rainfall events.

Figure 6.11 shows the probability of the occurrence of a rainfall event of duration D (yellow dashed line), $P(D)$, and the probability that when a landslide is observed that it is associated with a rainfall event of duration D (orange dashed line), $P(D|L)$, for a fixed interval of rainfall intensity $1 \leq I < 30$ mm/h.

These two quantities are responsible, from a mathematical point of view, for the difference between the prior landslide probability $P(L)$ and the posterior probability $P(D|L)$, since the ratio $P(D|L)/P(D)$ is the proportionality coefficient between the latter two quantities (see Eq. (6.3)).

If this factor was approximately equal to one, then it would demonstrate that $P(D|L)$ did not significantly differ from the prior probability $P(L)$:

$$\frac{P(D|L)}{P(D)} \approx 1 \Rightarrow P(L|D) \approx P(L) \tag{6.5}$$

In other words, the variable considered, D , would not play any role in triggering landslides.

The higher the ratio $P(D|L)/P(D)$, the higher is the significance of the variable considered, in this case the rainfall event duration, D . Based on the data, this factor varies from 0.8 to 2.0 (blue line in Figure 6.11) and, since the proportion is mirrored by the conditional probability $P(L|D)$, it means that $P(L)$ and $P(L|D)$ are different and there is a link between landslide episodes and the duration of the rainfall events (Figure 6.12).

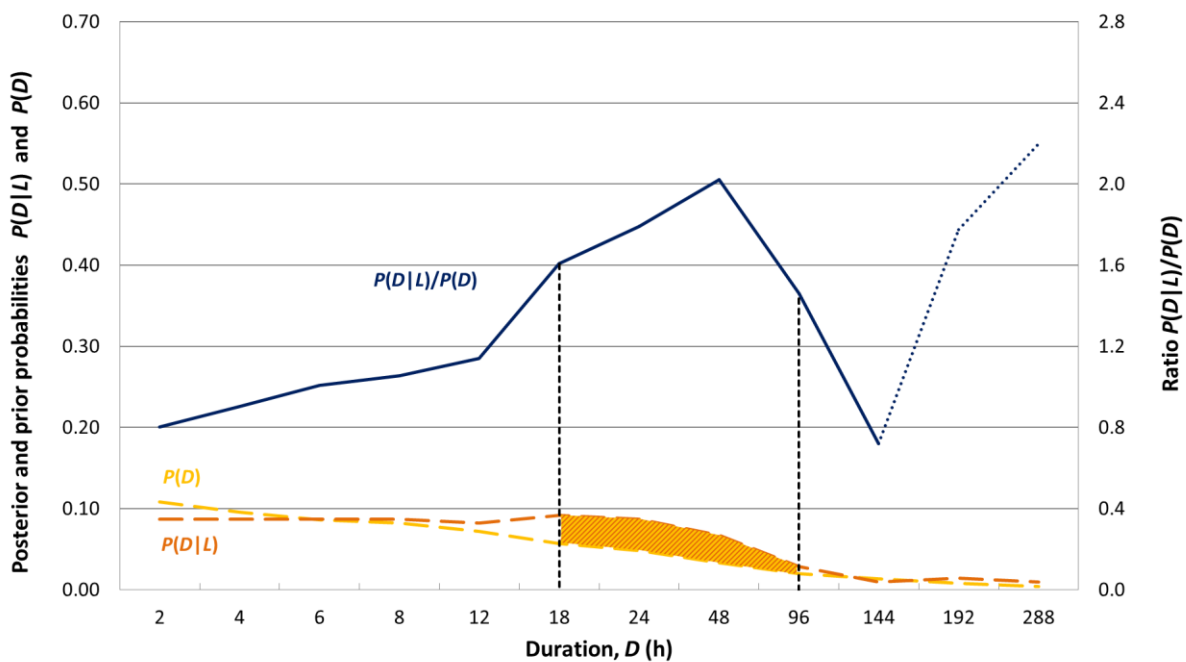


Figure 6.11: Posterior probability $P(D|L)$, prior probability $P(D)$ and their ratio for different values of rainfall duration, D . The higher the ratio $P(D|L)/P(D)$, the higher the conditional probability of a landslide given a rainfall of duration D , $P(L|D)$ (see Figure 6.12). (Note that intensity is treated as a constant in this analysis and the rainfall events within a large intensity interval have been considered: $1 \leq I < 30$ mm/h)

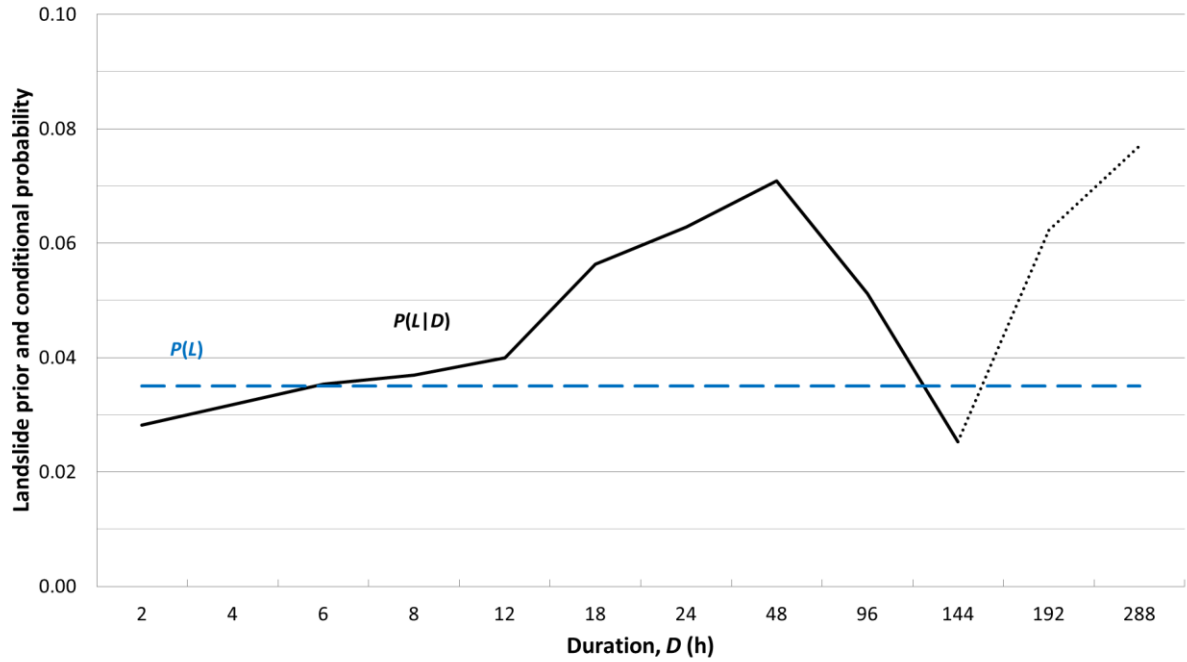


Figure 6.12: Prior and conditional probability of a landslide for different rainfall durations. The fact that the quantities differ means that the considered variable, D , is a significant predictor of landslides

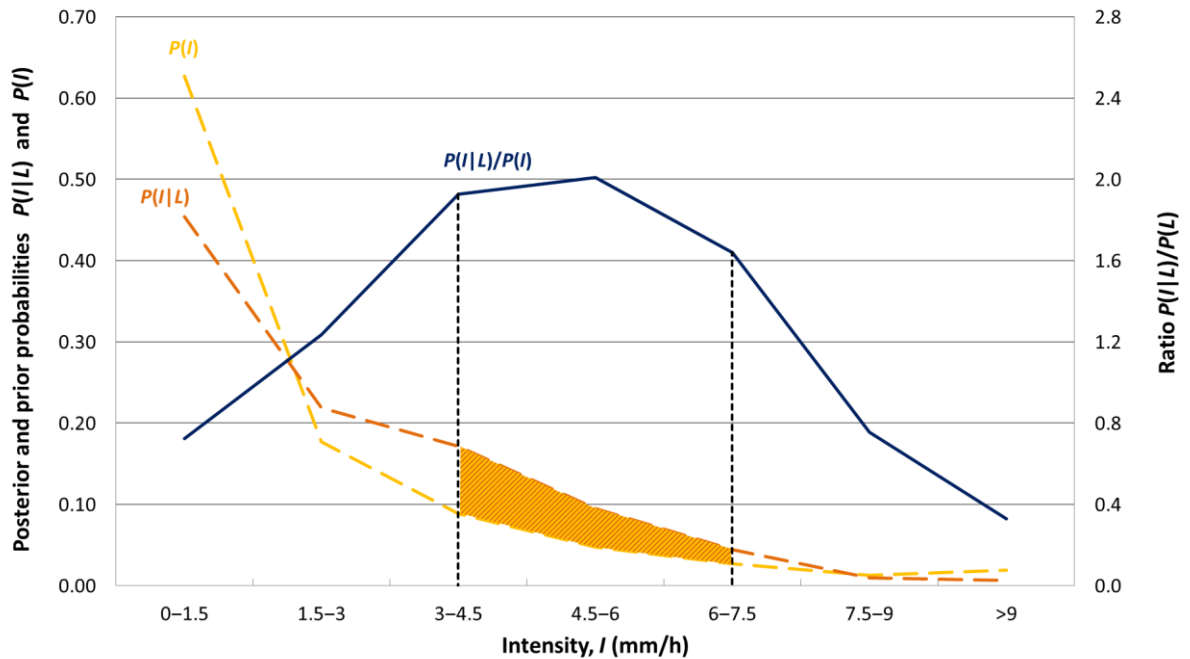


Figure 6.13: Posterior probability $P(I|L)$, prior probability $P(I)$ and their ratio for different values of the rainfall intensity, I . The higher the ratio $P(I|L)/P(I)$, the higher the conditional probability of a landslide given a rainfall of intensity I , $P(L|I)$ (see Figure 6.14)

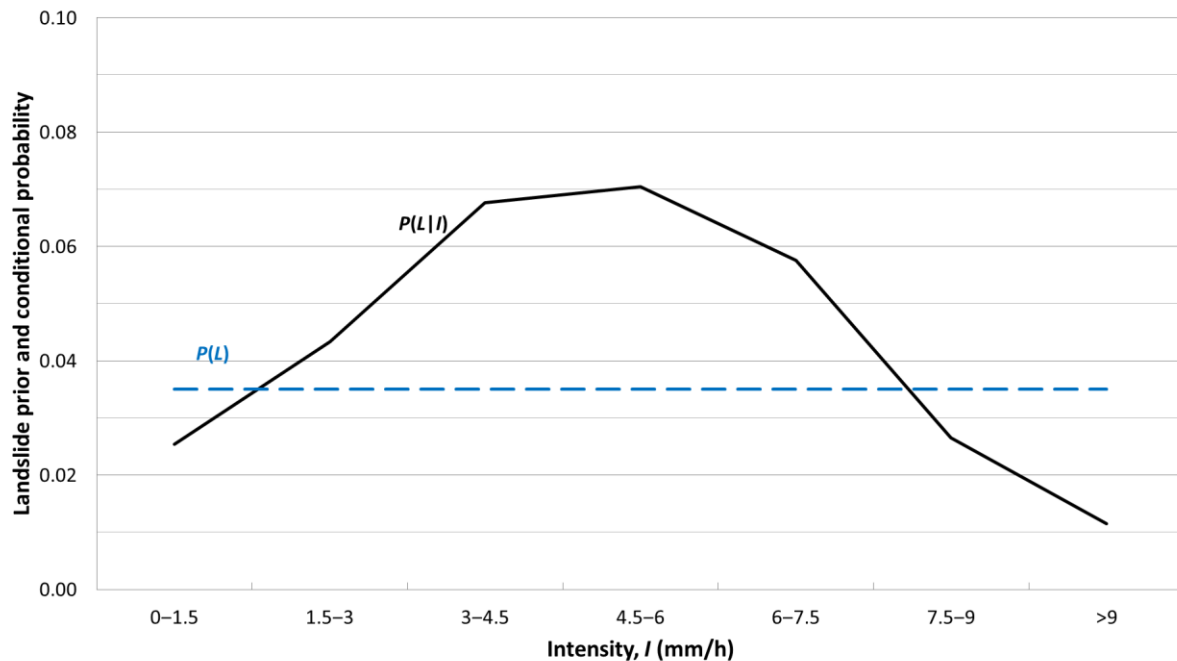


Figure 6.14: Prior and conditional probability of a landslide for different rainfall intensities. The fact that the quantities differ means that the considered variable, I , is a significant predictor of landslides

Figure 6.11 shows that the value of $P(D|L)/P(D)$ increases after 144 hours up to 288 hours (dotted blue line), but this behaviour does not necessarily reflect a physical phenomenon, since it is attributed to a small data sample; the number of rainfall events corresponding to the time windows 192 and 288 hours is only 39 and 21, respectively.

The highest value of $P(D|L)/P(D)$ in the data (excluding those at durations of 192 and 288 hours) corresponds to durations of between 18 and 96 hours (shaded area in Figure 6.11). This is therefore the maximum difference between the prior probability $P(L)$ and the conditional probability $P(L|D)$ and suggests that rainfall durations with the strongest influence on the triggering of landslides in the area of A83 Rest and be Thankful are those with a duration of at least 18 hours and generally up to around 96 hours.

Similarly, the variable rainfall intensity, I , is calculated for prior and posterior probabilities $P(I)$ and $P(I|L)$ using the frequency method (Eq. (6.1) and Eq. (6.2)). Figure 6.13 shows the results for different intensity intervals and the ratio between the two quantities, while Figure 6.14 shows the prior landslide probability and conditional landslide probability given an interval of intensities. It is noted that the latter of the two quantities is not the same, which indicates that landslide events also depend on the rainfall intensity. In particular, the highest probabilities are associated with rainfall events with intensities higher than 3 mm/h up to about 7.5 mm/h (shaded area in Figure 6.13).

It is also useful to understand whether, from the data, it is possible to link later antecedent rainfall to an occurrence of a landslide. The data relative to the longest rainfall duration available (288 hours or 12 days) was selected first. Multiplying the average rainfall intensity of a rainfall event by the duration gives the antecedent total rainfall for each event. Average rainfall intensity intervals of 25mm were considered (see Table 6.8), and the number of

rainfall events belonging to each of the intervals of total rainfall (E) was counted, N_E . The number of rainfall events which were associated to landslides for each interval, $N_{(E|L)}$, were extracted from the data in order to derive the prior and posterior probabilities using the frequency method. The results of the computation are shown in Table 6.8.

Table 6.8: Number of rainfall events for every average rainfall intensity interval for the duration of 288 hours and the associated prior and posterior probabilities. The resulting Bayesian probability $P(L|E)$ is shown in the last row

| Antecedent rainfall intervals, E (mm) | 0-25 | 25-50 | ... | 150-175 | 175-200 | 200-225 | 225-250 | >250 |
|---|-------------|-------------|-----|-------------|-------------|-------------|-------------|-------------|
| N_E | 9 | 29 | ... | 69 | 47 | 55 | 37 | 53 |
| $N_{(E L)}$ | 0 | 0 | ... | 6 | 2 | 2 | 5 | 3 |
| Probabilities | | | | | | | | |
| $P(E)=N_E/620$ | 0.01 | 0.05 | ... | 0.11 | 0.08 | 0.09 | 0.06 | 0.09 |
| $P(E L)=N_{(E L)}/21$ | 0.00 | 0.00 | ... | 0.29 | 0.10 | 0.10 | 0.24 | 0.14 |
| $P(E L)/P(E)$ | 0.00 | 0.00 | ... | 2.57 | 1.26 | 1.07 | 3.99 | 1.67 |
| $P(L)=21/620$ | 0.03 | 0.03 | ... | 0.03 | 0.03 | 0.03 | 0.03 | 0.03 |
| $P(L E)$ | 0.00 | 0.00 | ... | 0.09 | 0.04 | 0.04 | 0.14 | 0.06 |

Figure 6.15 shows that between total antecedent rainfall of 0 to 150mm that $P(E|L)/P(E)$, and therefore $P(L|E)$, remains below the reference factor of 1. This probability increases after total antecedent rainfall of more than 150mm, ranging between a factor of one and four. This implies that for a duration of 288 hours (12 days) a total rainfall amount in excess of 150mm increases the conditional probability, $P(L|E)$, of a landslide by a factor of up to four compared to the prior probability $P(L)$.

As noted in Section 6.2.3, Figure 6.10 shows that for longer durations the rainfall events associated with landslides were consistently in the upper range of all rainfall events. Therefore durations of 96, 144, 192 and 288 hours were considered for total antecedent rainfall, the conditional probability of each of the respective durations is given in Figure 6.16. Columns have black borders (e.g. the column representing $E = 150$ to 175mm; $D = 288$ h) are conditional probabilities that exceed that of the prior probability of a landslide ($P(L)=0.034$) and the key gives the shading coding for each columns respective sample size, the darker the column the higher sample size and therefore the more statistically significant the result. Figure 6.16 shows that the conditional probability ($P(L|E)$) becomes higher than the prior probability, $P(L)$, at higher total antecedent rainfalls. For durations of 96 and 144 hours the conditional probability exceeds the prior probability when total antecedent rainfall reaches >75mm, for a duration 192 hours this occurs when total antecedent rainfall reaches >100mm and for a duration of 288 hours this is >150mm.

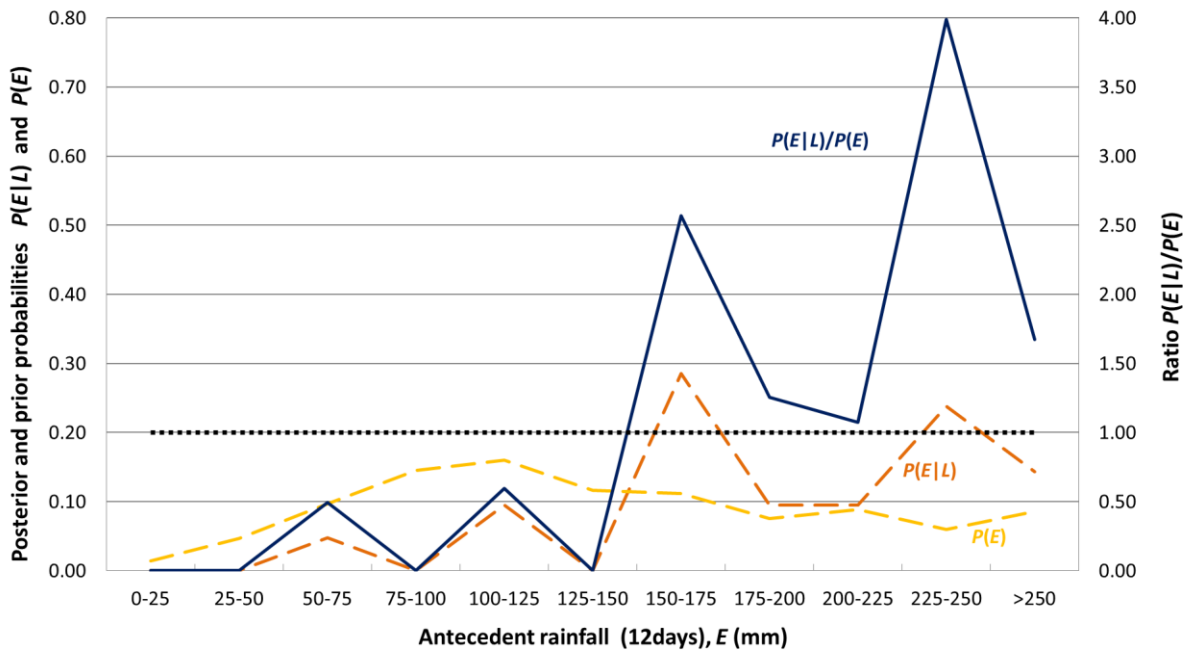


Figure 6.15: Posterior probability $P(E|L)$, prior probability $P(E)$ and their ratio for different values of antecedent rainfall, E . (The black dotted line provides a reference for the condition $P(E|L)/P(E)=1$)

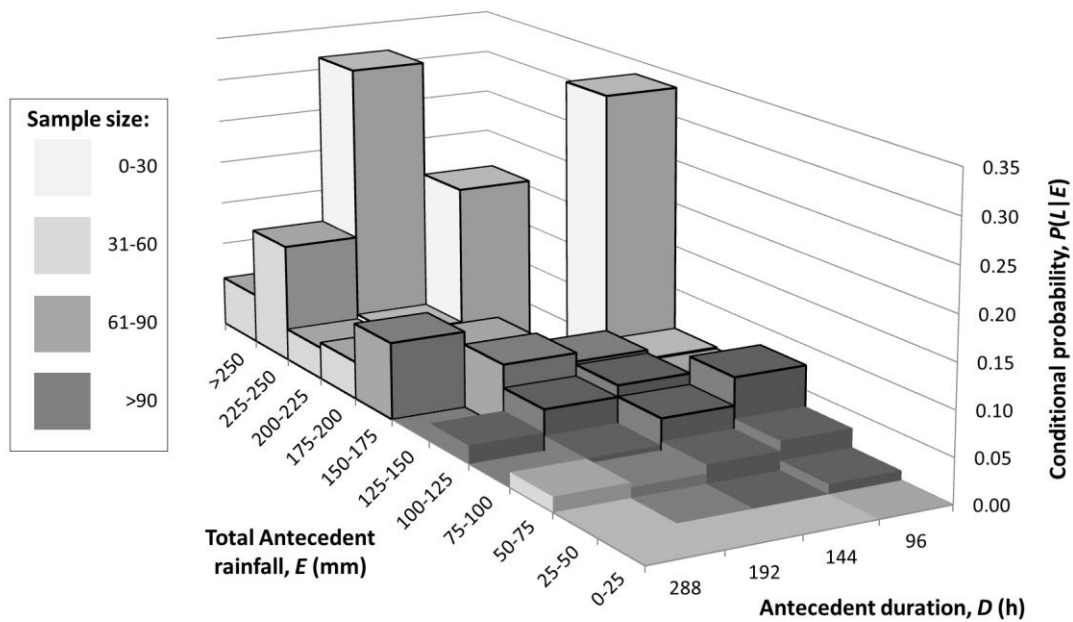


Figure 6.16: Conditional probability of a landslide for intervals of total antecedent rainfall $P(L|E)$ for durations of 96, 144, 192 and 288 hours. The sample size of each result is indicated by the shading of the column and indicated by the key

The variables, rainfall duration and rainfall intensity, have shown a clear connection with landslide occurrence. Accordingly, they have been selected for carrying out a two-

dimensional Bayesian analysis that considers the dependence of landslide occurrence on both of these rainfall variables (Section 6.2.5).

6.2.5 Two-dimensional analysis

For the two-dimensional analysis, both variables which proved to be relevant in causing landslides (Section 6.2.4), duration (D) and intensity (I) of a rainfall event, are considered simultaneously.

The generic variable R in Eq. (6.3) is substituted by combinations of D and I , and therefore the Bayesian probability takes the form:

$$P(L|D, I) = \frac{P(D, I|L)}{P(D, I)} \cdot P(L) \quad (6.6)$$

Where $P(D, I|L)$ is the probability that a rainfall event of duration D and intensity I is associated with a landslide L and $P(D, I)$ is the joint probability of a rainfall event of duration D and intensity I to occur.

According to Eq. (6.4) Bayes' theorem can be written in terms of relative frequencies, that is:

$$P(L|D, I) = \frac{N_{(D, I|L)}}{N_{D, I}} \quad (6.7)$$

Where $N_{(D, I|L)}$ is the number of rainfall events of duration D and intensity I that are associated with a landslide L , and $N_{D, I}$ is the total number of rainfall events characterised by duration D and intensity I that occurred.

The procedure followed was the same as for the one-dimensional analysis, except that the rainfall events are defined by the coupled variables (D, I). Using intensity intervals of 0.5mm/h, the number of rainfall events for duration and intensity is counted (Table 6.9), the same process is carried out for all events associated with a landslide (Table 6.10). For example, Table 6.9 shows that there were two rainfall events with an average antecedent rainfall intensity of between 0 and 0.5mm/h at 0.25 h prior to the event. Similarly, Table 6.10 shows that there were two rainfall events associated with landslides with an average antecedent rainfall intensity of between 0 and 0.5mm/h at 0.25 h prior to the event. The calculation of Eq. (6.7) is equivalent to dividing the numbers in the cells of Table 6.10 by the corresponding numbers in the cells of Table 6.9.

A sample threshold had been introduced in order to exclude the rarest, and therefore least statistically significant, combinations of rainfall duration and intensity. Accordingly, the value of $P(L|D, I)$ is calculated for only those cases for which at least three rainfall events have the characteristics of the paired values (D, I). For example, the two rainfall events of intensity 0 to 0.5 mm/h and duration 24 hours, have been omitted (see Table 6.9). After this final stage of data filtration there remain 140 rainfall conditions (i.e. coupled data pairs of (D, I)) for which the conditional probability of a landslide has been calculated.

Table 6.9: Extract from the table containing the number of rainfall events, $N_{(D,I)}$, of duration D for each intensity interval (the number following the square parenthesis is included in the range, the number preceding the curved parenthesis is excluded)

| $N_{(D,I)}$ | D (h) | Intensity intervals (mm/h) | | | | | | | | |
|-------------|---------|----------------------------|---------|---------|---------|---------|---------|---------|-----|-----|
| | | [0,0.5) | [0.5,1) | [1,1.5) | [1.5,2) | [2,2.5) | [2.5,3) | [3,3.5) | ... | >8 |
| 0.25 | | 2 | 15 | 0 | 20 | 42 | 0 | 54 | ... | 168 |
| 0.5 | | 14 | 8 | 21 | 28 | 73 | 45 | 36 | ... | 71 |
| 1 | | 16 | 30 | 62 | 55 | 90 | 49 | 66 | ... | 28 |
| 2 | | 38 | 65 | 89 | 81 | 78 | 58 | 47 | ... | 8 |
| 4 | | 51 | 110 | 117 | 84 | 68 | 59 | 51 | ... | 2 |
| 6 | | 71 | 137 | 114 | 87 | 85 | 48 | 25 | ... | 1 |
| 8 | | 82 | 144 | 139 | 103 | 56 | 38 | 16 | ... | 0 |
| 12 | | 87 | 189 | 160 | 76 | 55 | 19 | 17 | ... | 0 |
| 18 | | 51 | 296 | 146 | 68 | 26 | 22 | 5 | ... | 0 |
| 24 | | 2 | 386 | 140 | 55 | 18 | 15 | 2 | ... | 0 |
| 48 | | 152 | 308 | 118 | 36 | 5 | 1 | 0 | ... | 0 |
| 96 | | 226 | 299 | 88 | 7 | 0 | 0 | 0 | ... | 0 |
| 144 | | 252 | 304 | 64 | 0 | 0 | 0 | 0 | ... | 0 |
| 192 | | 285 | 296 | 39 | 0 | 0 | 0 | 0 | ... | 0 |
| 288 | | 344 | 255 | 21 | 0 | 0 | 0 | 0 | ... | 0 |

Table 6.10: Extract from table containing the number of rainfall events, $N_{(D,I|L)}$, associated with landslides and of duration D for each intensity interval (the number following the square parenthesis is included in the range, the number preceding the curved parenthesis is excluded)

| $N_{(D,I L)}$ | D (h) | Intensity intervals (mm/h) | | | | | | | | |
|---------------|---------|----------------------------|---------|---------|---------|---------|---------|---------|-----|----|
| | | [0,0.5) | [0.5,1) | [1,1.5) | [1.5,2) | [2,2.5) | [2.5,3) | [3,3.5) | ... | >8 |
| 0.25 | | 2 | 2 | 0 | 1 | 2 | 0 | 1 | ... | 2 |
| 0.5 | | 3 | 0 | 1 | 1 | 2 | 3 | 1 | ... | 1 |
| 1 | | 2 | 0 | 2 | 2 | 2 | 1 | 4 | ... | 0 |
| 2 | | 2 | 1 | 1 | 0 | 2 | 1 | 3 | ... | 0 |
| 4 | | 2 | 1 | 0 | 1 | 1 | 2 | 4 | ... | 0 |
| 6 | | 3 | 0 | 0 | 1 | 2 | 3 | 3 | ... | 0 |
| 8 | | 2 | 1 | 1 | 1 | 3 | 3 | 1 | ... | 0 |
| 12 | | 2 | 2 | 1 | 4 | 1 | 2 | 4 | ... | 0 |
| 18 | | 2 | 0 | 3 | 5 | 2 | 4 | 2 | ... | 0 |
| 24 | | 2 | 1 | 5 | 5 | 2 | 4 | 1 | ... | 0 |
| 48 | | 2 | 5 | 9 | 4 | 1 | 0 | 0 | ... | 0 |
| 96 | | 1 | 14 | 5 | 1 | 0 | 0 | 0 | ... | 0 |
| 144 | | 3 | 16 | 2 | 0 | 0 | 0 | 0 | ... | 0 |
| 192 | | 2 | 16 | 3 | 0 | 0 | 0 | 0 | ... | 0 |
| 288 | | 3 | 16 | 2 | 0 | 0 | 0 | 0 | ... | 0 |

Figure 6.17 shows the results of the calculation of the conditional probability of a landslide. The white areas without columns correspond to combinations of rainfall duration and intensity which did not occur (i.e. there is no data) or took place less than three times during the observation period.

The lightest pink squares (where there are no columns) on the D - I plane refer to rainfall conditions that are not associated with landslides and, as shown in Figure 6.18, cover about 16% of all the cases considered. (Note that Figure 6.17 does not cover all cases, excluding durations less than two hours and intensities greater than 7.5mm/h, in order to better highlight the combinations of higher probability of landslide occurrence.) The darker the shade the higher the conditional probability, the highest three columns (darkest reds) correspond to the highest three probabilities of 50%, 67% and 100%, these probabilities are however based on as sample size of four, three and three events, respectively. The darker pink columns correspond to conditional probabilities less than or equal to 0.4, and in particular there are five columns at $P(L|D,I)$ between 0.33 and 0.4.

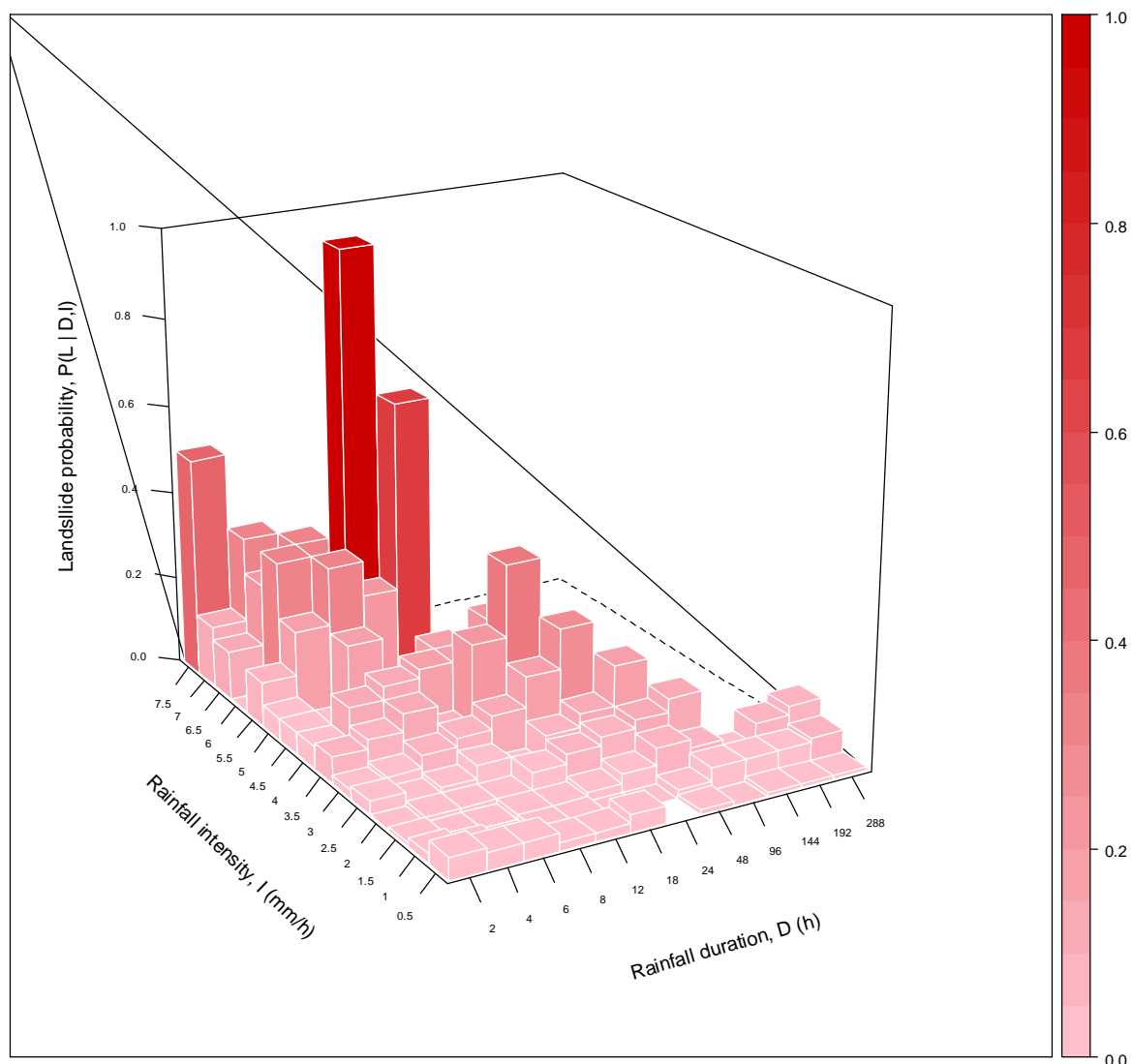


Figure 6.17: Conditional probability of landslide for a given rainfall event of duration D and intensity I , based on the data collected from the Rest and be Thankful. The intensity of the red corresponds to the values of $P(L|D,I)$ on the y-axis gauge

Figure 6.18 shows the number of rainfall conditions with a conditional probability of causing a landslide $P(L|D,I)$ in a certain range of values (orange line), regardless of the intensity or duration. The columns represent how many times a certain range of conditional probabilities appear in the data.

The graph shows that 16% of the (D,I) combinations, mostly for low intensities, are not associated with landslides and a probability of $P(L|D,I)$ of zero is implied. A further 61% of the (D,I) combinations have a $P(L|D,I)$ of greater than zero and less than or equal to 0.1 (10%) and thus 23% of the observations correspond to probabilities greater than 0.1 (10%). Probabilities of greater than 0.4 (40%) (i.e. the furthest two columns to the right of the graph) constitute only 2% of the (D,I) combinations. Due to the small sample size these higher probabilities are not statistically significant and therefore these figures must be viewed with caution until additional data can be added to the analysis; it is unlikely to be possible at present to derive probabilistic thresholds at probabilities greater than 0.4 (40%).

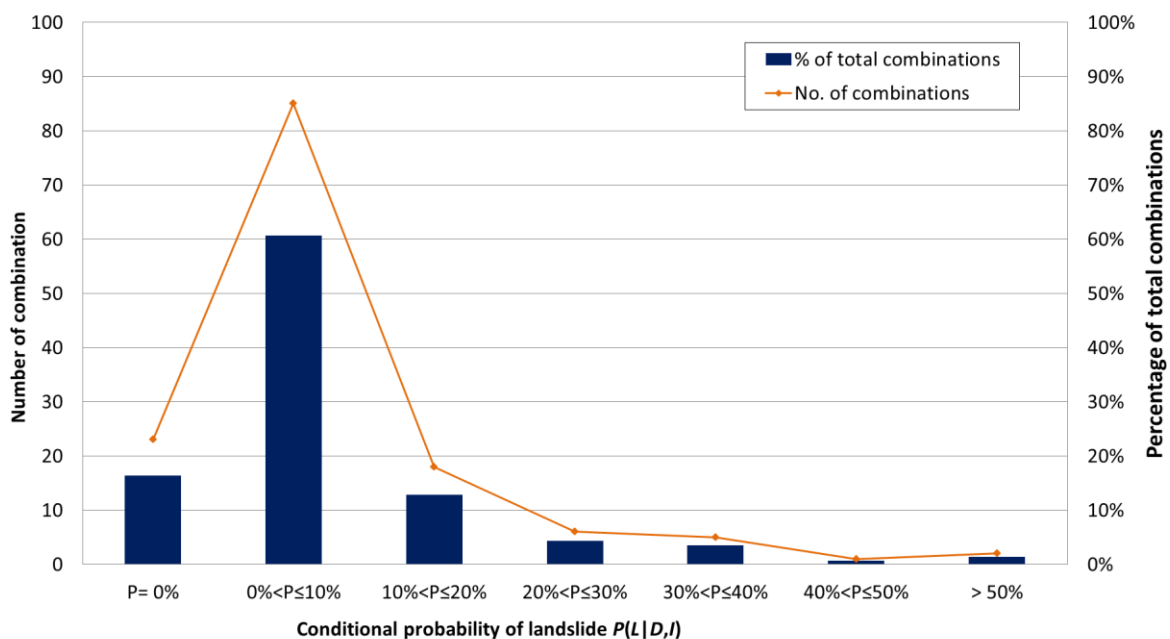


Figure 6.18: Number of rainfall combinations of intensity and duration for different intervals of the conditional landslide probability (line). The columns show the percentage of total combinations.

Figure 6.19 shows that, for each combination of (D,I) , it is possible to associate both the conditional probability and the sample size; the latter is represented by the dimension of the bubble, while the former is represented by the colour (as given in the key). Therefore, it is possible to infer the relative significance of the calculation. For example, there are 10 combinations of (D,I) which have $P(L|D,I)$ between 10 and 15% (dark blue), but not all of the pairs have the same statistical significance: the larger the bubble, the larger the sample and thus the more statistically reliable the result. The result for the rainfall events with $D=48h$ and $I=2mm/h$ ($10% < P(L|D,I) < 15%$) is more reliable than the same result for coupled variables such as $D=96h$ and $I=2mm/h$. Figure 6.19 also shows that results with higher probability such as coupled variables $D=8h$ and $I=6mm/h$ (dark orange), where the

conditional probability is 100%, is not particularly statistically significant as it is only based on a small sample (three events).

Figure 6.17 shows that the analysis revealed that rainfall events with intensity lower than 1.5mm/h are unlikely to generate landslides. However, among the coupled variables (D, I) available there are combinations of rainfall durations and intensity which are more likely to cause landslides; these follow a pattern, which can be visualised as an approximately linear trend in the semi-logarithmic plane of Figure 6.19. This trend broadly means, as expected, that the higher the intensity, the shorter is the time interval before a landslide occurs. Another way of articulating this is to state that the longer the rainfall duration, the lower the rainfall intensity required to cause a landslide.

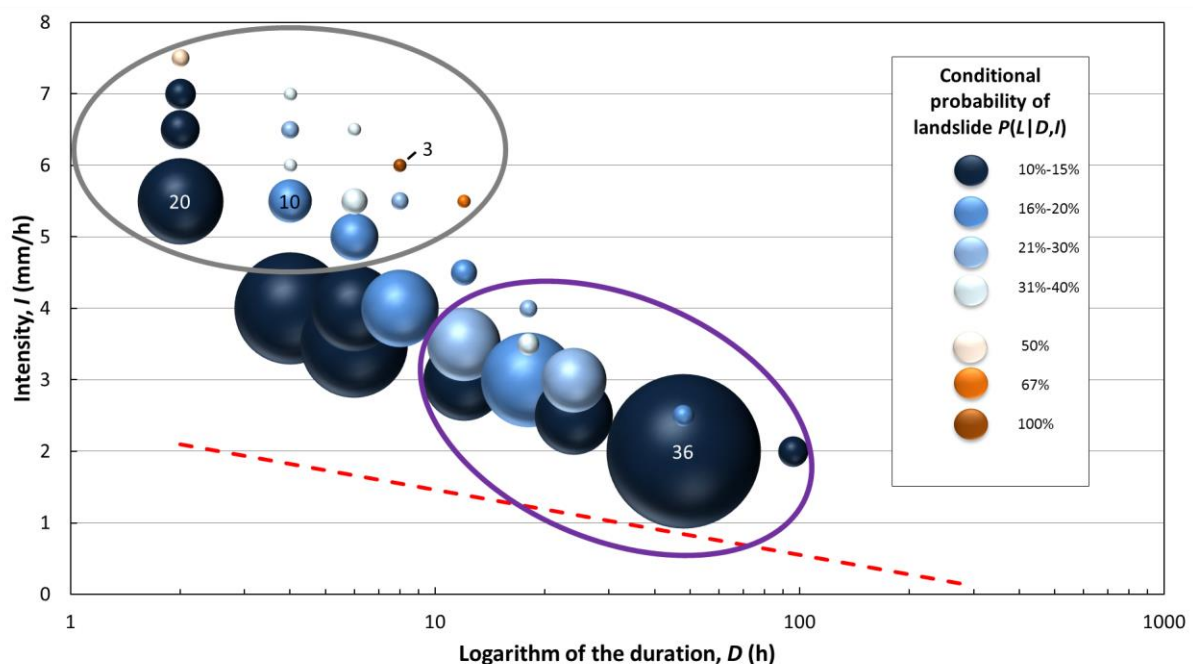


Figure 6.19: Coupled variable (D, I) with conditional probability of landslides higher than 10%. The dimension of the bubble is proportional to the sample size on which the calculation is based (four sample sizes are reported as references). The red dashed line represents the deterministic threshold developed by Winter et al. (2010)

An alternative way of displaying the result is to consider horizontal cross sections of the three-dimensional representation of Figure 6.17 that is, drawing the iso-density (i.e. same probability density) lines in a two-dimensional contour plot. The results of the Bayesian analysis are presented in Figure 6.20, where the lines corresponding the probabilities 0.025, 0.05, 0.1, 0.2, 0.3 and 0.9 (2.5%, 5%, 10%, 20%, 30% and 90%) are shown (the white surface corresponds to lack of data or to a number of rainfall events less than three).

This graphical technique helps to emphasize the variation in the dependent variable (i.e., the conditional probability, $P(L|D, I)$) as a function of the independent variables (i.e., the rainfall duration, D , and intensity, I). In particular the gradient of the function is revealed by the distance between the contour lines; the closer the contour (iso-density) lines, the greater the magnitude of the gradient, which means that the rate of change is greater. This area is shown in red in Figure 6.20 and identifies the combinations of rainfall duration and

intensity (centred around approximately 8 hours, 6mm/h) for which the conditional landslide probability, $P(L|D,I)$, is more sensitive. It is noted that this region corresponds to the highest probabilities, Figure 6.21 shows this area in detail.

Figure 6.20 suggests that rainfall durations from around four to 18 hours most strongly influence landslide occurrence; however, the statistical significance of this result is very low, due to the small sample size for these durations (see grey ellipse in Figure 6.19). The analysis also reveals that rainfall events of durations from 18 to 96 hours (Figure 6.20) are connected with landslide occurrences. This influence is less pronounced than the previous case; however, based on the available data, the reliability of this result is higher, since it is drawn from a larger sample size (see purple ellipse in Figure 6.19). This disparity in sample size is, however, a function of the physical process – there are more long duration, low intensity rainfall events than there are short duration, high intensity events (storms) – and it may be more appropriate to consider that this suggests that rainfall durations between four and 96 hours and intensities of between 4 and 7.5mm/h play a significant role in initiating in initiating landslide events. For values of $P(L|D,I)$ of around 30% (0.3), rainfall intensities of around 5.5mm/h to 6mm/h are indicated for durations of four to eight hours, respectively, while intensities of around 3mm/h to 4mm/h are indicated for durations of 12 to 18 hours.

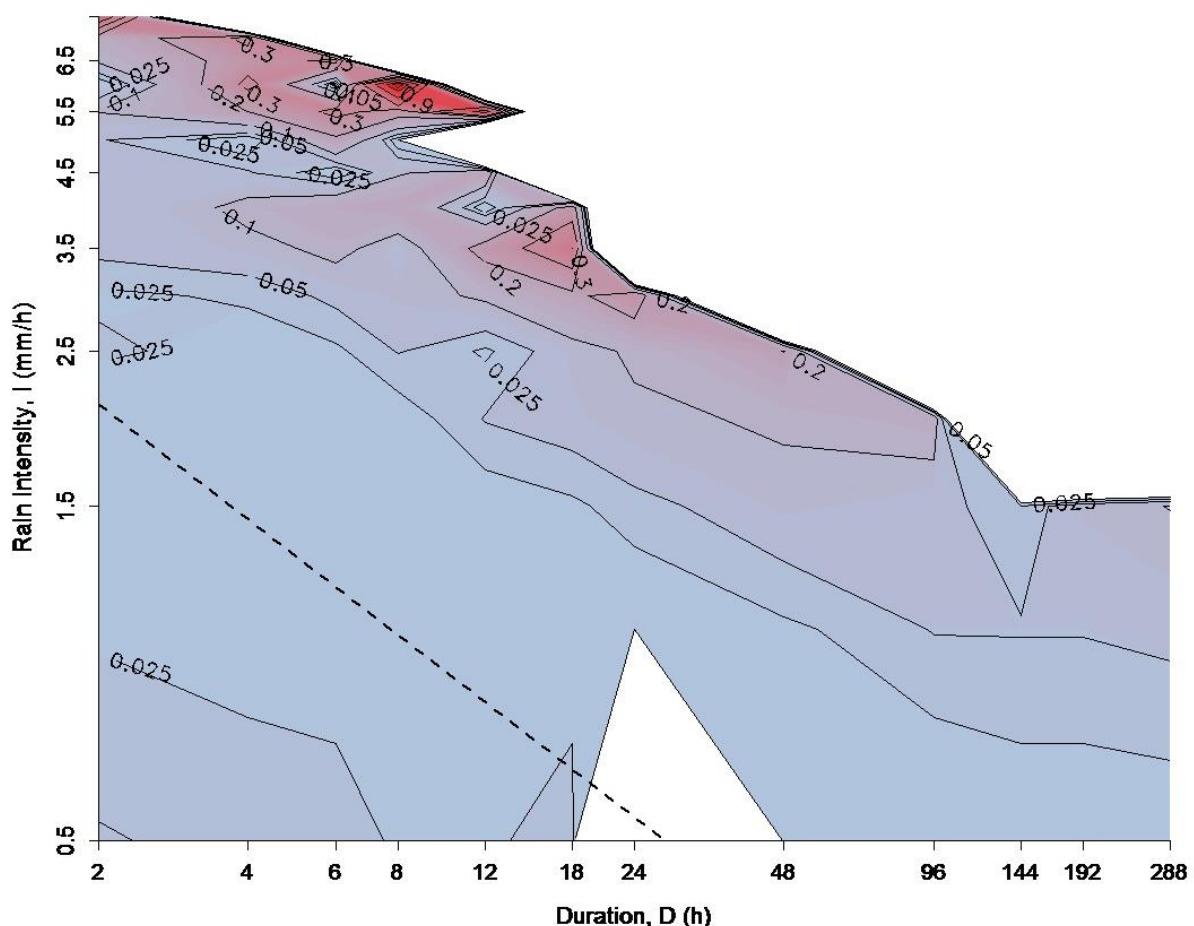


Figure 6.20: Conditional probability iso-lines $P(L|D,I)$ obtained from the Rest and be Thankful data. The dashed line represents the deterministic threshold developed by Winter et al. (2010)

The significant combinations of these two sets of independent variables, D and I , seem to follow the linear behaviour described above, that is, higher probabilities of landslide correspond to short periods of rain characterised by high intensities, or to low intensity events with long durations. It is noteworthy that the trend of this region is approximately parallel to the deterministic threshold (dashed line in Figure 6.20), and gives some comfort that the results are broadly consistent with previous work (Winter et al., 2010). This is especially the case as Winter et al. (2010) acknowledged that the nature of the rain gauge network was such that the tentative deterministic threshold was likely to be conservative (corresponding to a probability of around 0.025 or 2.5% in Figure 6.22) and an increase in the rainfall intensity (or duration) required to initiate a landslide being indicated by this work is entirely consistent with previous observations.

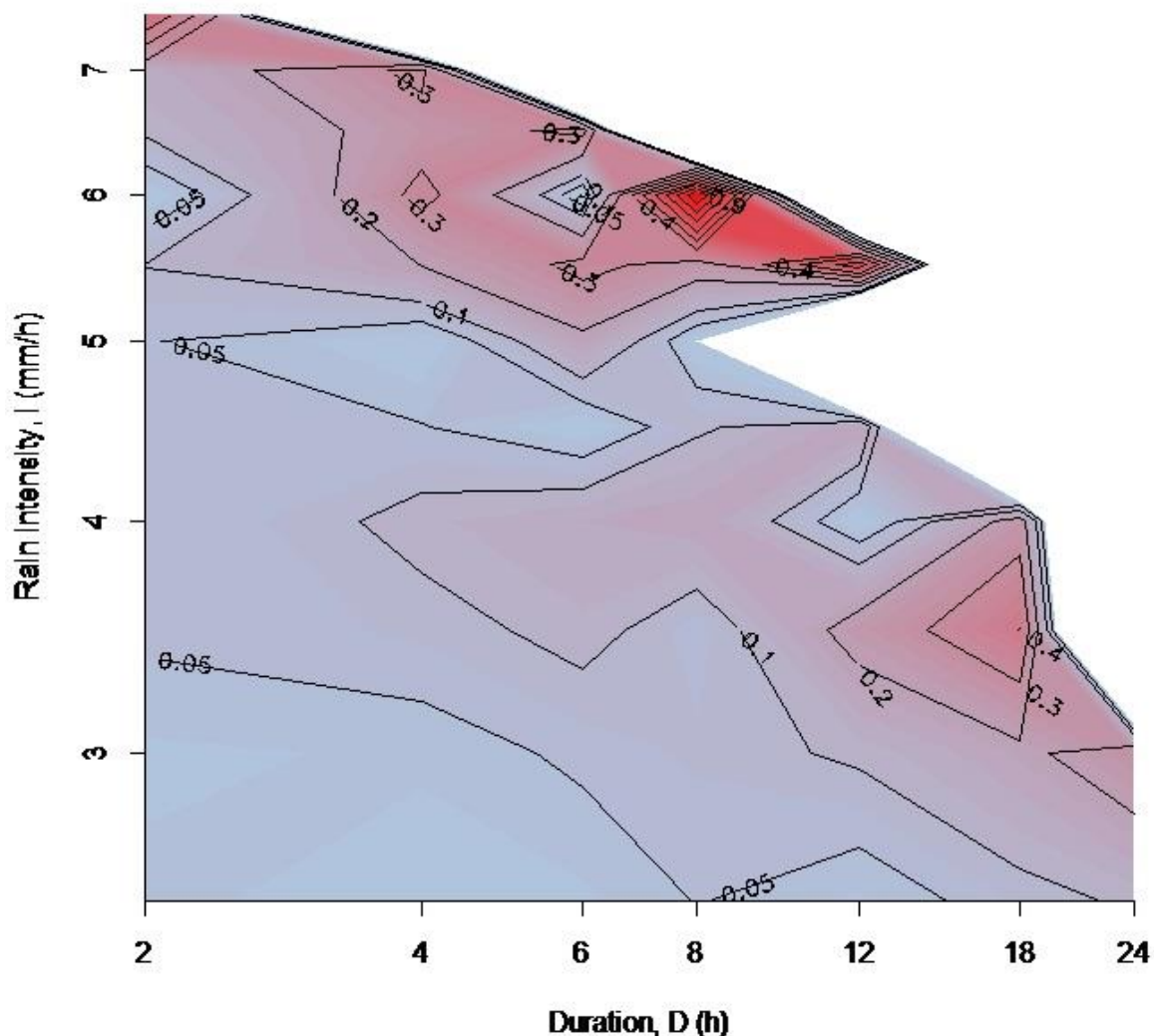


Figure 6.21: Conditional probability iso-lines $P(L|D,I)$ obtained from the Rest and be Thankful data (detail of Figure 6.20)

The deterministic threshold simply divides the D,I plane into two areas, roughly corresponding to coupled variables which are believed to cause landslides or not cause landslides; it does not provide an estimation of the likelihood of false positives and false negatives (see Section 3). The Bayesian analysis reported here adds information about the characteristics that a rainfall event must have in order to be considered critical. Specifically,

it is possible to associate rainfall events, defined by different durations and intensities, with a probability of a landslide being triggered.

The spacing of the contours in Figure 6.20 and Figure 6.21 decreases at rainfall intensities notionally in excess of 1.5mm/h indicates that the probability $P(L|D,I)$ increases more rapidly with increasing intensity and/or increasing duration. At probabilities greater than around 0.3 (30%) the spacing becomes sufficiently close that it is not practical to effectively define thresholds for higher probabilities as the differences between the intensities and durations linked to those probabilities are likely to be significantly less than the associated data ranges. Notwithstanding this it does appear possible to define lines that correspond to different actions similar to those set-out in Section 5 (Figure 5.5).

Figure 6.22 is based on the results presented in Figure 6.20 and gives thresholds for conditional probabilities of 5%, 10%, 20% and 30% of a landslide occurring given a combination of rainfall intensity, I , and duration, D . The black dotted line represents the available data within the study and the red dotted line represents the deterministic threshold from Section 5.

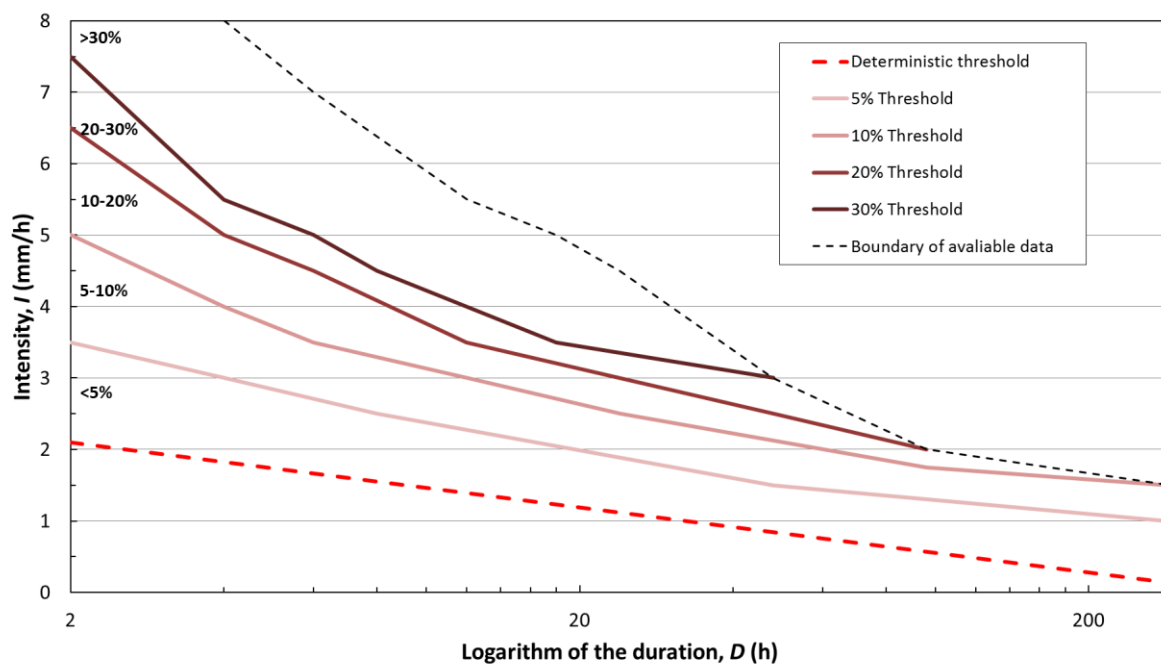


Figure 6.22: Conditional probability threshold of landslides given a rainfall event of Intensity I and Duration D , based on results given in Figure 6.20. The red dashed line represents the deterministic threshold developed by Winter et al. (2010)

Figure 6.22 potentially can be used for probabilistic estimates of the likelihood of a landslide occurring, based on forecast rainfall data, particularly on the A83 between Ardgartan and the Rest and be Thankful car park (Figure 6.1) given specific rainfall intensity and durations.

The analysis presented here is based on six years' of data but its robustness is very much dependent upon the number of landslide events. While the number of landslide events that it has been possible to incorporate in the analysis is significant in the context of Scotland, and indeed the rest of the UK, the number of landslide events available for analysis (21) is small in comparison to many other parts of the world. For this reason Winter et al. (2007b)

develop the approach used here that allows the use of data related to rainfall events that were not associated with landslides and this brings a further 599 events into the analysis (total rainfall events 620). This relative paucity of event data is a fact in the setting in which this work was conducted and it is not considered necessary to conduct further cycles of analysis that are not associated with an attempt to trial the operation of a probabilistic landslide forecast system, based on Figure 6.22, and associated with a risk management strategy. Such a forecast might be used, for example, to action specific landslide risk reduction actions such as the wig-wags described in Section 3 (see also Winter et al., 2013b; Winter & Shearer, 2017).

It is particularly important to note in this context that if such a trial is conducted that it is essential that rainfall data is used from the gauges at the Rest and be Thankful and/or Loch Restil. Winter et al. (2010) pointed out that the deterministic threshold was conservative due inter alia to the remote location and lower elevation of rain gauges that formed part of the national network at the time (i.e. the data that they acquired was closely related to the synoptic objective of the network). This is confirmed by the juxtaposition of the deterministic threshold and the probabilistic thresholds in Figure 6.22, with the deterministic threshold being located at considerably lower values of rainfall intensity as would be expected.

7 Conclusions and Recommendations

The link between rainfall and debris flow (and landslides more generally) is well-established in Scotland and a tentative threshold to describe the relation between rainfall and debris flow has been available for almost a decade.

This tentative, deterministic threshold is limited by the lack of data proximal to the debris flow events that occur and has always been considered to underestimate the amount of rain required to trigger an event. To this end two rain gauges were installed in the area around the A83 Rest and be Thankful, where debris flow events occur relatively frequently in Scotland.

This threshold is also limited by its deterministic nature, albeit at the time that it was developed there were no known probabilistic thresholds. Like all deterministic thresholds it simply divides the rainfall duration-intensity plane into two regions: one in which debris flow occurs and one in which debris flow does not occur. This binary approach is not well-matched to reality, which is significantly more complex, and in reality the two regions represent undefined, but greater and lesser, likelihoods of event occurrence. A probabilistic approach provides a more realistic, reliable and defensible rainfall trigger threshold for debris flow that is, additionally, based on similar principles to rainfall forecasts. This approach potentially yields a suite of rainfall thresholds, or rainfall states, that correspond to differing probabilities of debris flow occurrence given different rainfall duration-intensity pairings.

An evaluation of the effectiveness of wig-wag landslide warning signs, that are activated using rainfall levels closely related to the tentative deterministic threshold, suggests that around 90% of events occurred when the signs were activated. There were, however, at least two instances of 'false negatives' being indicated when landslides occurred when the wig-wag warnings were not active. Further a significant number of 'false positives' was reported, broadly correlating with the wig-wags being switched on seven times for each landslide event.

In this report an analysis is presented to demonstrate the potential of such a probabilistic approach to this problem. This approach has the additional advantage that data from rainfall events that did not lead to debris flow can be used in addition to data that did lead to debris flow. This goes some way towards overcoming the obstacle imposed by the relatively limited number of landslide events that are available for analysis. For the analyses presented here 21 rainfall events that were associated with a landslide and a further 599 rainfall events that were not associated with a landslide were included.

The analyses carried out include the determination of the prior probability of a landslide, $P(L)$; the one-dimensional probabilities for landslide occurrence given rainfall of a particular duration, $P(L|D)$, intensity, $P(L|I)$, or total, $P(L|E)$, has occurred; and the two-dimensional probability of a landslide occurring as a result of combinations of rainfall duration and intensity, $P(L|D,I)$. The key findings from the results are summarised in the following paragraphs.

The prior probability of a landslide, $P(L)$, is approximately 0.034 (3.4%) based on a minimum rainfall intensity of 0.5mm/h over a 24 hour period.

The one-dimensional analysis in which rainfall duration and intensity are treated separately in terms of the conditional probability of landslides occurring as a result of rainfall (i.e. $P(L|D)$, $P(L|I)$ and $P(L|E)$) suggests the following:

- The most important antecedent period is between 18 and 96 hours, which period is associated with the conditional landslide probability $P(L|D)$ approaching twice the value of the prior probability $P(L)$.
- Most landslides are associated with rainfall intensities between 3mm/h and 7.5mm/h (there is little data for intensities in excess of 7.5mm/h), again with conditional probabilities $P(L|I)$ approaching twice the value off the prior probability $P(L)$.
- For a duration of 288 hours (12 days) a total rainfall amount in excess of 150mm increases the value of conditional probability $P(L|E)$ of a landslide by a factor of up to four compared to the prior probability $P(L)$.
- For shorter durations the conditional probability $P(L|E)$ increases to values in excess of the prior probability $P(L)$ for lower rainfall totals. For example, for a 96 hour duration, a total rainfall of around 75mm is indicative of an increase in the conditional probability $P(L|E)$ to around twice the value of the prior probability $P(L)$.

Conclusions drawn from the two-dimensional analysis in which combinations of rainfall duration and intensity are considered in terms of the conditional probability of landslides occurring as a result of rainfall (i.e. $P(L|D,I)$) suggest the following:

- Rainfall durations of between four and 96 hours, and intensities of between 4mm/h and 7.5mm/h, play a significant role in initiating landslide events.
- The graph shows that 16% of the (D,I) combinations, mostly for low intensities, are not associated with landslides and a conditional probability of $P(L|D,I)$ of zero is implied. A further 61% of the (D,I) combinations have a $P(L|D,I)$ of 0.1 (10%) or less and 23% of the observations correspond to probabilities greater than 0.1 (10%). Probabilities of greater than 0.4 (40%) constitute only 2% of the (D,I) combinations.
- At higher intensities and shorter durations the lack of data as well as the rapid rate of change of the conditional probability $P(L|D,I)$ with increased rainfall means that it is not practical to estimate probabilities greater than around 0.3 (30%) for use in any meaningful hazard or risk management framework.

The two-dimensional analysis additionally allows probability thresholds for $P(L|D,I)$ from 0.05 (5%) to 0.3 (30%) to be established. It is not considered necessary to conduct additional cycles of analysis to further develop the threshold(s). However, trialling the operation of a probabilistic landslide forecast system is an option. Such a forecast ultimately might be used, for example, to action specific landslide risk reduction actions such as the wig-wags that are currently in use at the site. With a 0.3 probability threshold each time a forecast is made the likelihood of a landslide occurring is approximately 1 in 3. Although temporal variations are inevitable over an extended time period it is not unreasonable to expect an average of one landslide to occur for every three times the threshold is breached and a warning is issued (say) by switching on the wig-wag warning signs. This compares favourably with the current estimated one landslide for every seven time the wig-wags are switched on.

It is recommended that such a 'shadow' trial be considered at the A83 Rest and be Thankful. It is anticipated that, in time, the threshold might form the first level of a tiered warning system indicating 'higher probability of debris flow' (due to rainfall), 'debris flow near-imminent' (measurement of physical on-slope parameters or movement) and 'debris flow occurred' (potentially using seismic techniques).

Amongst the key issues that must be considered and resolved prior to a trial commencing are, the following:

- the approach to rainfall forecasting within the framework of the (D,I) plane, including specific the (D,I) combinations to be used in forecasting;
- whether the trial is 'live' with actions taken on the basis of the forecast or, at least in the initial stages, 'dummy' with hypothetical actions recorded on the basis of the forecast; and
- the hazard or risk management framework within which it is envisaged that the framework will be used.

It is suggested that a programme for the development of the trial should follow the actions below:

- Consultation with key stakeholders such as Transport Scotland, Traffic Scotland, Met Office, SEPA and the Operating Company.
- Determine forecasting and operational requirements and the interactions between such requirements.
- Determine the need for additional gauges and/or additional funding-support to continue the operation of the existing gauges.
- Determine the structure of the trial.
- Decide on the responsibility for data acquisition, analysis and delivery of 'shadow' warnings.
- Decide on responsibility for evaluation of the effectiveness of the warning system relative to the occurrence of landslides and setting the results within a hazard and risk management framework.
- Determine clear success criteria from the outset of the trial.
- Determine costs and programme for consideration by Transport Scotland senior management.

Whatever approach is taken to the trial it is essential that the rainfall data used is derived from the Rest and be Thankful and/or Loch Restil gauges (gauges even more proximal to the slope could be used but any such new gauges should conform to national standards set by the Met Office). This requirement to use local gauge data is a result of the conservative nature of the data that is acquired from the remote and lower elevation gauges and that form part of the national network; the national network is designed for synoptic purposes and not for the purposes set out in this report. This may require an upgrade to the current installations in order to allow data to be acquired in real time or near-real time.

If the trial proves successful and is used operationally at the A83 Rest and be Thankful then the introduction of landslide warnings to the broader north-west region of Scotland for other areas prone to rainfall-induced debris flows also could be considered.

Implementation of the new probabilistic rainfall threshold implies an increase in rainfall levels over the current deterministic threshold. While this is the case, the wider context is that the current threshold is based on data remote from the area that is less than representative of rainfall at the site while the new the threshold is based on local data. This confirms the expectation that local rainfall is considerably greater than would be anticipated from the national network upon which the deterministic threshold is based.

Acknowledgements

The authors are grateful for the inputs of Louise Lloyd and Iain Yorke in developing the outline conceptual approach to the Bayesian analysis.

Stuart Dunning, Rupert Bainbridge (Newcastle University), Mike Lim and Bradley Sparkes (Northumbria University) and thanked for their work and assistance in identifying events from late-2014 onwards, particularly through the use of time-lapse photography and LiDAR.

The initial rainfall data analysis that is reported in Section 6.1 was undertaken by Met Office under contract to TRL. The methodology was developed and the initial analysis (2012 to 2014 data) was undertaken by John Fullwood and subsequent analyses were undertaken by Jill Dixon (2012 to 2015 data) and Matthew Perry (2012 to 2018 data).

References

- Ahmad, R. 2003. Developing early warning systems in Jamaica: rainfall thresholds for hydrogeological hazards. *Proceedings, National Disaster Management Conference*. Ocho Rios (St Ann), Jamaica: Office of Disaster Preparedness and Emergency Management. (Sourced from <http://www.mona.uwi.edu/uds/> June 2006.)
- Aleotti, P. 2004. A warning system for rainfall-induced shallow failures. *Engineering Geology*, **73**, 247-265.
- Anon. 1989. *The climate of Scotland – some facts and figures*. London: The Stationery Office.
- Anon. 2007. *Rainfall thresholds for the initiation of landslides*. Istituto di Ricerca per la Protezione Idrogeologica, Italy. (Accessed June 2007 <http://rainfallthresholds.irpi.cnr.it/>.)
- Anon. 2013. A83 Trunk Road Route Study: Part A – A83 Rest and be Thankful. Final Report. Report prepared by Jacobs for Transport Scotland, 212p. (Accessed March 2013, <http://www.transportscotland.gov.uk/road/maintenance/landslides/>.)
- Barnett, C., Perry, M., Hossell, J., Hughes, G. & Procter, C. 2006a. A handbook of climate trends across Scotland; presenting changes in the climate across Scotland over the last century. 58p. *SNIFFER Project CC03*. Edinburgh: Scotland and Northern Ireland Forum for Environmental Research.
- Barnett, C., Perry, M., Hossell, J., Hughes, G. & Procter, C. 2006b. Patterns of climate change across Scotland: technical report, 102p. *SNIFFER Project CC03*. Edinburgh: Scotland and Northern Ireland Forum for Environmental Research.
- Berti, M., Martina, M. L. V., Franceschini, S., Pignone, S., Simoni, A. & Pizziolo, M. 2012. Probabilistic rainfall thresholds for landslides occurrence using a Bayesian approach. *Journal of Geophysical Research*, **117**(F04006), 1-20.
- Brunetti, M. T., Peruccacci, S., Rossi, M., Luciani, S., Valigi, D. & Guzzetti, F. 2010. Rainfall thresholds for the possible occurrence of landslides in Italy. *Natural Hazards and Earth System Sciences*, **10**(3), 447-458.
- Caine, N. 1980. The rainfall intensity-duration control of shallow landslides and debris flows. *Geografiska Annaler*, **62 A**, 23-27.
- Campbell, R. H. 1975. Soil slips, debris flows, and rainstorms in the Santa Monica Mountains and vicinity, southern California. *US Geological Survey Professional Paper 851*, 51p.
- Cannon, S. H., Gartner, J. E., Wilson, R. C., Bowers, J. C. & Laber, J. L. 2008. Storm rainfall conditions for floods and debris flows from recently burned area in southwestern Colorado and southern California. *Geomorphology*, **96**(3-4), 250-269.
- Eyles, R. J. 1979. Slip-triggering rainfalls in Wellington City, New Zealand. *New Zealand Journal of Science*, **22**(2), 117-122.
- Flentje, P. & Chowdury, R. 2009. Observational approach for urban landslide management. *Engineering Geology for Tomorrow's Cities*, Geological Society Engineering Geology Special Publication No 22, Paper No 522, 12p. London: The Geological Society.
- Fukuoka, M. 1980. Landslides associated with rainfall. *Geotechnical Engineering*, **11**, 1-29.

- Hurlimann, M., Rickenmann, D. & Graf, C. 2003. Field and monitoring data of debris flow events in The Swiss Alps. *Canadian Geotechnical Journal*, **40**, 161-175.
- Jones, F. O. 1973. Landslides of Rio de Janeiro and the Serra das Araras Escarpment, Brazil. *US Geological Survey Professional Paper 697*, 42p.
- Kendon, M., McCarthy, M. & Jevrejeva, S. 2015. *State of the UK climate 2014*. Exeter: The Met Office.
- Kendon, M., McCarthy, M., Jevrejeva, S. & Legg, T. 2016. *State of the UK climate 2015*. Exeter: The Met Office.
- Kendon, M., McCarthy, M., Jevrejeva, S. & Legg, T. 2017. *State of the UK climate 2016*. Exeter: The Met Office.
- Kendon, M., McCarthy, M., Jevrejeva, S., Matthews, A. & Legg, T. 2018. State of the UK climate 2017. *International Journal of Climatology*, **38**(S2), 1-35.
- Ko, F. W. Y. 2005. Correlation between rainfall and natural terrain landslide occurrence in Hong Kong. *GEO Report No. 168*. Hong Kong SAR: Geotechnical Engineering Office.
- McAdam. 1993. *Edinburgh – a landscape fashioned by geology*. Edinburgh: Scottish Natural Heritage and British Geological Survey.
- McGregor, P. & MacDougall, K. 2009. A review of the Scottish rain-gauge network. *Proceedings, Institution of Civil Engineers (Water Management)*, **162**(2), 137-146.
- Milne, F. D., Werritty, A., Davies, M. C. R. & Browne, M. J. 2009. A recent debris flow event and implications for hazard management. *Quarterly Journal of Engineering Geology and Hydrogeology*, **42**(1), 51-60.
- Roberts, N. M., Cole, S. J., Forbes, R. M., Moore, R. J. & Boswell, D. 2009. Use of high-resolution NWP rainfall and river flow forecasts for advance warning of the Carlisle flood, north-west England. *Meteorological Applications*, **16**, 23-34
- Selby, M. J. 1976. Slope erosion due to extreme rainfall: a case study from New Zealand. *Geografiska Annaler*, **58 A**, 131-138.
- Sidle, R. C. & Swanson, D. N. 1982. Analysis of a small debris slide in coastal Alaska. *Canadian Geotechnical Journal*, **19**(2), 167-174.
- Sparkes, B, Dunning, S, Lim, M & Winter, M G. 2017. Characterisation of recent debris flow activity at the Rest and be Thankful, Scotland. *Advancing Culture of Living with Landslides: Volume 5, Landslides in Different Environments* (Eds: Mikoš, M, Vilímek, V, Yin, Y & Sassa, K), 51-58. Switzerland: Springer.
- Sparkes, B, Dunning, S A, Lim, M & Winter, M G. 2018. Monitoring and modelling of landslides in Scotland: characterisation of slope geomorphological activity and the debris flow geohazard. *Published Project Report PPR 852*. Wokingham: Transport Research Laboratory.
- Toll, D. G. 2001. Rainfall-induced landslides in Singapore. *Proceedings, Institution of Civil Engineers (Geotechnical Engineering)*, **149**(4), 211-216.

-
- VanDine, D.F. 1996. Debris flow control structures for forest engineering. *Ministry of Forests Research Program, Working Paper 22/1996*. Victoria, BC: Ministry of Forests.
- Wieczorek, G. F. 1987. Effect of rainfall intensity and duration on debris flows in central Santa Cruz Mountains, California. Debris Flow/Avalanches: Process, Recognition and Mitigation (Eds: Costa, J.E. & Wieczorek, G.F.). *Reviews in Engineering Geology*, **VII**, 93-104. Boulder, CO: Geological Society of America.
- Winter, M. G. 2013. Discussion Session 4.3: Landslides. *Geotechnics of Hard Soils – Weak Rocks: Proceedings, XV European Conference on Soil Mechanics and Geotechnical Engineering*, (Eds: Anagnostopoulos, A, Pachakis, M. & Tsatsanifos, C.) **4**, 427-434. Amsterdam: IOS Press.
- Winter, M. G. 2014a. A strategic approach to landslide risk reduction. *International Journal of Landslide and Environment*, **2**(1), 14-23.
- Winter, M. G. 2014. The vulnerability shadow cast by debris flow events. *Engineering Geology for Society and Territory, Volume 6: Applied Geology for Major Engineering Works* (Eds: Lollino, G., Giordan, D., Thuro, L., Carranza-Torres, C., Wu, F., Marinos, P. & Delgado, C.), 641-644. Heidelberg: Springer.
- Winter, M. G. 2018. The quantitative assessment of debris flow risk to road users on the Scottish trunk road network: A85 Glen Ogle. *Published Project Report PPR 799*. Wokingham: Transport Research Laboratory.
- Winter, M. G. 2019. Debris flows. In: *Geological Hazards in the UK: their Occurrence, W and Mitigation* (Eds: Giles, D. P. & Griffiths, J. S.). Engineering Geology Special Publication 29. London: Geological Society. (In Press)
- Winter, M. G. & Bromhead, E.N. 2012. Landslide risk – some issues that determine societal acceptance. *Natural Hazards*, **62**, 169-187.
- Winter, M. G. & Corby, A. 2012. A83 Rest and be Thankful: ecological and related landslide mitigation options. *Published Project Report PPR 636*. Wokingham: Transport Research Laboratory.
- Winter, M. G. & Shearer, B. 2013. Climate change and landslide hazard and risk - a Scottish perspective. *Published Project Report PPR 650*. Wokingham: Transport Research Laboratory.
- Winter, M. G. & Shearer, B. 2017. An extended and updated technical evaluation of wig-wag signs at the A83 Rest and be Thankful. *Published Project Report PPR 743*. Wokingham: Transport Research Laboratory.
- Winter, M. G., Macgregor, F. & Shackman, L. (Eds.). 2005. *Scottish road network landslides study*, 119p. Edinburgh: The Scottish Executive.
- Winter, M. G., Heald, A., Parsons, J., Shackman, L. & Macgregor, F. 2006. Scottish debris flow events of August 2004. *Quarterly Journal of Engineering Geology and Hydrogeology*, **39**(1), 73-78.
- Winter, M. G., Shackman, L. & Macgregor, F. 2007a. Landslide management and mitigation on the Scottish road network. *Landslides and Climate Change: Challenges and Solutions* (Eds: McInnes, R., Jakeways, J., Fairbank, H. & Mathie, E.), 249-258. London: Taylor & Francis.
-

Winter, M. G., Parsons, J. A., Nettleton, I. M., Motion, A., Shackman, L. & Macgregor, F. 2007b. Proactive debris flow detection in Scotland. *Landslides and Society – Integrated Science, Engineering, Management and Mitigation* (Eds: Schaefer, V. R., Schuster, R. L. & Turner, A. K.), 225-233. Association of Environmental & Engineering Geologists Special Publication 23. Wisconsin, USA: OMNI Press.

Winter, M. G., Macgregor, F. & Shackman, L. (Eds.). 2009. *Scottish road network landslides study: implementation*, 278p. Edinburgh: Transport Scotland.

Winter, M. G., Dent, J., Macgregor, F., Dempsey, P., Motion, A. & Shackman, L. 2010. Debris flow, rainfall and climate change in Scotland. *Quarterly Journal of Engineering Geology & Hydrogeology*, **43**(4), 429-446.

Winter, M. G., Harrison, M., Macgregor, F. & Shackman, L. 2013a. Landslide hazard assessment and ranking on the Scottish road network. *Proceedings, Institution of Civil Engineers (Geotechnical Engineering)*, **166**(GE6), 522-539.

Winter, M. G., Kinnear, N., Shearer, B., Lloyd, L. & Helman, S. 2013b. A technical and perceptual evaluation of wig-wag signs at the A83 Rest and be Thankful. *Published Project Report PPR 664*. Wokingham: Transport Research Laboratory.

Winter, M. G., Smith, J. T., Fotopoulou, S., Pitilakis, K., Mavrouli, O., Corominas, J. & Argyroudis, S. 2014. An expert judgement approach to determining the physical vulnerability of roads to debris flow. *Bulletin of Engineering Geology and the Environment*, **73**(2), 291-305.

Winter, M G, Sparkes, B, Dunning, S A & Lim, M. 2017. Landslides triggered by Storm Desmond at the A83 Rest and be Thankful, Scotland: panoramic photography as a potential monitoring tool. *Published Project Report PPR 824*. Wokingham: Transport Research Laboratory.

Wong, J. F. C. & Winter, M. G. 2018. The quantitative assessment of debris flow risk to road users on the Scottish trunk road network: A83 Rest and be Thankful. *Published Project Report PPR 798*. Wokingham: Transport Research Laboratory.

Appendix A The procedure for sorting and analysing 15-minute rainfall data

Stage 1

1. Sort data into descending order with newest date first and if the last day is only a partial day delete this last day. Note the data are archived against the 15 minute period ending with the time shown so, for example, the first entry for 16/01/2015 00:00 relates to the 15 minute period 23:45:01 on 15/01/2015 to 00:00:00 on 16/01/2015.
2. Calculate the average 15 minute rainfall intensity by multiplying the 15-minute rainfall total by 4.
3. Create columns headed 15 minutes, 30 minutes, 1 hour, 2 hours, 4 hours, 6 hours, 8 hours, 12 hours, 18 hours, 24hours, 48 hours, 96 hours, 144 hours, 192 hours and 288 hours. For every 15-minute rainfall intensity calculate the average antecedent rainfall intensity over the preceding 1, 2, 4, 8, 16, 24, 32, 48, 96, 192, 384, 576, 768 and 1152 observations (equivalent to preceding 15 minutes, 30 minutes, 1 hour, 2 hours, 4 hours, 6 hours, 8 hours, 12 hours, 18 hours, 24hours, 48 hours, 96 hours, 144 hours, 192 hours and 288 hours) and allocate to appropriate column.
4. Find the maximum 15 minute rainfall intensity in each day.
5. Also calculated at this stage were hourly rainfall totals and the maximum 15 minute rainfall intensity in each hour (although may not be required).

Stage 2

6. Identify the 15 minute value that has the maximum intensity in the day.

Stage 3

7. Delete all rows that relate to days with a maximum rainfall intensity of zero and store in a folder 'Cuts_Zero', except for landslip dates – see 9 below.
8. Identify the 15 minute value that has the maximum intensity in the day and delete all other values in that day and store in a folder 'Cuts_Non_Max_Hours', except for landslip dates – see 3. Note, if the maximum intensity occurs on more than one occasion in a day, leave only the latest occurrence in the day, the other values to be stored in a folder 'Cuts_Duplicates'. Check if the maximum value occur at the midnight observation (which has the date of the next day) to ensure there are not two values for one day. There were none for 'Rest and Be Thankful' and two occasions at Loch Restil (on two consecutive days!) highlighted in green in spreadsheet - 25/12/2014 (00:00) which relates to the last hour of the 24th plus 24/12/2014 (00:00) which relates to the last hour of the 23rd so there is no double-counting.
9. For all landslip days (highlighted in yellow) identify the time when the landslip occurred (or for one date when the time was unknown so the period with the later highest intensity was chosen) and delete all other hours and place in 'Cuts_Non_Max_Hours' even if they have higher values than that associated with the time of the landslip. However, it was noted that on eight occasions significantly higher intensities occurred during a period of approximately 2 hours (or less) prior to the landslip. These maybe of

significance in identifying lag effects; they have been removed but stored in a folder called 'Cuts_On_Landslip_Days'.

Final

10. The final spreadsheet contains all the sorted days (745) of data with the landslide dates highlighted in yellow and in appropriate time slot.

Graph

11. As Final but with the landslide events removed from list and archived separately at the bottom enabling landslide events and non-landslide events to be treated separately initially to produce individual graphs, then merged into one graph.

Appendix B Application of Bayes Theorem to a Hypothetical General Scenario

Hypothetically, assume that during a certain time interval 24 rainfall events (blue squares in Figure B.1) and four landslides (yellow squares in Figure B.1) are observed. The rainfall events are recorded and divided into three groups according to a chosen variable (it could be for instance the intensity, the total rainfall, the duration, etc.). Eight events belong to the group R_1 (i.e. they are characterised by a value R_1 for the selected variable), 12 events are in the R_2 group and four are in the R_3 group. Two landslides are associated with two rainfall events of the type R_1 , the other two are associated with two rainfall events of type R_2 .

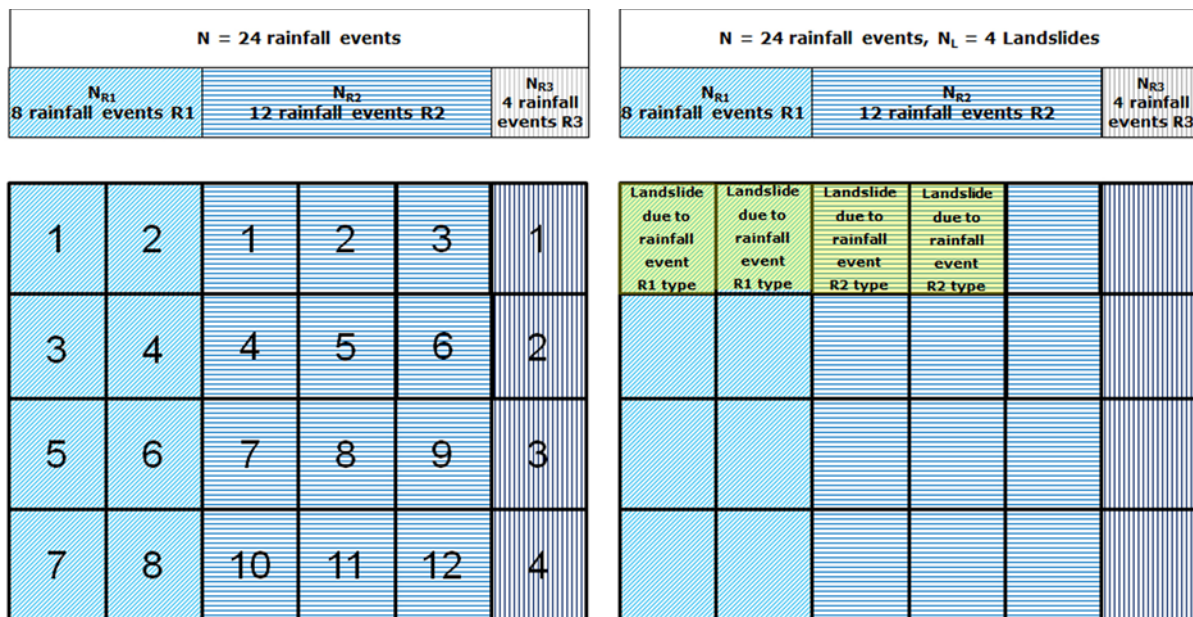


Figure B.1: Hypothetical scenario where 24 rainfall events (blue squares) and four landslides (yellow squares) are observed (see text for details).

According to the relative frequency method and on our data, the prior probability that a rainfall of type R_1 occur is given by the ratio between the number of times it happens and the total number of rainfall events recorded. In our example, $P(R_1) = N_{R1}/N = 8/24 \cong 0.33$ (recurring). Similarly, it is calculated for the rainfall events in the group R_2 and R_3 (see Figure B.2) that the $P(R_2)$ and $P(R_3)$ ratios are 0.50 and 0.17, respectively.

The prior probability of a landslide is equal to the number of landslides observed divided by the total number of rainfall events; that is, in the example, $P(L) = N_L/N = 4/24 \cong 0.17$. (Note that the explicit assumption is that landslides are always associated with rainfall.) This prior probability tells us that in cases where rain occurs, there is a probability of 17% that a landslide occurs. This approach does not link the landslide event with a particular type or amount of rainfall (R_1 , R_2 or R_3); it simply states that every time it rains there is a 17% probability of a landslide. But this conclusion can be misleading if there is an underlying connection between the characteristics of the rainfall event we are studying and landslide occurrence. In our case, for instance, the rainfall events belonging to the third group have not been linked temporally with a landslide, therefore if we in future observe another R_3 type of rainfall, it would not be appropriate to affirm that there is a 17% of probability that a landslide takes place.

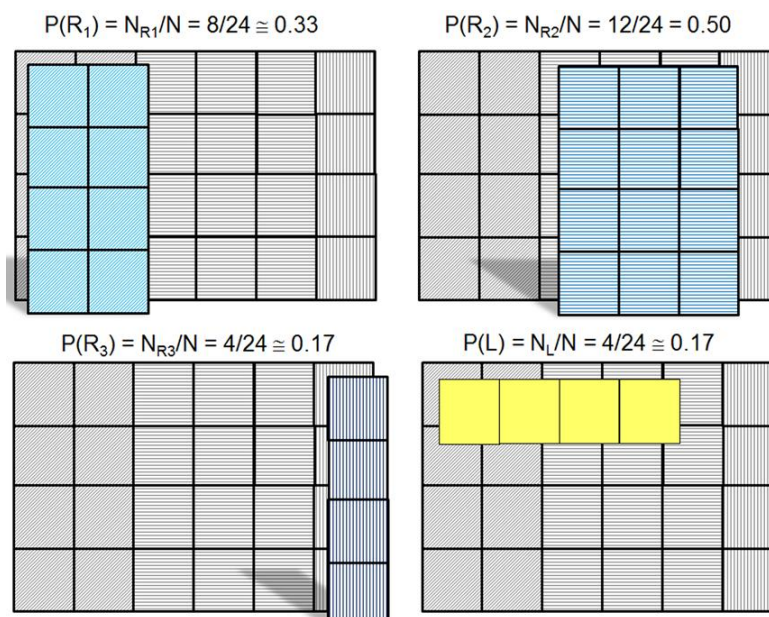


Figure B.2: Example of calculation of prior rainfall and landslide probabilities based on the relative frequency method.

However, through the Bayes' theorem more information is taken into account, and this leads to more accurate expectations. The analysis allows a focus on selected characteristics of the potential cause (e.g. the rainfall intensity) and testing whether it is relevant, and to what extent for the phenomenon under study (see point 2 in Section 6.2.2).

In the example two landslides out of four (50%) are associated with rainfall of type R_1 . This can be rephrased saying that, if a landslide occurs, there is a 50% probability that the associated rainfall was of type R_1 or that the posterior probability of R_1 being associated with the recorded landslide, L , is 50%:

$$P(R_1|L) = N_L(R_1)/N_L = 2/4 = 0.5$$

where $N_L(R_1)$ is the number of landslides in the data which has been attributed to rainfall events of type R_1 (left-hand picture in Figure B.3).

Similarly for the other two landslides we have: $P(R_2|L) = N_L(R_2)/N_L = 2/4 = 0.5$.

We want to know the probability that a rainfall of type R_1 is associated with a landslide. From Bayes' theorem, Eq. (6.1), we have:

$$P(L|R_1) = \frac{P(R_1|L) \cdot P(L)}{P(R_1)} = \frac{0.5 \cdot 0.17}{0.33} = 0.25$$

If the calculation is repeated for the group R_2 , we obtain a posterior landslide probability of 17% ($= [0.5 \cdot 0.17] / 0.50$), while for the type R_3 , it is equal to 0%, since $P(R_3|L) = 0\%$.

Based on this, it can be concluded that the hypothetical rainfall events of type R_1 are most responsible for generating landslides, with a probability of a landslide occurring as a result of that type of rainfall being 25% (well above the 17% of $P(L)$); rainfall events of type R_2 are associated with landslides with a probability of 17% identical to the simple event probability; while R_3 events are unlikely to be linked to landslide phenomena.

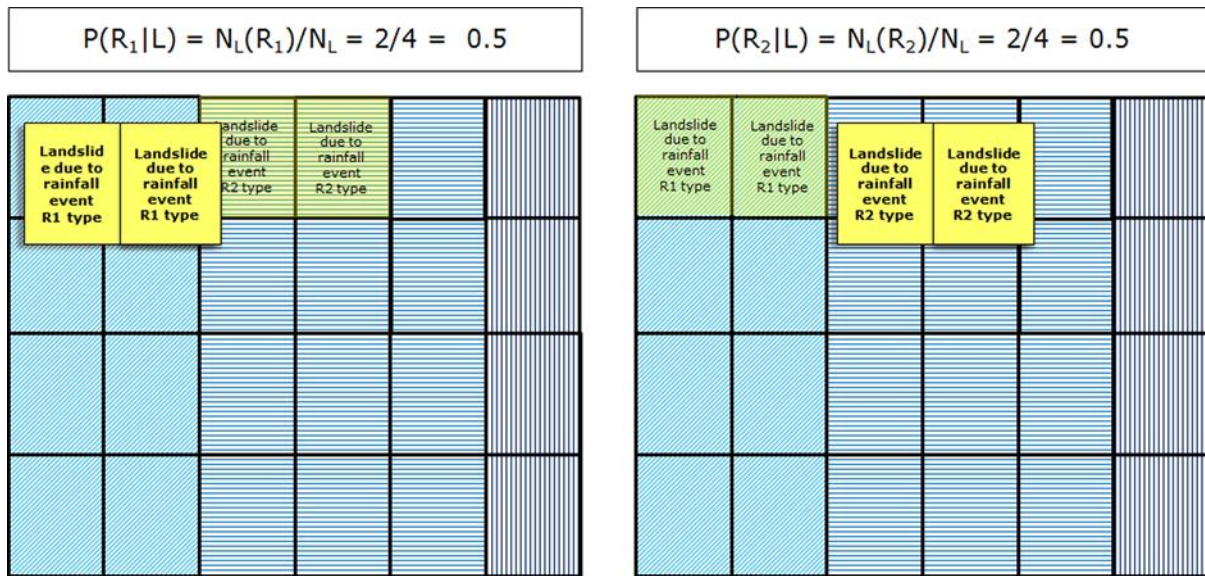


Figure B.3: Posterior probability of a rainfall given a landslide.

Appendix C Explanation of Probability of Rainfall Duration $P(D)$

For explanatory purposes, we can consider five rainfall events and eight durations, from 0.25 to 12 hours (Table C.1). If we chose $1 \text{ mm/h} \leq I < 5 \text{ mm/h}$, we have $N_{\Delta I, tot} = 22$ (blue figures in Table 5). For each time interval (duration) D , we count the number of cells with the intensity in the selected range (red figures in the Table C.1). From these values, we calculate the probability of having a rainfall event of duration D (for ΔI in the selected interval) as described in the last row in Table C.1.

Table C.1: Section of the original rainfall events data table used to illustrate the procedure followed for calculating the probabilities (see text for more details).

| $D(\text{h})$ | 0.25 | 0.5 | 1 | 2 | 4 | 6 | 8 | 12 |
|----------------------------------|-------------|-------------|-------------|-------------|-------------|-------------|-------------|-------------|
| Event 1 | 11.20 | 9.20 | 8.00 | 7.50 | 7.60 | 6.40 | 5.00 | 3.47 |
| Event 2 | 4.80 | 2.80 | 1.60 | 1.00 | 0.85 | 1.73 | 2.10 | 1.80 |
| Event 3 | 17.60 | 12.00 | 6.00 | 3.30 | 2.00 | 2.27 | 3.75 | 5.45 |
| Event 4 | 5.60 | 4.40 | 3.80 | 3.20 | 5.50 | 5.67 | 5.45 | 4.32 |
| Event 5 | 8.80 | 5.20 | 3.40 | 3.50 | 3.30 | 3.07 | 2.83 | 3.07 |
| N_D | 1 | 2 | 3 | 4 | 2 | 3 | 3 | 4 |
| $P(D) = N_D / N_{\Delta I, tot}$ | 1/22 | 2/22 | 3/22 | 4/22 | 2/22 | 3/22 | 3/22 | 4/22 |

This report considers the recent history of debris flow in Scotland as it relates to the trunk (strategic) road network and the rainfall climate of Scotland. The development of a deterministic rainfall threshold for Scotland is described in the context of a brief review of international rainfall trigger thresholds. This highlights the potential for a probabilistic approach to be taken to the development of such thresholds; and for rainfall event data that does not lead to a landslide, as well as rainfall event data that does lead to a landslide, to be incorporated into the analysis. The probabilistic analyses presented here use Bayes' theorem to undertake both one-dimensional analyses (for rainfall duration and intensity, and total rainfall) and two-dimensional analyses (for paired values of rainfall duration and intensity) to determine conditional landslide probability. Probabilistic thresholds for the conditional probability of landslide occurrence dependent on rainfall duration and intensity $P(D|I)$ are derived in the range 0.05 (5%) to 0.3 (30%). It is proposed that a formal trial be undertaken of a probabilistic landslide forecast system.

Other titles from this subject area

- PPR 852** Monitoring and modelling of landslides in Scotland: characterisation of slope geomorphological activity and the debris flow geohazard. B Sparkes, S A Dunning, M Lim & M G Winter. 2018
- PPR 824** Landslides triggered by Storm Desmond at the A83 Rest and be Thankful, Scotland: panoramic photography as a potential monitoring tool. M G Winter, B Sparkes, S A Dunning & M Lim. 2017
- PPR 798** The quantitative assessment of debris flow risk to road users on the Scottish trunk road network: A83 Rest and be Thankful. J F C Wong & M G Winter. 2018
- PPR 743** An extended and updated technical evaluation of wig-wag signs at the A83 Rest and be Thankful. M G Winter & B Shearer. 2017

TRL

Crowthorne House, Nine Mile Ride,
Wokingham, Berkshire, RG40 3GA,
United Kingdom
T: +44 (0) 1344 773131
F: +44 (0) 1344 770356
E: enquiries@trl.co.uk
W: www.trl.co.uk

ISSN 2514-9652

ISBN 978-1-912433-90-2

PPR901